# Morphological and physiological changes of shoot apex during stem cell senescence and death process in *Arabidopsis thaliana*

# シロイヌナズナにおける茎頂幹細胞の老化と死プロセスの形態学的/生理学的解析

Yukun Wang
Nara Institute of Science and Technology
Division of Biological Sciences
Plant Stem Cell Regulation and Floral Patterning
(Toshiro Ito)
2021.09.20

Division of Biological Sciences Doctoral Thesis Abstract

| Laboratory (Supervisor) | Plant Stem Cell Regulation and Floral Patterning (Toshiro Ito) | | |
|---|---|---|---|
| Name | Yukun Wang | Date | 09, 20, 2021 |
| Title | Morphological and physiological changes of shoot apex during stem cell senescence and death process in *Arabidopsis thaliana* | | |


Monocarpic plants have a single reproductive phase, in which their longevity is developmentally programmed by molecular networks. In the reproductive phase of *Arabidopsis thaliana*, the inflorescence meristem (IM) maintains a central pool of stem cells and produces a limited number of flower primordia, which results in seed formation and the death of the whole plant. In this study, I observed morphological changes in the IM at cellular and intracellular resolutions until the end of the plant life cycle. I observed four biological events during the periods from 1 week after bolting (WAB) till the death of stem cells: 1) the gradual reduction in the size of the IM, 2) the dynamic vacuolation of IM cells, 3) the loss of the expression of the stem cell determinant *WUSCHEL* (*WUS*), and 4) the upregulation of the programmed cell death marker *BIFUNCTIONAL NUCLEASE1* (*BFN1*) in association with the death of stem cells. These results indicate that the stem cell population gradually decreases in IM during plant aging and eventually is fully terminated. I further show that the expression of *WUS* becomes undetectable in IM at 3 WAB prior to the loss of *CLAVATA3* (*CLV3*) expression at 5 WAB; CLV3 is a negative regulator of *WUS*. Moreover, *clv3-2* plants show delayed loss of *WUS* and lived six weeks longer compared with wild type plants. These results indicate that the prolonged expression of *CLV3* at 4-5 WAB may be a safeguard that inhibits the reactivation of *WUS* and promotes plant death. Through transcriptome analysis, I revealed that reactive oxygen species (ROS) are involved in the control of plant longevity, and eight ROS-metabolism-related-candidate genes are isolated. Furthermore, I found that main components of ROS, superoxide anion ($O_2^{\cdot-}$) and hydrogen peroxide ($H_2O_2$), displayed dynamic changes along with the plant growth. Applications of 5 mM and 50 mM exogenous $H_2O_2$ could inhibit *WUS* and promote dPCD marker *ORESARA 1* (*ORE1*) expressions, respectively. The results indicate that ROS acts as an intracellular signal and plays important roles in regulating stem cell fate during plant senescent period. My work presents a framework for the regulation of plant longevity in *Arabidopsis* at morphological, physiological, and gene expression levels. The findings provide novel insights into ROS-mediated signaling pathways involved in stem cell fate regulation towards the understanding of plant longevity control.

## Table of contents

# Introduction

Shoot apical stem cells are located on the top of main shoot in plants. Generally, these stem cells are thought of as a cell population that has infinite abilities of proliferation. The daughter cells of stem cells mainly have two kinds of functions: one is to maintain the stable number of stem cells and the other is to form the differentiated cells. The renewable capacity ensures the dynamic balance and continuity of shoot stem cells, and has a close relationship with plant longevity. In the current study, I try to investigate the relationship between stem cell longevity and whole plant lifespan. I not only monitor stem cell activities but also expect to uncover the possible pathways resulting in stem cell death in model plant *Arabidopsis thaliana*.

**Advances of stem cell regulating mechanism in *Arabidopsis***

The aerial part is originated from shoot apical meristem (SAM) in plants. In *Arabidopsis*, SAM generally refers to the top area above leaf primordia (vegetative stage) or floral primordia (proliferative stage) (Figure 1). In cellular and structural levels, SAM is made up of central zone (CZ), peripheral zone (PZ), and rib zone (RZ) (Figure 2A) (Steeves and Sussex, 1989; Meyerowitz, 1997). Stem cell population is harbored in CZ (Figure 2A). Through slow cell division, stem cells can self-renew and keep the undifferentiated status. PZ cells divide faster than stem cells, thereby differentiate into different organic primordia. Similar to PZ cells, RZ cells also divide fast to ensure stem growth (Steeves and Sussex, 1989; Meyerowitz, 1997). Based on the features of division and differentiation of stem cells, the SAM domain can be separated into three layers, including the epidermal L1 layer, subepidermal layer L2, and inner layer L3 (Figure 2B) (Fletcher, 2002).

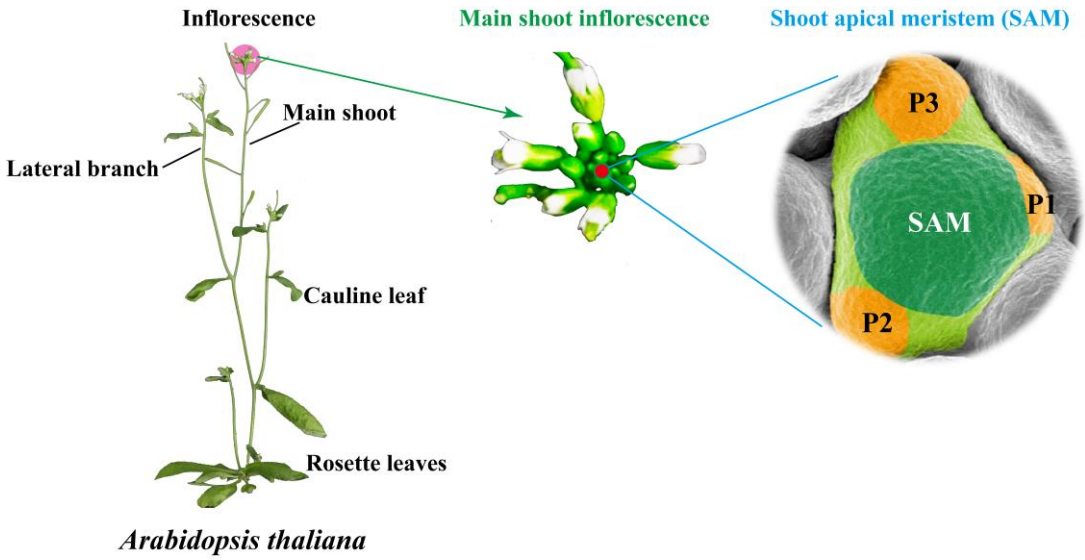


**Figure 1** Morphology of *Arabidopsis thaliana* seedling (Landsberg *erecta*, L*er*) and the shoot apical meristem (SAM). The structure of *Arabidopsis thaliana* seedling and the relative locations of inflorescence meristem (IM) and SAM are denoted. P1-P3 indicate floral primordia.

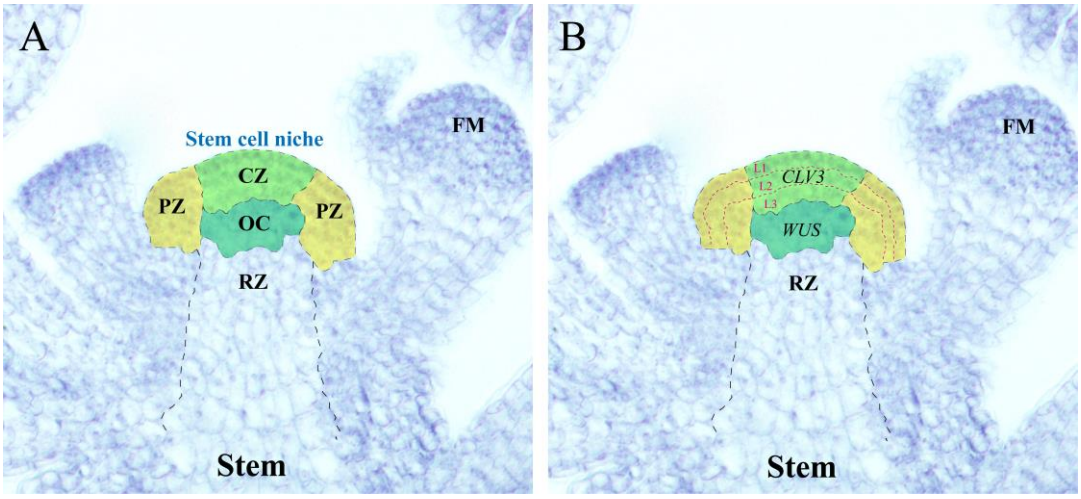


**Figure 2** The structure of shoot apical meristem (SAM). (**A**) The relative positions of different zones in SAM. OC: organizing center. CZ: center zone. PZ: peripheral zone. RZ: rib zone. FM: floral meristem. (**B**) Schematic diagram of different cell layer (L1-L3) and the expression domains of *WUS* and *CLV3* in SAM domain. FM: floral meristem.

During plant growth and development, stem cell fate is dynamically controlled by several signals from the stem cell microenvironment. A set of cells, known as the organizing center (OC) and located under CZ, determine the number and fate of stem cells (Figure 2). This part of cells plays a conclusive role in the maintenance of stem cells. The core signal pathway is the negative feedback loop formed by *WUSCHEL* (*WUS*) and *CLAVATA3* (*CLV3*). *WUS* encodes a plant-specific homeotic transcription factor and is a basic member of the *WUSCHEL-related homeobox* (*WOX*) gene family (van der Graaff et al., 2009). *WUS* is expressed in OC cells (Figure 2). In *wus* mutant, the domelike SAM is absent in the seedling stage as well as in inflorescence meristem (IM). Some differentiated cells appear in the CZ of *wus* mutant, indicating that *WUS* plays role in preventing stem cell differentiation (Mayer et al., 1998; Laux et al., 1996). Overexpression of *WUS* can induce an intumescent SAM and the production of ectopic stem cells, suggesting that WUS can determine the stem cell properties (Brand et al., 2002; Lenhard et al., 2002; Schoof et al., 2000). *CLV3* encodes a protein that contains 96 amino acids and belongs to CLV3/EMBRYO SUPPOUNDING REGION (CLE) protein family (Cock and McCormick, 2001). *CLV3* is expressed in CZ approximately (Figure 2B). The number of cells that expressing *CLV3* in L3 is lower than that in L1; therefore the *CLV3* expression domain is not precisely equivalent to the CZ area. In the *clv3*-2 mutant, SAM is more extensive than in wild type (WT) and forms more floral organs than WT. These results demonstrate that *CLV3* plays opposing role in regulating stem cell maintenance (Clark et al., 1995). By contrast, the *CLV3*-overexpressed plants show the same phenotype as that in the *wus* mutant, and the *WUS* expression is inhibited (Brand et al., 2000; Lenhard and Laux, 2003). By combining these findings, the *WUS-CLV3* feedback loop is established to explain the molecular foundation of stem cell homeostasis. However, these evidence can not uncover the precise functions of *WUS* and *CLV3* on stem cell maintenance. Subsequently, researchers found that *CLV3* can inhibit the dedifferentiation of PZ cells (close to CZ) to prevent these cells from becoming stem cells and inhibit the mitotic speed in PZ cells to maintain the SAM size (Reddy and Meyerowitz, 2005). Furthermore, inducible activation of *WUS* in CZ results in the transformation of outer PZ cells into stem cells. It promotes the mitotic speed of PZ cells, therefore regulates the differentiated PZ cell ratio (Yadav et al., 2010).

In the SAM domain, *WUS* mRNA is transcribed in OC, but WUS protein can move into CZ via plasmodesmata to promote the expression of *CLV3* in stem cells (Yadav et al., 2011; Holt et al., 2014; Daum et al., 2014). WUS protein can bind to several TAAT elements existing in the promotor and 3' regulatory region of *CLV3* (Yadav et al., 2011). A proposed model presents that monomeric WUS activates *CLV3* in CZ at a low concentration whereas represses *CLV3* in OC via forming homodimer at a high concentration (Perales et al., 2016). There is an 18 amino acid-length signal peptide in the N-terminus of CLV3 protein and a 14 amino acid-length EMBRYO SURROUNDING REGION (CLE) conversed domain in the C-terminal (Cock and McCormick, 2001; Fletcher et al., 1999; Ito et al., 2006). In plants, CLV3 precursor protein is spliced as a 13 amino acid-length bioactive peptide CLV3p via

extracellular hydrolysis (Kondo et al., 2006; Ohyama et al., 2009). After the secretion, CLV3p moves from CZ to OC area, where existing leucine-rich repeat (LRR) containing receptors, therefore inhibiting the expression of *WUS* (Katsir et al., 2011). There are four kinds of CLV3 receptors, the first one is CLV1, the second one is CLV2/CORYNE (CRN) complex, the third one is Receptor-like Protein Kinase 2 (RPK2), and the last one is BARELY ANY MERISTEM (BAM) family receptor. *CLV1* encodes a LRR receptor-like kinase and is mainly expressed in RZ (Clark et al., 1997). CLV3 peptide can directly bind the LRR domain of CLV1 (Ogawa et al., 2008). CLV2 and CRN form a CLV3 receptor complex largely independent of CLV1 (Jeong et al., 1999; Müller et al., 2008; Bleckmann et al., 2010). The phenotype of *rpk2* mutant is weaker than that in *clv1* and *clv2*, but stem cells are still diffused. The phenotype of *clv1 clv2 rpk2* is very similar to *clv3*, indicating that the RPK2-mediated pathway plays subordinate and independent roles (Kinoshita et al., 2010). *BAM* encodes LRR functional domain-containing receptor kinase. In *bam1 bam2 bam3* mutant, the SAM size is smaller than in WT, suggesting that BAMs play roles in suppressing stem cell proliferation (DeYoung et al., 2006) (Figure 3).

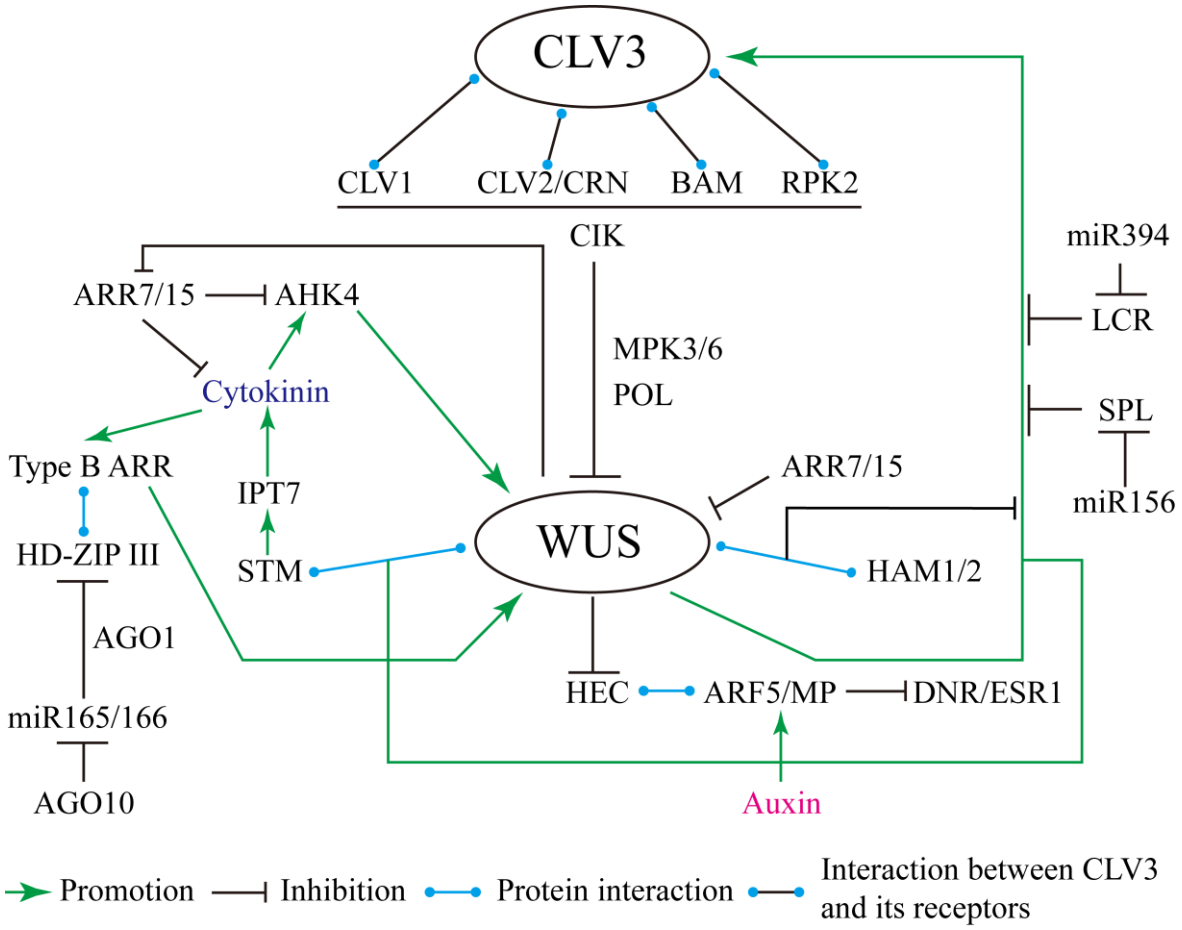


**Figure 3** The regulatory network of factors involved in WUS-CLV3 feedback loop.

So far, the signaling cascade from CLV3 to *WUS* remains to be studied. Current studies reveal that several kinases and phosphatases take part in this cascade. CLAVATA INSENSTIVE RECEPTOR KINASES (CIKs) act as interacting partners of the CLV3 receptors in the control of SAM size, and the *cik1 2 3 4* quadruple mutant displays an inflated SAM (Hu et al., 2018). *POLTERGEIST* (*POL*), which encodes a protein phosphatase 2C, acts as a negative component of the CLV1 receptor kinase signaling pathway to possibly regulate downstream of the CLV receptors (Yu et al., 2003). In addition, the mitogen-activated protein kinases (MAPK) MPK3 and MPK6 act in an intracellular signaling cascade to play an important role in the maintenance of SAM development. The application of exogenous CLV3 peptide triggers rapid signaling in the SAM via dynamic activation of MPK3 and MPK6 (Betsuyaku et al., 2010; Lee et al., 2019) (Figure 3).

There are several players involved in the WUS-CLV3 feedback loop. The first group of genes is *HAIRY MERISRTEM (HAM)* genes. *HAM* genes encode GRAS domain transcription factors that act as inhibitors of the differentiation of shoot stem cells (Stuurman et al., 2002; Schulze et al., 2010). In Arabidopsis, HAM1 and HAM2 directly interact with WUS protein and act as transcriptional cofactors with WUS to regulate the formation of shoot stem cells. Moreover, *HAM1/2* are co-expressed in RZ with *WUS*, and synergistically regulate the expression of *TOPLESS* (*TPL*), indicating WUS protein needs transcriptional cofactors (Zhou et al., 2015). Besides, in the rib meristem, the expression patterns of *CLV3* and *HAM1/2* are mostly complementary, and the 3D computational simulation and experimentation show WUS-HAM complex controls the expression of *CLV3* (Zhou et al., 2018). In *ham123* mutant, *CLV3* is expressed restrictedly in the axillary meristem, indicating HAM proteins regulate the initiation and maintenance of the WUS-CLV3 feedback loop (Zhou et al., 2018). Some microRNAs have been reported to play roles in SAM development. *MicroRNA156* and its target gene *SQUAMOSA PROMOTER BINDING PROTEIN-LIKE* (SPL) form a pathway to control SAM size during vegetative development (Fouracre and Poethig, 2019). In Arabidopsis, five *HOMEODOMAIN-LEUCINE ZIPPER III* (*HD-ZIP III*) genes regulate the SAM formation during embryonic development stage (Prigge et al., 2005; McConnell et al., 2001; Green et al., 2005). Loss-of-function of *HD-ZIP III* genes results in the termination of SAM (Emery et al., 2003; Williams and Fletcher, 2005). In the SAM domain, *HD-ZIP III* genes are the targets of *microRNA165/166* (Liu et al., 2009). *MicroRNA165/166* are precisely regulated by *ARGONAUTE1* (*AGO1*) and *AGO10* (Moussian et al., 1998; Lynn et al., 1999; McConnell and Barton, 1995). *MicroRNA165/166* reduce the expression levels of *HD-ZIP III* via AGO1-mediated pathway, whereas *AGO10* can silence *microRNA165/166* to stabilize the *HD-ZIP III* expression (Zhu et al., 2011). Another microRNA, *microRNA394*, is only expressed in L1 in SAM during the embryonic period. MicroRNA 394 can specifically repress its target *LEAF CURLING RESPONSIVENESS* (*LCR*) in inner layers of SAM, thereby enables WUS protein to control the expression of *CLV3* (Knauer et al., 2013) (Figure 3).

Besides, phytohormone cytokinin (CK) and auxin also take part in the WUS-CLV3 feedback loop. Type A *ARABIDOPSIS RESPONSE REGULATOR* (*ARR*) genes, including *ARR7* and *ARR15*, are negative regulators of the CK signaling pathway. WUS directly inhibits *ARR7* and *ARR15* expression levels (Leibfried et al., 2005). The relationship between WUS activity and CK is found in OC in SAM. *ARABIDOPSIS HISTIDINE KINASE 4* (*AHK4*) gene is the receptor of CK, and it is expressed in OC. *AHK4* induces WUS expression and inhibits CLV1 expression (Gordon et al., 2009). Some studies have revealed that the type B ARR proteins can directly bind to the *WUS* promoter region and promote *WUS* expression (Meng et al., 2017; Xie et al., 2018). Due to the regulatory functions of CK, the expression of WUS can respond to nitrate availability (Landrein et al., 2018), light (Pfeiffer et al., 2016), and a long-distance mobile signal mediated by *BYPASS1* (Lee et al., 2019). It has been reported that CK acts as a regulator of WUS protein stability (Snipes et al., 2018). In short, WUS mediates the CK signaling pathway, and in turn, enhances the expression of *WUS*. Auxin (or indole-3-acetic acid) is another important phytohormone that regulates the WUS-CLV3 feedback loop. AUXIN RESPONSE FACTOR 5/MONOPTEROS (ARF5/MP) is a key factor in the ARF-mediated auxin signaling pathway and can directly inhibit the expression of *ARR7/15* in CZ, resulting in the CK signal activation (Zhao et al., 2010). ARF5/MP can repress the expression of *DORNROSCHEN/ENHANCER OF SHOOT REGENERATION 1* (*DRN/ESR1*), which plays a role in the activation of *CLV3* in the SAM domain (Luo et al., 2018). The HECATE (HEC) transcription factor family members are downstream components of WUS, and they have been reported that possibly regulate stem cells via the interaction with ARF5/MP (Schuster et al., 2014; Gaillochet et al., 2017) (Figure 3).

In addition to the WUS-CLV3 feedback pathway, another parallel signaling pathway led by SHOOT MERISTEMLESS (STM), also regulates shoot stem cell fate. Like WUS, STM is also a homeodomain transcription factor. Loss-of-function of *STM* induces the termination of SAM. In *stm* mutant, there is no recognizable SAM (Endrizzi et al., 1996). Ectopic expressions of *WUS* and *STM* can induce different downstream genes. The main function of WUS is the transformation of CZ cells into stem cells, whereas the function of STM is to inhibit the differentiation and promote the proliferation of stem cells (Lenhard et al., 2002). STM directly activates *ISOPENTENYL TRANSFERASE 7* (*IPT7*) and *ARR5* to regulate stem cell maintenance (Jasinski et al., 2005; Yanai et al., 2005). Similar to WUS, STM in the stem cells can activate the expression of CLV3 (Brand et al., 2002; Lenhard et al., 2002). Recently, the molecular mechanism of synergistically regulate stem cell fate by WUS and STM is uncovered. WUS and STM interact directly with each other, and WUS activates the expression of STM. STM interacts with WUS to enhance WUS binding to the *CLV3* promoter (Su et al., 2020) (Figure 3).

In brief, the functions of WUS and CLV3 on stem cell formation and maintenance are irreplaceable. All regulations of *WUS* and *CLV3* can change the stability of the WUS-CLV3 feedback loop, in turn, to influence the stem cell fate directly or indirectly.

**WUS-mediated network in control of plant development**

As a master regulator in plant growth and development, functions of *WUS* and *WUS-related homeobox* (*WOX*) transcription factors have been largely estimated in plants (Jha et al., 2020). During the plant growth and development, *WUS* is not only regulated directly or indirectly by a series of factors but also regulates several targets via transcriptional levels. Recently, the structural basis of WUS protein has been uncovered. This finding provides us a detailed understanding of the binding mechanism of WUS transcription factor. It is quantitatively delineated that WUS can bind to three divergent DNA motifs such as 'TGAA,' 'TAAT,' and 'G-box.' Among these motifs, WUS maintains a strong interaction with the 'TGAA' motif (Sloan et al., 2020).

Some works reveal the WUS-mediated gene expression maps in *Arabidopsis* shoot apical meristem in past years (Yadav et al., 2009; Busch et al., 2010). In these studies, WUS is thought as a key regulator, and several WUS targets and response genes were isolated by ChIP-seq. WUS can directly bind to DNA motifs in more than 100 target promoters (Busch et al., 2010). A total of 675 isolated WUS response genes, including direct WUS targets CLV1 and TOPLESS, are clustered into seven modules, including cell division hormone signaling, regulation of polar auxin transport, inhibition of auxin signaling, meristem-related processes, modulation of jasmonate signaling, activation of cytokinin signaling, and cell division (Busch et al., 2010). For instance, WUS directly binds to promoters of *CLV1* and *TOPLESS* to promote the expression of *CLV1* and repress the expression of *TOPLESS* (Busch et al., 2010). By deeply excavating these targets, a subsequent study showed that WUS could act as an auxin response rheostat to maintain apical stem cells (Ma et al., 2019). Several genes, such as *TRANSPORT INHIBITOR RESPONSE 1* (*TIR1*), *AUXIN RESPONSE TRANSCRIPTION FACTORs* (*ARFs*), *INDOLEACETIC ACID-INDUCED PROTEIN* (*IAA*), *LOB DOMAIN-CONTAINING PROTEIN 38* (*LBD38*), and *TARGET OF MONOPTEROS 3* (*TMO3*), are directly bound by WUS in their promoter regions (Ma et al., 2019). In the list of responsive genes with annotated activities in "auxin response" to WUS, *ORESARA 1/NAC092*, which is known as a programmed cell death regulator in papilla cells (Gao et al., 2018), is regulated by WUS via deacetylation (Ma et al., 2019).

In addition to the roles in *WUS*-mediated regulation of the shoot meristem, WUS also maintains important functions in regulating plant development. In floral meristem development, the *WUS* expression pattern is controlled by an epigenetic mechanism (Cao et al., 2015). During male organogenesis, *WUS* is expressed in the precursor cells of the stomium and terminated before the stomium cells enter terminal differentiation. In *wus* mutants, there are fewer and malformed lobes compared to the WT, indicating that *WUS* plays essential role in regulating another development in *Arabidopsis* (Deyhle et al. 2007). In *Chrysanthemum morifolium*, WUS can interact with CYCLOIDEA 2 (CYC2) transcription factor to regulate the development of floral organs and pistils (Yang et al., 2019). In addition, *WUS* is reported to show important roles in plant embryogenesis. During somatic

embryogenesis, *WUS* expression is upregulated in several plant species (Jha et al., 2020), suggesting that *WUS* is essential for embryogenesis.

So far, the potential functions of WUS and its targets have only been studied rarely. The expression patterns and functional behavior of WUS suggest that it is still a long way until we understand WUS function in plant growth and development. More importantly, the linkage between WUS and programmed cell death (specific reference of stem cell death) and its targets in this bioprocess is still unknown. Most recently, WUS has been reported to play decisive roles in regulating innate antiviral immunity in plant stem cells (Wu et al., 2020). Through inhibiting the expressions of related genes, WUS restrain the virus replication in plant stem cells (Wu et al., 2020). This new finding reminds us that the WUS functions have not been uncovered fully yet.

**The relationship between stem cell activity and plant lifespan**

Plant lifespan means the maximal life expectancy at birth in plants. The variations of lifespan in different plant species, including individual and clonal plants, are tremendous (Thomas, 2013). For instance, a tree plant named Bristlecone pine (*Pinus longaeva*) has 4,600 years' lifespan, but only a few months' lifespan in model plant *Arabidopsis thaliana*. In order to understand the control of plant lifespan, it is necessary to know the plant structure. Usually, except for root parts, the plant body is made up of one or more shoots, which topically reiterates the same species-specific architecture or configuration (Klimešová et al., 2015). Based on origins, shoots can be classified as primary shoots and axillary shoots (or lateral shoots). The primary shoot is initiated on the shoot pole of the embryo (Klimešová et al., 2015). Given that all parts of plant body are derived from stem cells in SAM; therefore, SAM is sometimes considered as the 'fountain of youth' (Baurle and Laux, 2003).

In 1994, a study observed the arrest of inflorescences in *Arabidopsis thaliana* and found that the inflorescence arrest occurs normally. During the inflorescence arrest process, each inflorescence ceases to open flowers and enters the arrested status. This phenomenon is defined as the global proliferative arrest (GPA) (Hensel et al., 1994). The production of the GPA process is probably due to the fruit formation. Fruit removal or lack of fruits (in some male sterile mutants) demonstrates a precaution of inflorescence arrest. The SAM activities keep relatively high levels due to new flower formations continuously (Hensel et al., 1994).

Not far from now, a study depicted that the arrested inflorescence meristem status is strongly similar to the dormancy in lateral inflorescences, indicating that the GPA represents a formation of bud dormancy through controlling the inflorescence meristem activities (Wuest et al., 2016). Another current study shows that the delayed inflorescence arrest exists in *fruitfull* mutants and points out the inflorescence arrested process was regulated by a FRUITFULL–APETALA2 regulatory pathway. Meanwhile, the authors also monitored the spatio-temporal expression patterns of *WUS* and *CLV3* and found that terminations of *WUS* and *CLV3* expressions are necessary for inflorescence arrest (Balanzà et al., 2018). Most

recently, a study declared that an auxin-mediated inflorescences arrest model. They found that the end-of-flowering in *Arabidopsis* has not occurred synchronously between different branches, and this phenomenon is driven by auxin export from fruit proximal to the inflorescence apex (Ware et al., 2020), indicating that the concept of GPA is still controversial. Furthermore, the authors pointed out that the inflorescences arrest happened when they reach a certain developmental age (Ware et al., 2020). These current findings, at least in part, suggest that the SAM activity is associated with the whole-plant lifespan.

Shoot stem cells are harbored in the SAM domain. The activities of SAM depend on stem cell activities. Unlike animals, theoretically, plants have an endless supply of stem cells (Weigel and Jürgens, 2002; Singh and Bhalla, 2006). These stem cells take charge of tissue homeostasis and repair. Given this, some researchers surmise that stem cells may hold the key to determining plants' longevity (Dijkwel and Lai, 2019).

**Intracellular changes in plant senescent and dying cells**

Several studies revealing that senescent plant cells take place with obvious changes (Figure 4). In mesophyll cells, the content of chlorophyll negatively correlates with senescence (Martin and Thimann, 1972). Chlorophyll degradation is the most distinct feature in senescent leaves (Lesgemy, 1981). In senescent rice leaves, the decreased contents of chlorophyll and related proteins can be recognized as reliable traits of leaf senescence (Biswas and Choudhuri, 1980).

The homeostasis of normal cells is maintained by a balanced system, which is combined by synthesis and decomposition. Proteins keep a relatively constant turnover. However, the relatively constant turnover is broken once the plant cell enters the senescent stage. Several studies have demonstrated that protein degradation is a basic feature of senescence (Ray and Choudhuri, 1980; Ryan, 1973; Matile and Winkenbach, 1971). Thus, the increase of proteinase activities should be an important intracellular change in senescent cells.

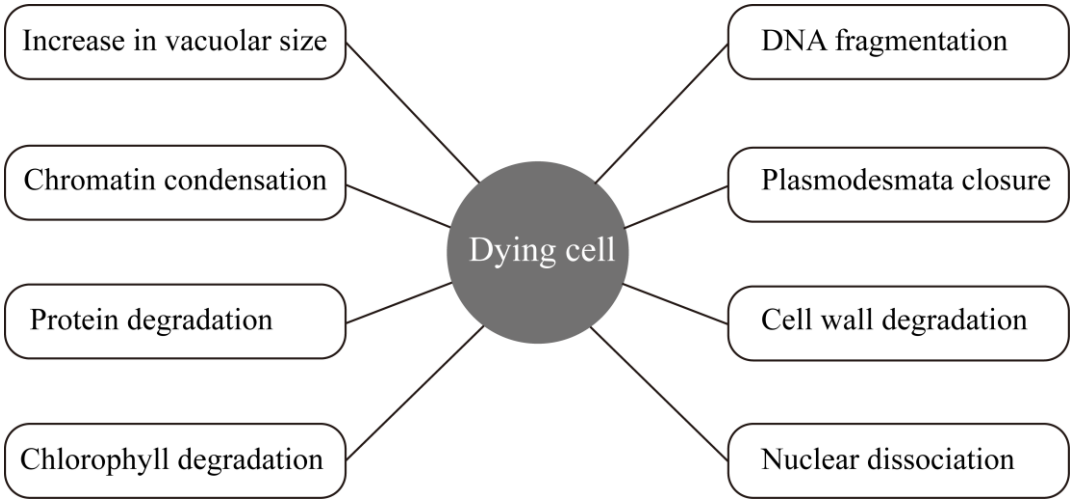


**Figure 4** Summary of morphological changes and physiological features in dying cells.

In addition, various morphological features are mostly considered autophagy-like processes, such as the increase in vacuolar size, chromatin condensation, and nuclear dissociation (Shibuya et al., 2016). Usually, the degradation of the cytoplasm is mediated by lytic vacuoles in senescent and dying cells. Lytic vacuoles contain acid phosphatases and hydrolytic enzymes (Shibuya et al., 2016). In the cytochemical study in root-tip stem cells, the results showed the lytic vacuoles are derived from tubules formed on the *trans* side of the Golgi body (Marty, 1999). In young plant cells, several small lytic vacuoles are formed during cell differentiation (Marty, 1997). Subsequently, these small lytic vacuoles will merge and form one or a few large vacuoles (Shibuya et al., 2016). Thus, the formation of large vacuoles in senescent or dying cells is an important feature as well. Chromatin condensation is often initially happened somewhere in the nucleus and then extends the whole of the nucleus. In dying *Ipomoea* petal cells, chromatin condensation induces decreased nucleus size (Yamada et al., 2006b). In some cases, DNA degradation is observed when chromatin condensation happens (Shibuya et al., 2016). Nuclear dissociation has also been reported in some plant dying cells (Wojciechowska and Olszewska, 2003). In the dying petal cells in *Ipomoea*, *Petunia*, and *Argyranthemum*, nuclear fragmentation is observed (Yamada et al., 2006a; Yamada et al., 2006b).

Moreover, the plasmodesmata closure has also been thought of as senescent feature (Kamdee et al., 2015). So far, plasmodesmata closure has been studied in petal cells of *Iris* (van Doorn et al., 2003). Besides, the cell wall degradation is also a noticeable feature in senescent and dying cells and is now thought of as a contributor to cell death. Cell wall degradations always induce turgor loss and tonoplast rupture, resulting in the cell collapse. So far, cell wall degradation has been confirmed in Ipomoea, Iris, and Dendrobium. The decrease in cellulose and hemicellulose, the secretion of hydrolytic enzymes, and swelling of cell walls can trigger the cell wall degradation during cell senescent and dying stages (Wiemken-Gehrig et al., 1974; van Doorn, 2011; Kamdee et al., 2015). Overall, all evidence mentioned above can be utilized as the traits to distinguish normal and dying cells (Figure 4).

**Roles of reactive oxygen species in plant growth, development, and death**

Reactive oxygen species (ROS) are kinds of intracellular signaling components produced by metabolic pathways in almost all cells (Mhamdi and Van Breusegem, 2018). The roles of ROS in biotic and abiotic-related processes have been widely uncovered in these years (Huang et al., 2019). More generally, the roles of ROS in regulating numerous biological processes, such as root, shoot, and flower growth and development, have also been largely revealed (Mhamdi and Van Breusegem, 2018).

ROS is a cluster of any oxygen derivative and is more reactive than oxygen molecule ($O_2$) (Foyer and Noctor, 2009; Mittler, 2017). In plants, ROS usually includes singlet oxygen ($^1O_2$), superoxide ($O_2^{\bullet-}$), hydroxyl ($OH^{\bullet}$), and hydrogen peroxide ($H_2O_2$) (Mhamdi and Van Breusegem, 2018) (Figure 5). Comparing with $^1O_2$ and $O_2^{\bullet-}$, $H_2O_2$ is relatively stable, and its

half-life time is more than 1 ms. Therefore, it is always considered the main component of ROS involved in intracellular signal pathways (Mhamdi and Van Breusegem, 2018). There are several enzymes involved in $H_2O_2$ metabolism. Catalases (CATs) and ascorbate peroxidases (APXs) are two key enzymes in $H_2O_2$ metabolic pathway. Besides, glutathione S-transferases (GSTs), peroxiredoxins (PRXs), and glutathione peroxidases (GPXs), which are now known as thioredoxin (TRX)-dependent peroxiredoxins, are important players in processing $H_2O_2$ metabolism (Dixon and Edwards, 2010; Dietz, 2011; Iqbal et al., 2006; Bela et al., 2015). Indeed, the main superoxide-processing enzymes are superoxide dismutases (SODs), and $OH^{\bullet}$ and $O_2^{\bullet-}$ are mainly processed by non-enzymatic reactions (Fridovich, 1997; Triantaphylidès and Havaux, 2009; Noctor et al., 2012; Richards et al., 2015). In plant cells, ROS are produced in mitochondrial respiration, photosynthesis in chloroplasts, photorespiratory reactions in the peroxisome, and also in some other enzymatic reactions by NADPH oxidases (Mhamdi and Van Breusegem, 2018). Several phytohormones, such as salicylic acid (SA), jasmonic acid (JA), ethylene (ET), abscisic acid (ABA), and gibberellic acid (GA), can also regulate ROS levels in plant cells through the complex crosstalk (Noctor et al., 2015; Considine and Foyer, 2014; Diaz-Vivancos et al., 2015; Tognetti et al., 2017).

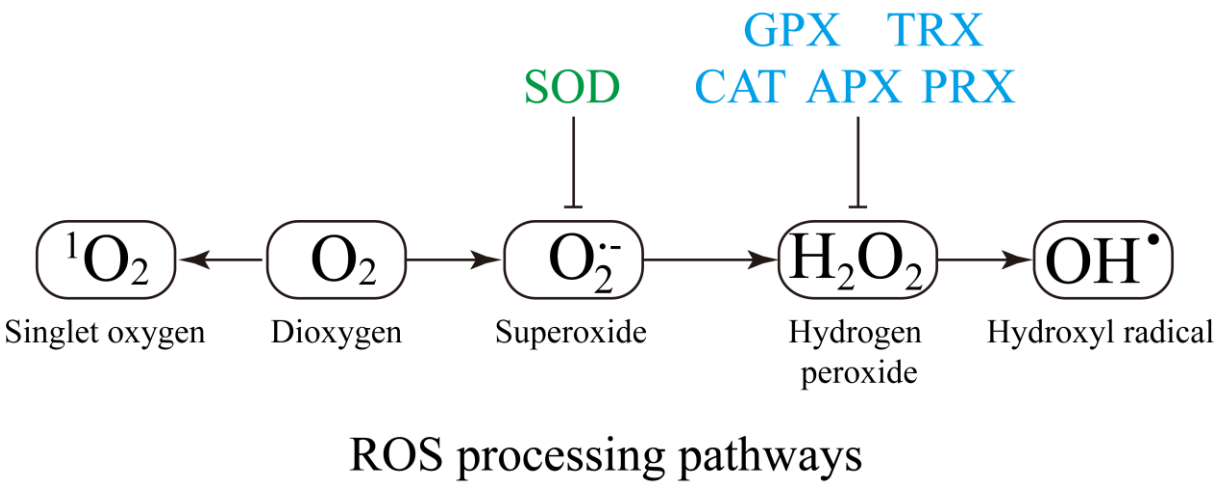


**Figure 5** An overview of ROS processing pathways and the major enzymes in plants.

The functions of ROS and ROS homeostasis in regulating plant growth and development have been largely revealed. During seed germination, ROS homeostasis is tightly controlled (Stacey et al., 2006; Bailly et al., 2008). So far, APX6 and mitochondrial thioredoxin O1 (TRXO1) are involved in seed germination by regulating ROS levels (Chen et al., 2014; Ortiz-Espín et al., 2017). Meanwhile, a key player of the ABA signaling pathway, ABI5, is also involved in regulating $H_2O_2$ homeostasis by binding to the promoter of *CAT1* (Skubacz et al., 2016; Bi et al., 2017). In root growth, several studies have shown that ROS homeostasis takes part in restricting the growth of the primary root, regulating lateral root emergence, and promoting the growth of root hair (Foreman et al., 2003; Orman-Ligeza et al., 2016). During these developmental processes, two auxin-regulated transcriptional factors, ROOT HAIR DEFECTIVE 6-LIKE 4 (RSL4) and MEDIATOR 25 (MED25), are confirmed as the key regulators in promoting root hair elongation (Sundaravelpandian et al., 2013; Mangano et al., 2017). A fine-turned balance between $H_2O_2$ and superoxide contents can regulate cell differentiation in root hairs (Sundaravelpandian et al., 2013). In lateral root emergence, the RBOH-peroxidase system, also a ROS source in plants, plays essential role. RBOHD and RBOHF are involved in lateral root emergence via altering the superoxide levels in root tips (Li et al., 2015). In addition, several mutants of ROS processing pathway-related members show abnormal growth defects. In *cat2* mutant, the plant growth is inhibited due to the increased photorespiratory $H_2O_2$ (Queval et al., 2007). In *gpx5* mutant, the embryo development is defective (Pagnussat et al., 2005). In *gpx1* and *gpx7* mutants, the root architectures are altered (Passaia et al., 2014).

Moreover, some evidence show a clear relationship between redox signaling and flower development. The roles of ROS in regulating petal development, pollen tube growth, and gametophyte formation have been reported. Some plant-specific class III CC-type GRXs, also known as ROXYs, have functions on petal development (Gutsche et al., 2015). Arabidopsis *roxy1* mutant shows a reduced number of petal primordia and exhibits abnormalities during further petal development (Xing et al., 2005). Subsequently, ROXY1 can interact with PETAL LOSS (PTL) to promote petal initiation (Quon et al., 2017). For pollen tube development, the appropriate ROS accumulation in pollen tube tips is necessary (Potocký et al., 2012). *RBOHH* and *RBOHJ* are important for the proper growth of pollen tubes, and pollen tubes in *rbohH rbohJ* mutant show an abnormal collapse (Duan et al., 2014). For gametophyte development, GRXs- and TRXs-encoded genes are required. In Arabidopsis, *NTRA* and *NTRB* encode two NADPH-dependent thioredoxin reductases, and loss-of-function of *NTRA* and *NTRB* induce fertility decrease and slow growth ratio in corresponding mutants (Reichheld et al., 2007). Besides, *ROXY1* and *ROXY2* are also required during anther development. In *roxy1* and *roxy2* single mutants, anther development is normal but abnormal in *roxy1 roxy2* double mutant (Xing and Zachgo, 2008). Further, a study showed that ROXY proteins could interact with TGA9/TGA10 to control anther development (Murmu et al., 2010).

Furthermore, the redox-linked reactions take part in dictating meristem development in both the shoot apical meristem (SAM) and the root apical meristem (RAM) (Schippers et al., 2016; Mhamdi and Van Breusegem, 2018). The activities of RAM are highly sensitive to the alterations of ROS levels in root stem cells, and the $H_2O_2$ treatment can decrease the number of stem cells (Tsukagoshi et al., 2010). In root meristem, $H_2O_2$ accumulation is induced by DNA double-strand breaks. FLAVIN-CONTAINING MONOOXYGENASE 1 (FMO1) is induced by high levels of $H_2O_2$ during the DNA double-strand breaks process, resulting in the decrease of root meristem size (Tsukagoshi et al., 2010; Chen and Umeda, 2015). In SAM development, the roles of ROS have also been uncovered, and the SAM activities are controlled by the antagonistic actions of superoxide and $H_2O_2$. The expression of *WUS* is promoted by superoxide and inhibited by $H_2O_2$, and *PRX* genes are associated with stem cell fate (Zeng et al., 2017).

In recent years, more and more studies reveal that ROS metabolism has a close relationship with plant senescence. Plant senescence is described as a slow and complex process that is associated with the increased availability of ROS (Breeze et al., 2011; Guo and Gan, 2012; Munné-Bosch et al., 2013; Rogers and Munné-Bosch, 2016). Several transcription factors are showing altered expression patterns during ROS-induced senescence. Members of the *NAC* and *WRKY* gene families display downregulated expression profiles (Rosenwasser et al., 2011; Allu et al., 2014). *NAC3/ORS1* and *NAC2/ORE1* are involved in salt stress-induced senescence and participate in $H_2O_2$-dependent signaling crosstalk (Balazadeh et al., 2010, 2011). Overexpression of the NAC transcription factor JUNGBRUNNEN 1 can enhance expressions of ROS-responsive genes and regulate longevity in Arabidopsis (Wu et al., 2012). *WRKY75* is required to link between age-dependent increased ROS and SA synthesis (Guo et al., 2017). In addition to transcription factors, ROS metabolism-related enzymes CAT2 and APX1 are also involved in senescence regulation through triggering of the $H_2O_2$ peak (Zimmermann et al., 2006).

It is well known that death is an integral part of life, and cell death is a necessary process for the normal growth and development of plants. Plant cell death is intimately linked with ROS production (Van Breusegem and Dat, 2006). ROS is thought of as an intracellular signal that can trigger cell death, and the tightly controlled ROS homeostasis is necessary for response to the complex stimuli during the cell death process (Foyer and Noctor, 2005). In *Arabidopsis*, *LSD1*, which encodes a zinc-finger protein, can integrate with LOL1 and LOL2 to sense the changes of ROS homeostasis and repress a default death pathway (Jabs et al., 1996; Dietrich et al., 1997; Epple et al., 2003). Loss-of-function of the *Arabidopsis Executer1* gene can decrease the plant sensitivity to singlet oxygen and results in the complete abolishment of singlet oxygen-induced cell death (Wagner et al., 2004). Moreover, mitogen-activated protein kinases (MAPKs) are also found to play important roles in ROS-dependent cell death events (Ren et al., 2002; Samuel and Ellis, 2002; Samuel et al., 2005; Nakagami et al., 2004).

Taken together, ROS acts as a crucial signal that is required in almost all biological processes, and ROS homeostasis is a rheostat that regulates the plant growth, development, and death underlying the complex molecular network. The different ROS threshold levels in plant cells may determine the cell status and fate.

**Roles of programmed cell death in regulating plant development**

Programmed cell death (PCD) acts as an essential and complex biological process in eukaryotes. It is originally introduced as a process activated by plant-pathogen defensive reactions in 1923 (Jones, 2001). Although the definition of PCD is proposed by plant scientists initially, in fact, achievements on the plant PCD studies are hysteretic as compared to that on animal PCD (Jones, 2001; Daneva et al., 2016). It has been a long journey for scientists to uncover the regulatory mechanisms of animal PCD too. In 1966, animal cell death was observed during the tadpole tail development, and it was firstly considered cell death as an actively controlled biological process (Tata, 1966). In 1972, Kerr et al. came up with the term "apoptosis", which has been known as the first kind of PCD morphotype, to describe a series of morphological features, such as cell shrinkage, nuclear pyknosis, membrane blebbing, and rapid elimination by phagocytosis (Kerr et al., 1972; Daneva et al., 2016). In 2002, the Nobel Prize in Physiology or Medicine was awarded to the scientists who studied the nematode *Caenorhabditis elegans* for their findings on the crucial roles of PCD on organ development (Putcha and Johnson, 2004). In the 1990s, the researches of plant PCD entered into a flourishing period (Beers, 1997), and many studies had been done to uncover the apoptosis in different types of plant PCD processes (Locato and De Gara, 2018). Although some hallmarks of apoptosis have been observed in several plant PCD processes, plant homologs of major regulators in animal apoptosis are rare (Daneva et al., 2016). This finding suggests that some differences exist between plant PCD and animal PCD, and there must be plant-specific regulators in the regulatory mechanism of PCD in the plant kingdom (Van Hautegem et al., 2015; Daneva et al., 2016).

More and more evidence show that the plant PCD is caused in multiple contexts and has a multitude of functions in regulating growth and development (Locato and De Gara, 2018). Up to date, many scientists are inclined to distinguish the plant PCD from a functional point of view. Based on this viewpoint, the plant PCD can be divided into environmentally induced PCD (ePCD) and developmentally regulated PCD (dPCD) (Huysmans et al., 2017). The ePCD is mainly induced by external stimuli, which include pathogen attack as well as abiotic stress (Wu et al., 2014; Petrov et al., 2015), and it is not highlighted in this study. However, dPCD is elicited by different internal signals or stimuli and is controlled precisely in a spatio-temporal manner. So far, dPCD has been observed and studied on various growth and developmental processes in plants, such as tracheary element differentiation, xylem formation, trichome formation, fertility regulation, and self-incompatibility response (Daneva et al., 2016; Locato and De Gara, 2018).

As an important regulatory pathway in plant growth and development, PCD is tightly controlled on the genetic aspect. Clusters of NAC, MYB, and bHLH transcription factors are mainly associated with the regulations of PCD process in different events. In xylem formation, NAC clade *VASCULAR-RELATED NAC-DOMAIN* (*VND*) genes play key roles in regulating PCD (Kubo et al., 2005; Endo et al., 2015; Tan et al., 2018; Yamaguchi et al., 2010a, 2010b). In root cap PCD, NAC transcription factor SMB/ANAC033 is identified as a master regulator (Fendrych et al., 2014). In addition, *ANAC087* and *ANAC046* have also been identified to regulate the root cap PCD (Huysmans et al., 2017). In plant organ senescence processes and age-induced PCD, such as leaf senescence and stigma cell death, NAC transcription factors ORESARA1 (ORE1), ANAC019, ANAC055, and KIRA1 are necessary (Kim et al., 2014; Shibuya, 2018; Gao et al., 2018). Alongside NAC transcription factors, MYB transcription factors also show crucial functions in plant PCD regulation. During tapetal cell death, *MYB* genes control the proper timing of tapetal PCD (Gu et al., 2014; Zhu et al., 2008; Cai et al., 2015). During pollen tube development, *MYB97*, *MYB101*, and *MYB120* show a regulatory function on pollen tube rupture (Leydon et al., 2013; Liang et al., 2013). Similar to NAC and MYB transcription factors, bHLH transcription factors also take part in regulating plant PCD. DISFUNCTIONAL TAPETUM1 (DYT1) is required in the tapetum and the development of microspores (Zhang et al., 2006). During embryo development, the endosperm-specific bHLH genes, *RETARDED GROWTH OF EMBRYO1* (*RGE1*)/*ZHOUPI* (*ZOU*) and *INDUCER OF CBP EXPRESSION1* (*ICE1*), are required and co-expressed in the endosperm. Lacking functions of these two genes can induce endosperm breakdown due to the abnormal endosperm PCD process (Kondou et al., 2008; Yang et al., 2008; Denay et al., 2014; Fourquin et al., 2016).

In addition to transcription factors, several proteases also participate in regulating PCD process in different plant tissues and organs. XYLEM CYSTEINE PROTEASE1 (XCP1) and XCP2 are two proteases that show functions in the cytoplasmic clearance of dying xylem vessels (Avci et al., 2008). METACASPASE9 (MC9) also takes part in the cytoplasmic clearing after tonoplast rupture (Escamez et al., 2016). In lateral root cap cell death, the expression patterns of several PCD-associated hydrolytic enzymes-encoding genes, including *RIBONUCLEASE3* (*RNS3*), *BIFUNCTIONAL NUCLEASE1* (*BFN1*), and *PUTATIVE ASPARTIC PROTEINASE3* (*PASPA3*), are upregulated, indicating that these enzymes may play some unknown roles (Olvera-Carrillo et al., 2015). Before this, a study has already shown PASPA3 and BFN1 are the downstream targets of *SMB/ANAC033*, which acts as the master regulator of root cap PCD (Fendrych et al., 2014). BFN1 is also the target of *ANAC046* and *ANAC087*, and its expression patterns are directly regulated by these two NAC transcription factors during root cap cell death (Huysmans et al., 2018). Moreover, BFN1 is thought of as a potential target of *ORE1* and *KIRA1* in papilla cell death (Gao et al., 2018). As a member of nuclease I enzymes, *BFN1* is induced during leaf and stem senescence in *Arabidopsis* (Pérez-Amador et al., 2000). By the further analysis of the expression profiles,

*BFN1* was found to be expressed in differentiating xylem and the abscission zone of flowers, suggesting that *BFN1* is a PCD-associated marker gene (Farage-Barhom et al., 2008). Apart from BFN1, a papain-like cysteine protease CYSTEINE ENDOPEPTIDASE1 (CEP1), which is indirectly regulated by *MYB80*, also takes part in the PCD process in tapetum (Zhang et al., 2014). In endosperm degradation, PASPA3 and BFN1 are possible targets of *RGE1/ZOU* (Fourquin et al., 2016).

In summary, PCD process is an indispensable event that keeps the plants growing normally in the natural environment. The roles of PCD are not only the necessary step for some organ or tissue formations but also the limitation that restricts the plant growth and development status.

**The knowledge gap in the regulation of stem cell longevity**

In recent years, the study on plant longevity is always a hot point. In this research field, several theories are coming up with, such as "source-sink," "death hormone," and "determinate or indeterminate apex" (Thomas, 2013). However, these viewpoints are still lacking conclusive evidence. For the research of plant apex, as early as 1994, Hensel et al. (1994) examined the arrest of inflorescences and designated this arrested process as GPA using WT *Arabidopsis thaliana* (Landsberg *erecta*, L*er*) line. However, a current study shows that the GPA is inapplicable in the WT *Arabidopsis thaliana* (at least Columbia accession, Col-0) line (Ware et al., 2020). In Col-0 *Arabidopsis*, the arrest of inflorescences between different branches is not synchronous, and this arrested process is a local process, which is driven by auxin export from fruit proximal (Ware et al., 2020). These findings suggest that it is difficult work that monitors the plant longevity from the whole-plant level, and auxin may be a kind of "death hormone". In genetic aspect, a recent study showed that inflorescence arrest is mediated by a FRUITFULL–APETALA2 regulatory module (Balanzà et al., 2018). Moreover, the *Arabidopsis AT-HOOK MOTIF NUCLEAR LOCALIZED 15 (AHL15)* gene, which acts as a suppressor of axillary meristem maturation, contributes to longevity in monocarpic *Arabidopsis* and tobacco (Karami et al., 2020). However, the findings mentioned above are either the description of the macroscopical phenomenon based whole-plant or not decisive evidence for the regulation of plant longevity.

As mentioned above, stem cell longevity maintains a key relationship with plant lifespan; therefore, uncovering the regulatory mechanism of stem cell longevity may be a good direction. Unfortunately, such kind of study is rare so far. In the past decades, lots of good jobs have largely revealed mechanisms of stem cell formation and stem cell activity maintenance (reviewed in the above part), whereas much remains unclear about the status of stem cells during the plant aging period. It is still blank in the mechanism of how plants control stem cell fate during the senescent period.

Herein, I observed that the gradual reduction of inflorescence meristem (IM) size and the dynamic vacuolation of stem cells began at one week after bolting (WAB). Moreover, the

expression of *WUS* was dynamically reduced until 3 WAB, and the upregulation of the programmed cell death marker *BFN1* was detected at 5 WAB and was associated with the death of stem cells. These results indicate that the stem cell population in the IM is decreased during plant aging. In addition, RNA-Seq and imaging analyses revealed that the reactive oxygen species (ROS) module was involved in the death of IM cells. I proposed that the aging of the IM in *Arabidopsis* consists of three phases. Besides, I also found that the levels of ROS components superoxide anion ($O_2^{\cdot-}$) and hydrogen peroxide ($H_2O_2$) displayed dynamic changes in the IM domain. By utilizing the different concentrations of exogenous $H_2O_2$, I found that the expressions of *WUS* and *ORE1* were inhibited and promoted, respectively. These results indicated that ROS played integrative roles in regulating stem cell final fate. Overall, the results of this study may help us to elucidate the regulatory mechanism governing plant longevity in *Arabidopsis*.

# Materials and methods

## Plant materials and growth conditions

*Arabidopsis thaliana* seed stocks used in this study were the Landsberg *erecta* (L*er*) background. The *clv3-2* mutant was described previously (Clark et al., 1995). The reporter lines *proWUS::GFP-ER*, *proCLV3::GFP-ER*, and *proWUS::GUS* were reported previously (Sun et al., 2019; Lenhard and Laux, 2003; Gordon et al., 2007; Rodriguez et al., 2016). *proBFN1::GUS-GFP* and *proORE1::GUS-GFP* in *clv3-2* background were generated by crossing with *clv3-2* mutant line. Homozygous *acx1-3* mutant (Columbia background) was from Arabidopsis Biological Resource Center (ABRC, Ohio, USA) with accession number CS66497. *Arabidopsis* seeds were sown in pots containing vermiculite and Metro-Mix and incubated at 4 °C in the dark for 3 days to promote germination. All plants were cultured in an illumination incubator (BiOTRON, LPH-411SP, Japan) under a 16-hour light (100 μmol $m^{-2}$ $s^{-1}$)/8-hour dark light cycle with 60% humidity and at 22 °C.

## Phenotypic definitions and measurements

To observe the development of each Arabidopsis plant precisely during aging, I applied "weeks after bolting" (WAB) as the temporal unit (Balanzà et al., 2018). When the stem length approached 1 cm, this time point was defined as the initiation of bolting (Noodén and Penney, 2001). For the counting of flower numbers on the primary stem, the siliques and flowers older than stage 7 were counted. The flower stage was referenced to the criterion described by Smyth et al. (1990). The measurement of IM size was estimated by measuring the IM circumference from a maximum diameter (Daum et al., 2014). The measurements of IM circumference and diameter were performed using FIJI (v1.50b, https://fiji.sc/) (Schindelin et al., 2012).The IM circumference were defined by the boundary between IM and the floral primordium. The cells with a large vacuole in the IM domain were judged by the area ratio between the vacuole (or vacuoles) and the whole cell. If the area ratio was over 40% in a cell (using FIJI to measure the size of the cell and vacuole), then the cell was considered to be a cell with a large vacuole. To ensure that the observed cells were stem cells, a total of 18 and 6 cells in the stem cell layers were observed in the WT and *clv3-2* mutant, respectively. In *clv3-2* mutant, only L1 cells were selected because other layers were disorganized. The ratio of cells with large vacuoles was the ratio between the number of cells with large vacuoles and total cells observed. The morphological observations of inflorescences on primary shoots were performed using an optical camera (Canon EOS 600D).

## Scanning electron microscope

Inflorescences of primary WT shoots were fixed in FAA solution overnight at room temperature and dehydrated with an ethanol and acetone series. Critical point drying with

liquid $CO_2$ and a gold coating were performed using EM CPD300 (Leica, Germany) and E-1010 (Hitachi, Japan), respectively. The inflorescences were observed using an S-4700 scanning electron microscope (SEM) (Hitachi, Japan) with an accelerating voltage of 15 kV.

**Transmission electron microscope**

For transmission electron microscopy (TEM) observation, inflorescences of primary shoots of Arabidopsis WT plants and *clv3-2* mutant plants were harvested at each time point (1-6 WABs). The methods of sample fixation and sectioning were described previously (Yamaguchi et al., 2018). Photographs were taken using an H-7100 TEM (Hitachi, Japan).

**GUS staining and tissue sectioning**

Inflorescences of primary shoots of reporter lines were fixed in 90% acetone for 15 min at room temperature, rinsed with double-distilled water, and subsequently stained with GUS staining solution. The staining method was described previously (Shirakawa et al., 2014). Tissue sectioning was performed as described previously (Yamaguchi et al., 2018). The slides were stained with 0.05% neutral red (Wako Chemicals, Japan) or 0.01% toluidine blue (Wako Chemicals, Japan).

**Confocal microscopy**

To observe the GFP signal in the longitudinal sections of the IMs on *proWUS::GFP-ER* primary shoots, the floral buds older than stage 7 were removed with tweezers under a light microscope, and then the IMs were embedded into 5% agar (Difco) and sliced with a Liner Slicer PRO7 vibratome (Dosaka, Japan) (Yamaguchi et al., 2018). The resulting tissue sections were immersed in moderate volumes of 1/10 Murashige and Skoog (MS) solution on glass slides. The GFP signal was immediately observed under an FV 1000 (Leica, Germany) microscope with FV10-ASW software. To detect the GFP signal in *proCLV3::GFP-ER*, the IMs on primary shoots were immersed in moderate volumes of 1/10 MS containing FM4-64 (Thermo Fisher, 5 μg/ml) on glass slides and covered with coverslips for 10 min. The images of the transverse orientation (XY axis) were taken with an inverted ZEISS LSM710 confocal laser-scanning microscope. The images of longitudinal orientation were reconstructed from Z-stack images along the XY axis by ZEN software. GFP was excited with the 488-nm Argon laser, and the emission was detected between 495 and 545 nm. FM4-64 was excited with the 561-nm laser and the emission was detected between 570 and 620 nm (Shi et al., 2018).

**RNA-seq**

The IMs (including floral buds up to stage 7) on primary shoots of WT at 2 and 4 WAB were collected as the RNA-seq samples. For each sample, at least 50 individual IMs were collected under microscopes using sterile forceps and freezed in liquid nitrogen

immediately. The RNeasy Plant Mini Kit (Qiagen, Germany) was used to extract total RNA from the four biological replicates. DNA was removed using the RNase-Free DNase Kit (Qiagen, Germany). The methods of library construction and sequencing were described previously (Uemura et al., 2018). Briefly, the mRNA was fragmented using magnesium ions at elevated temperatures, after which the polyA tails of mRNA were primed using an adapter-containing oligonucleotide for cDNA synthesis with DNA Polymerase I (Thermo Fisher Scientific). The 5′ adapter addition was performed using breath capture to generate strand specific libraries. The final PCR enrichment was performed using oligonucleotides containing the full adapter sequence with different indexes and Phusion High-Fidelity DNA Polymerase (New England Biolabs). The cleanup and size selection of the resulting cDNA was performed using AMPure XP beads (Beckman Coulter). The size distribution and concentration of the libraries were measured using agarose gel electrophoresis and a microplate photometer, respectively, to enable the pooling of libraries for Illumina sequencing systems. The libraries were sequenced by NextSeq 500 (Illumina). The produced bcl files were converted to fastq files by bcl2fastq (Illumina). Mapping to the Arabidopsis thaliana reference (TAIR10) was conducted using Bowtie with the following options "--all --best --strata --trim5 8." The number of reads mapped to each reference was counted. After normalization, the false-discovery rate (FDR) and fold change were calculated using the edgeR package for R. (Wu et al., 2019). The differentially expressed genes (DEGs) were isolated with a log2 fold change ≥ 1 or log2 fold change ≤ -1, and false discovery rate (FDR) < 0.05 (Wang et al., 2018). Gene Ontology (GO) term enrichment analysis of DEGs was carried out using Blast2GO (q-value ≤ 0.05). Kyoto Encyclopedia of Genes and Genomes (KEGG) pathway analysis was performed (q-value ≤0.05) using BlastX searches against the KEGG pathway database (Wang et al., 2018).

**Reverse-transcription PCR and quantitative RT-PCR**

The RNeasy Plant Mini Kit (Qiagen, Germany) was used to extract total RNA. The RNase-Free DNase Set (Qiagen, Germany) was used to eliminate the contamination of genomic DNA in RNA samples. Reverse-transcription PCR was performed using PrimeScript™ RT Master Mix (Takara, Japan). Quantitative RT-PCR was applied as described previously (Yamaguchi et al., 2018). *Arabidopsis ACTIN2* (*AT3G18780*) was used as the internal reference. Each experiment was repeated three times with four technical replicates. The relative expression level of each gene was calculated using the $2^{-\Delta\Delta CT}$ method (Livak and Schmittgen, 2001).

**Plasmid construction and plant transformation**

To generate the *proBFN1::GUS-GFP* construct, a genomic DNA fragment covering a sequence 2.0 kb upstream of the BFN1 translation start site was subcloned into the pENTR/D-TOPO vector according to the manufacturer's protocol (Thermo Fisher, Germany).

After confirmation by sequencing, the plasmid containing the fragment was employed in the LR reaction with the pBGWFS7 vector, which was a gateway vector containing GUS and GFP coding sequences, according to the manufacturer's protocol (Gateway™ LR Clonase™ II Enzyme mix, Thermo Fisher, Germany). The recombinant construct *proBFN1::GUS-GFP* was transformed into *Agrobacterium tumefaciens* strain GV3101 by using the freeze–thaw method. *proORE1::GUS-GFP* line (2.5 kb promoter) was generated using the same method mentioned above. The *Agrobacterium*-mediated floral dip method was performed to perform transgene analysis (Zhang et al., 2006). T1 seeds were collected and screened using the chemical Basta. More than 20 T1 plants were obtained, and the representative lines were chosen for further study.

**DAB and NBT staining**

The methods of DAB (3,3'-diaminobenzidine, Sigma-Aldrich) and NBT (4-Nitro blue tetrazolium chloride, Sigma-Aldrich) staining of IM were performed using methods described previously (Zeng et al., 2017). The chlorophyll in stained IM tissues was discolored in boiling ethanol (ethanol:glycerin:glacial acetic acid = 3:3:1). For each experiment, at least 5 individual inflorescences were stained.

**Fluorescein diacetate and propidium iodide staining**

Fluorescein diacetate (FDA) (Sigma) was dissolved in acetone to produce a 1 mg/ml stock solution. The working solution (20 μg/ml) of FDA was prepared by diluting 20 μl of the stock solution in 1 ml of 1/10 MS solution. 1 mg/ml stock solution of propidium iodide (PI) (Sigma) was prepared by dissolving 1 mg PI in 1 ml sterile water. 10 μg/ml working solution of PI was prepared by diluting 10 μl of the stock solution in 1 ml of 1/10 MS solution. IMs without any dissection were stained 20 min. Then, samples were put on glass slides and covered with coverslips. FDA was excited with the 488-nm laser line of the Argon laser, and the emission was detected between 495 and 545 nm, and PI was excited with a 561-nm diode laser and detected between 580 and 680 nm. (Gao et al., 2018). The images of the transverse orientation (XY axis) were taken with an inverted ZEISS LSM710 confocal laser-scanning microscope. The images of longitudinal orientation were reconstructed from the Z-stack images along the XY axis by the ZEN software.

**Exogenous hydrogen peroxide treatments**

For treatments in *proWUS::GUS* line, individual inflorescences were immersed in 5, 10, and 20mM hydrogen peroxide ($H_2O_2$, WAKENYAKU, Japan) liquid containing 0.01% Silwet L-77 for 10s. The 1WAB-old plants were treated until 2WAB. After the confirmation of the optimal concentration, individual inflorescences of *proWUS::GUS* line were immersed in 5mM $H_2O_2$ liquid to treat for 1, 2, 3, 4, 5, and 6 days to confirm the response speed of *WUS* expression. For treatments in *proORE1::GUS-GFP* and *proBFN1::GUS-GFP* lines,

individual inflorescences were immersed in 5, 20, 40, and 50 mM $H_2O_2$ liquid for 10 s. The 2 WAB-old plants were treated until 3 WAB. The gene expression signals were detected using GUS staining after treatments. For Mock treatments, double distilled water containing 0.01% Silwet L-77 was used. For each experiment, at least 5 individual inflorescences were treated.

**Data statistics and availability**

In this study, one-way ANOVA or Student's t-test (two-tailed, $p < 0.05$) was performed to detect differences as required. All primers used in this study are listed in Table 1. The RNA-seq data sets were submitted to the DNA Data Bank of Japan with the accession number DRA010789.

**Table 1** The primers used in this study

| Gene name | Forward (5'-3') | Reverse (5'-3') | Annotation |
|---|---|---|---|
| *proORE1* | CACCGAGCCAGAAAACGGTCTTTGGGTAA | TGCCTCGTAATCCATTTTATCCTA | Cloning of 2.5kb promoter |
| *proBFN1* | CACCGTTGGAAATTAAGTATTTACCTGC | ATCTTCAAAGTTTGAAACTTATATAATG | Cloning of 2.0kb promoter |
| *CAT1* | GATGATAAGCTACTCCAGACCC | TTGTTGTGGTGAGCACATTTAG | |
| *CAT3* | CTTGTGGTTCCTGGAATCTACT | AGGATCAAACTTTGAGGGGTAG | |
| *GPX6* | GGAATCAAGAGCCTGGTACTAA | TTTGTCACCGTTAACATCAACC | |
| *PRX51* | GGATTCGACACCGTCATTAAAG | TGAGTTGGTTGAGATCAAAGGT | |
| *PRX53* | AAACGCAACATTTTACTCTGGG | CAACAACGTTGAATCCTCTAGC | Gene validation by using Real time PCR |
| *PRX70* | AGGGACAGATTCTTCAACTACG | AGGTACGACGTATCAAATTGGT | |
| *ACX1* | GAGGATATGAAGATCGTCTGGG | TCATTGAGACGAAGCTCGATAA | |
| *DOX2* | TATCGACGGAGAAGATAGACCT | TCATCATCTGTCAACTCTTCCC | |
| *CLV3* | GTTCAAGGACTTTCCAACCGCAAGATGAT | CCTTCTCTGCTTCTCCATTTGCTCCAACC | |
| *ACTIN2* | GAAAAGATCTGGCATCACACTTTATA | ACATACATAGCGGGAGAGTTAAAGGT | Inner reference |

## Chapter I Morphological and physiological framework underlying plant longevity in *Arabidopsis thaliana*

### Results

#### Growth and termination of the primary inflorescence

In my growth conditions, the WT Landsberg *erecta* (L*er*) plants were bolted 35 days after germination, and they reached the maximum height at 3 weeks after bolting (WAB) (Figure 6A). After 3 WAB, multiple siliques were produced, and aging began with the change in plant color from green to brown (Figures 6A and B). At 4 WAB, the aging of plants progressed, resulting in that some siliques started to turn yellow. At 5 and 6 WAB, mature siliques were dehisced, and plants dispersed seeds (Figure 6B). During the whole life cycle of plants, the sum of the number of both flowers and siliques increased continuously until 4 WAB (Figure 6C).

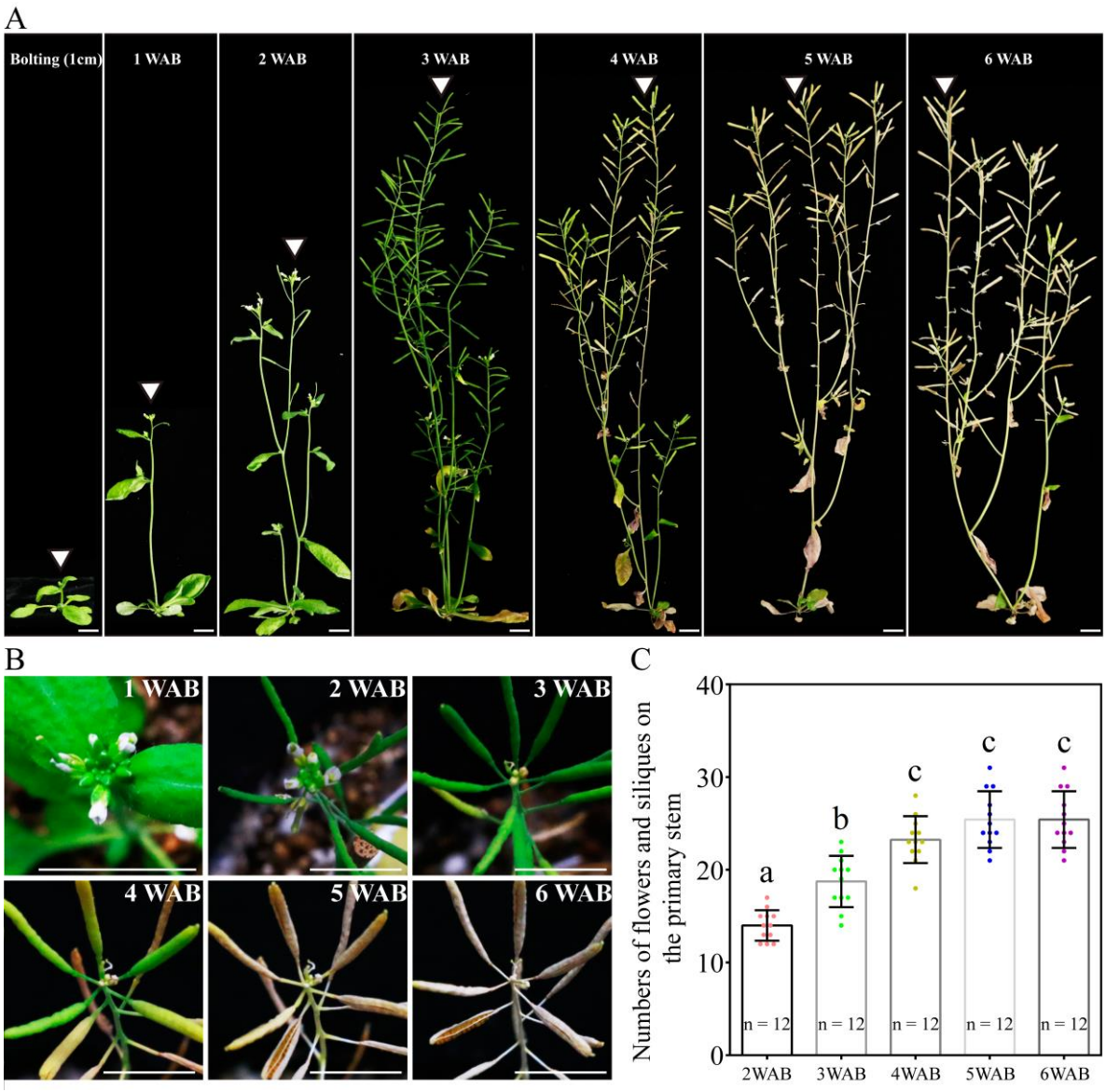


**Figure 6** Growth and termination of the primary inflorescence of *Arabidopsis thaliana*, Landsberg *erecta*. (A) Photographs of plant morphologies at the bolting time point (the stem length was reached at 1 cm) and from 1 week after bolting (WAB) to 6 WAB. White triangles mark the primary inflorescence at each time point. Scale bars = 1 cm. (B) Serial top views of the primary inflorescences at 1-6 WABs. Twelve individual plants were observed, and representative images are shown. Scale bars = 1 cm. (C) The quantification of numbers of flowers and siliques on primary stems of 12 individual plants. The flowers beyond floral stage 7 were counted. Dots represent numbers of flowers and siliques from each sample. Error bars represent SD. One-way ANOVA followed by the Tukey-Kramer test was performed ($p < 0.01$). Different letters indicate significant differences, while the same letters indicate no significant differences.

**The gradual decrease in the size of the inflorescent meristem (IM)**

I hypothesized that IM activity was limited and lost at the end of the plant life cycle because the total number of flowers and siliques was controlled (Figure 6). To examine whether IM size is reduced during aging, I measured IM sizes by using scanning electron microscopy (SEM) from 1 WAB to 6 WAB (Daum et al., 2014) (Figures 7A and B). IM sizes were notably reduced from 1 WAB until 6 WAB, and IM sizes at 5 and 6 WAB were minimal (Figure 7B). Consistent with these results, the maximum width of IM in cross-sections was also notably reduced until 5 WAB, and the IM width at 5 and 6 WAB was minimal (Figure 7C and D). At 4 WAB, the total number of flowers and siliques reached a maximum number (Figure 6C). Taken together, these results suggested that IM activity before 4 WAB is required for the production of seeds. These results suggested that the IM gradually shrinks during the aging of plants.

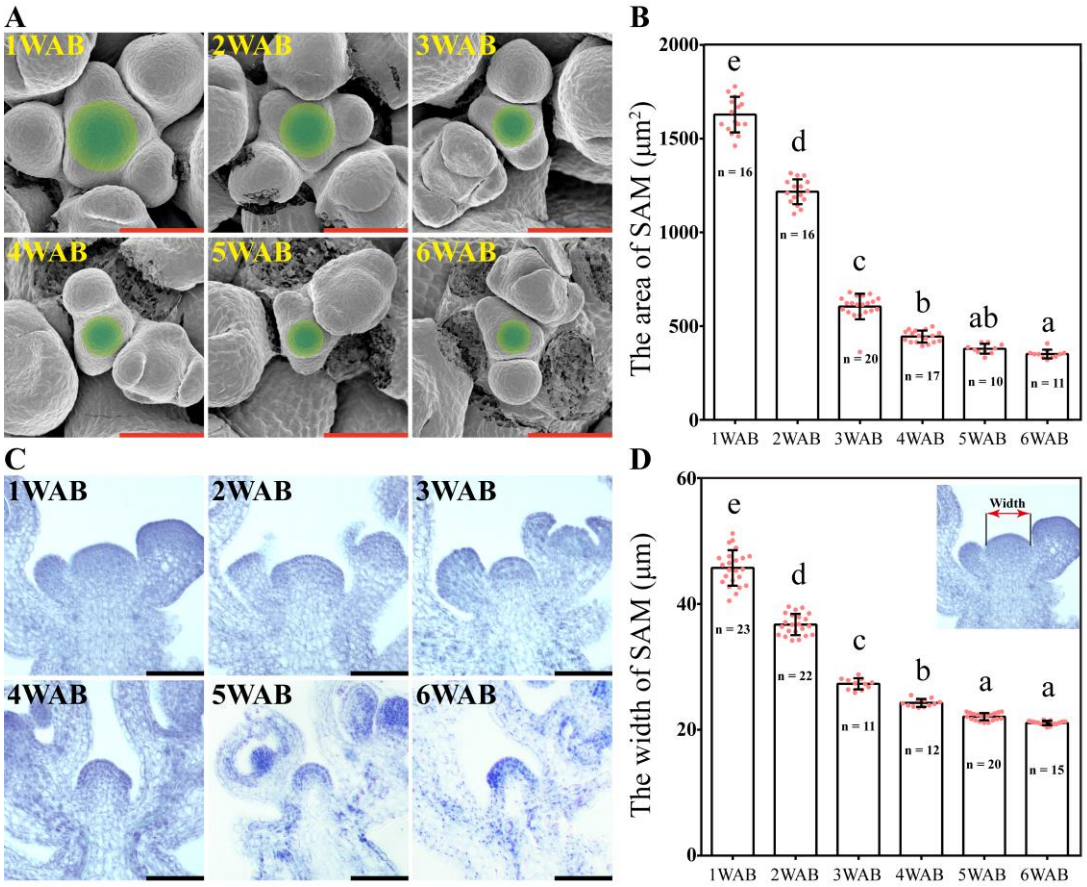


**Figure 7** Size of the inflorescent meristem gradually decreased. (A) The top views of inflorescent meristem (IM) domains of WT from 1 WAB to 6 WAB. Scanning electron microscopy (SEM) was used. Green circles indicate IM domains (including central zones and peripheral zones) (Daum et al., 2014). Scale bars = 40 μm. (B) The area of IM domains of WT from 1 WAB to 6 WAB. The number (n) of observed samples at each time point is shown. Dots represent the area of IM from each sample. Error bars indicate SD. One-way ANOVA followed by the Tukey-Kramer test was performed ($p < 0.01$). Different letters indicate significant differences, while the same letters indicate no significant differences. (C) Longitudinal views of IMs of WT from 1 WAB to 6 WAB by using histologic sections. Scale bars = 40 μm. (D) The width of IM domains of WT from 1 WAB to 6 WAB. The image at the top right corner indicates the definition of the SAM width (Daum et al., 2014). The number (n) of observed samples at each time point is shown. Dots represent the width of IM from each sample. Error bars indicate SD. One-way ANOVA followed by the Tukey-Kramer test was performed ($p < 0.01$). Different letters indicate significant differences, while the same letters indicate no significant differences.

**The dynamic transition of intracellular structures of stem cells in L1 and L2 of IM**

At 4 WAB, the IM size was almost minimal (Figure 7). Next, I analyzed the transition of the ultrastructure of cells in both L1 and L2 (L1/2) of IM by using transmission electron microscopy (TEM). At 2 WAB, all cells in L1/2 were filled with electron-dense materials (dark gray color), and intracellular spaces were occupied primarily by a large nucleus and cytoplasm (Figure 8A and B left). Combined with the expression data of stem cell markers (described below), these cells have high proliferative potential. At 3 WAB, some of the cells in L1/2 had large vacuoles whose sizes were nearly equal to the sizes of the nuclei (Figure 8A and B right). After 3 WAB, the numbers of cells with large vacuoles increased until 6 WAB (Figure 8A and C). Almost all cells in the IM had a central large vacuole at 6 WAB. Large vacuoles are one of the indicators of differentiated cells. Combined with the results regarding plant growth (Figure 6) and IM size (Figure 7), these results suggested that even stem cells in the IM were getting differentiated.

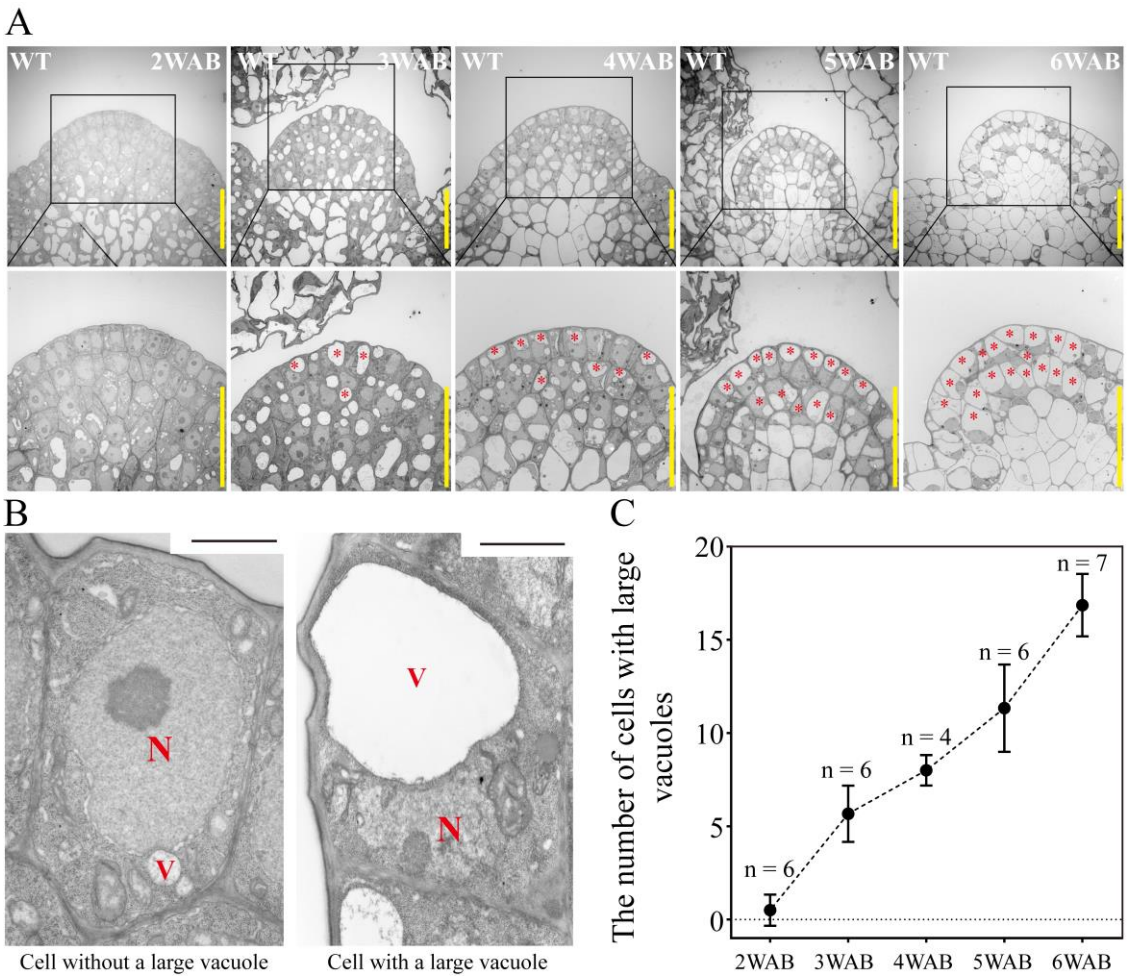


**Figure 8** Dynamic transition of intracellular structures of stem cells in L1 and L2 of IM. (A) The intracellular ultrastructures of stem cells in L1 and L2 of IM of WT from 2 WAB to 6 WAB by using transmission electron microscopy (TEM). Images in the lower panels indicate the magnified images of the black box area in the upper panels. Red stars indicate cells with large vacuoles that occupied over 40% of the cell size. Scale bars = 20 μm. (B) Representative images of cells without or with a large vacuole in IM. N: nucleus. V: vacuole. Scale bars = 1.5 μm. (C) The number of cells with large vacuoles in IM of WT from 2 WAB to 6 WAB. The number of samples at each time point is shown. Error bars indicate SD.

**Expression patterns of stem cell markers in the IM domain during aging**

How do plants lose the proliferative activity of IM at approximately 4 WAB? To examine how the morphological changes and stem cell marker gene expression levels during aging were coordinated, I examined the dynamic expression patterns of two stem cell marker genes, *WUS* and *CLV3*, during the aging of the IM (Figure 9 and Figure 10). *CLV3* was expressed at cells in L1 and L2 (L1/2) of the central zone (CZ) of the IM, and *WUS* was expressed at the organizing center (OC), which is located below the CZ (Schoof et al., 2000; Brand et al., 2000) (Figure 9). The expression level of *WUS* at 1 WAB was highest and then gradually decreased during aging until 3 WAB. No expression signal was detected at 3 WAB in either the GFP reporter or the GUS reporter (Figure 9A and B). After 3 WAB, *WUS* expression was not reactivated (Figure 9B). Combined with the morphological data, these results suggested that IM cells began to lose stem cell/proliferative activity after 1 WAB because they began to reduce the expression levels of *WUS*. This hypothesis is consistent with the results demonstrating that the IM size at 3 WAB was less than 50% of the IM size at 1 WAB (Figure 7B) and that some IM cells at 3 WAB had large vacuoles (Figure 8). Compared with *WUS*, the expression of *CLV3* maintained longer to 4 WAB, and no expression signal was detected at 5 WAB in the GFP reporter (Figure 10). These results suggested that the expression period of *CLV3* was two weeks longer than that of *WUS*. A similar observation was reported by using *proCLV3::GUS* lines (Balanzà et al., 2018). These results suggested that *CLV3* might play an additional role in the regulation of plant longevity (described below).

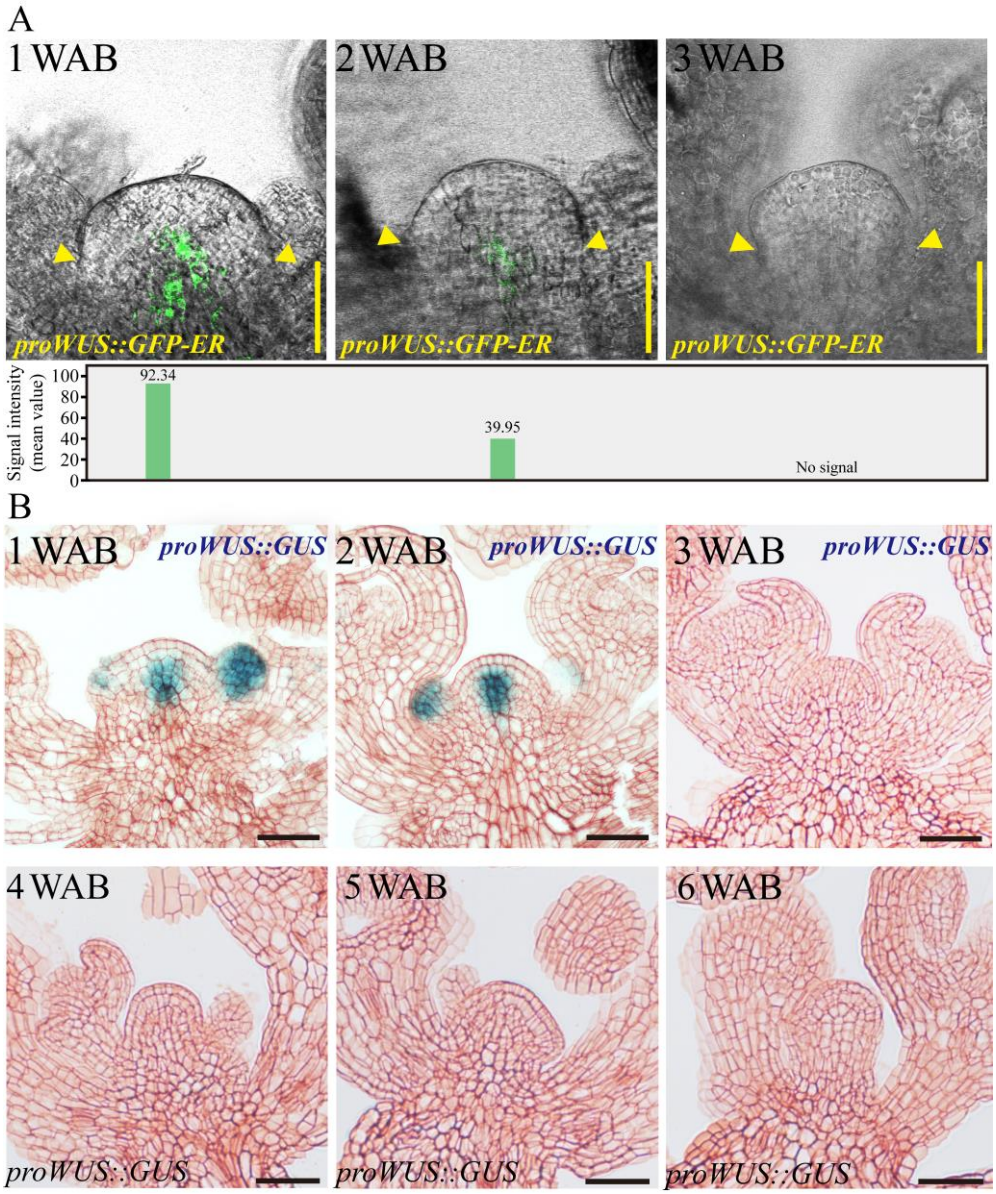


**Figure 9** Expression patterns of *WUS* in the IM domain during aging. (A) The spatiotemporal expression patterns of *WUS* from 1 WAB to 3 WAB. The *proWUS::GFP-ER* line were used. The GFP signal intensity was quantified and is shown in the lower panel and yellow triangles denoted boundaries of SAMs. n = 5. (B) The spatiotemporal expression patterns of *WUS* from 1 WAB to 6 WAB. *proWUS::GUS* line were used. Scale bars = 25 μm in (A) and (B).

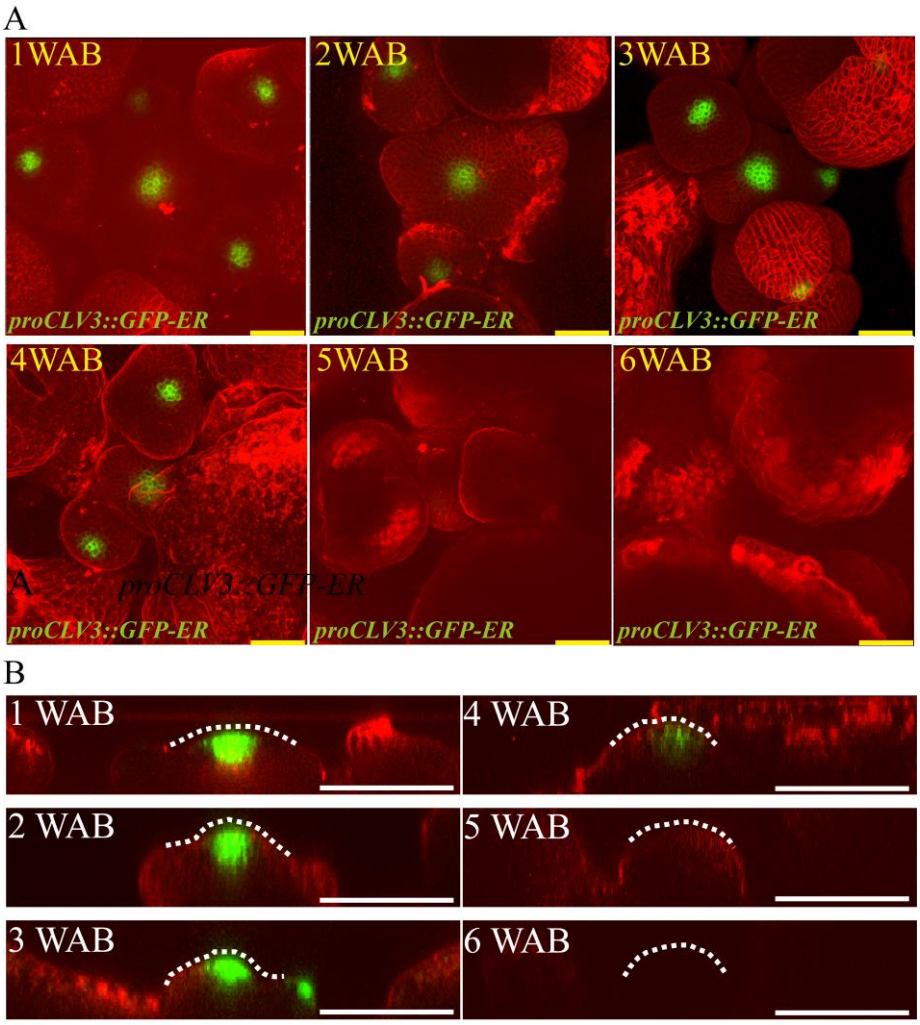


**Figure 10** The spatiotemporal expression patterns of *CLAVATA3* (*CLV3*). The *proCLV3::GFP-ER* line was used. The top view of confocal images is shown in (A), and the side view is shown in (B). To visualize the outline of cells, I stained IM with FM4-64 dye (red). White dotted lines indicate SAM shapes. Scale bars = 25 μm in (A) and 50 μm in (B).

**ROS are involved in the death of stem cells in the IM**

I hypothesized that the dynamic changes of gene expressions might occur between 2 WAB and 4 WAB because the size of IMs was reduced dynamically, the intracellular vacuolations were progressed, and the expression of *WUS* was lost during these two weeks. To clarify the transcriptional dynamics of plant aging, I compared RNA sequencing (RNA-seq) profiles of four independent IMs samples between 2 WAB and 4 WAB. I isolated 547 differentially expressed genes (DEGs), including 492 upregulated DEGs and 55 downregulated DEGs (Figure 11). To understand the putative functions of these DEGs, I performed GO term enrichment and KEGG pathway analysis. Notably, I found that some DEGs were specifically clustered into ROS-related GO terms and KEGG pathways. Five DEGs were clustered into "Catalase activity" (GO: 0004096), seven DEGs were gathered into "Oxidoreductase activity acting on peroxide as acceptor" (GO: 0004601), and 25 DEGs were enriched into "Antioxidant activity" (GO: 0022857) (Figure 12A). Based on the results of KEGG pathway analysis, we found six DEGs involved in the KEGG pathway "Peroxisome" (ko04146) (Figure 12B). By removing the redundant DEGs, I obtained eight ROS-related DEGs (Table 2). By qPCR analysis, I confirmed that all eight DEGs were significantly upregulated at 4 WAB compared with those at 2 WAB (Figure 14). These results were highly consistent with the RNA-seq data (Table 2) that ROS-related genes are upregulated during the aging of IMs. In addition, in keeping with the results of the *proCLV3::GFP-ER* reporter lines, my qPCR analysis indicated a significant reduction in the expression levels of *CLV3* (Figure 14).

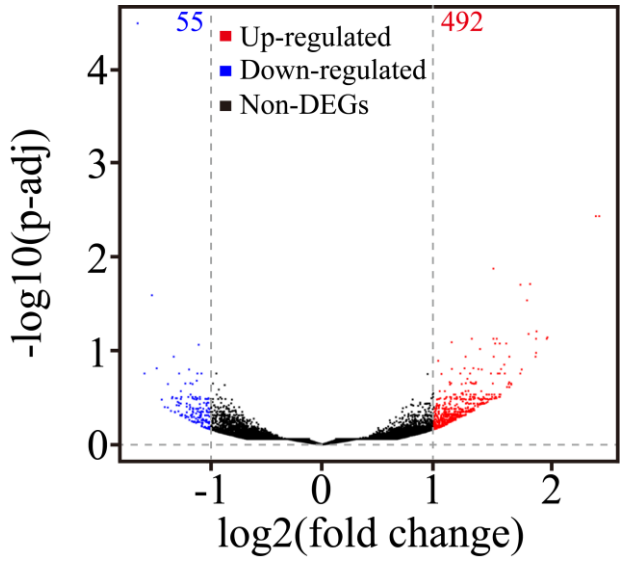


**Figure 11** Volcano plot of DEGs isolated from RNA-seq data sets. The numbers of up- and downregulated DEGs are indicated.

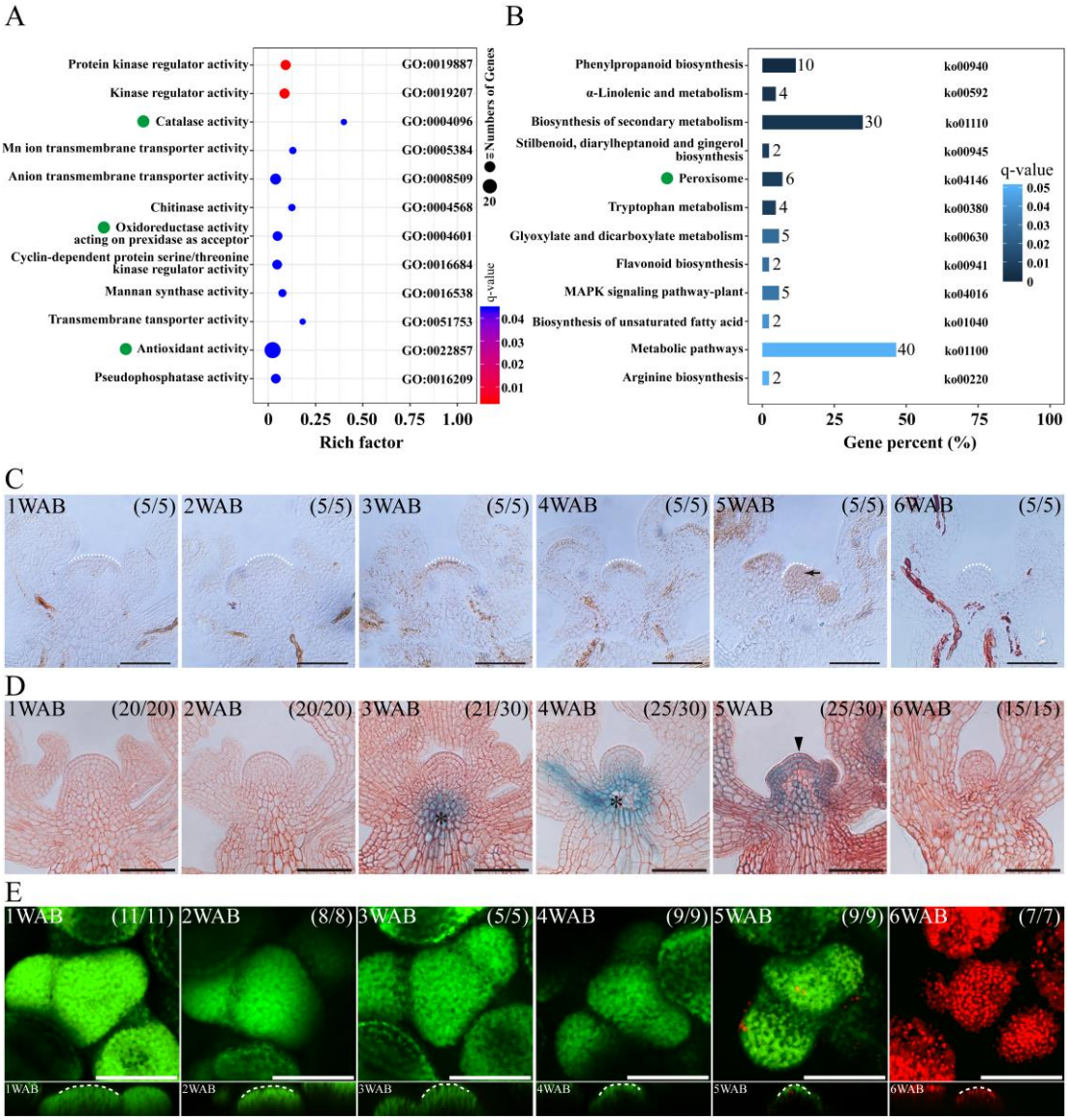


**Figure 12** $H_2O_2$ is involved in the death of stem cells in IM. (A-B) Omics analyses of differentially expressed genes (DEGs) of IMs between 2 WAB and 4 WAB. RNA-Seq was performed with four biological replicates of each sample. In both analyses, ROS-related genes were enriched. (A) GO term enrichment of the DEGs of IMs between 2 WAB and 4 WAB. Green dots indicate ROS-related GO terms (Catalase activity, Oxidoreductase activity, and Antioxidant activity). (B) KEGG pathway analysis of the DEGs. Green dots denote ROS-related pathways (Peroxisome). (C) DAB staining of IM from 1 WAB to 6 WAB. White dotted lines indicate IM shape. The black arrow indicates the accumulation of the $H_2O_2$ signal in IM. Scale bars = 50 μm. (D) The spatial-temporal expression patterns of a PCD marker gene, *BFN1*, in IM from 1 WAB to 6 WAB. Scale bars =50 μm. The black arrowhead indicates the GUS signal in stem cells in the central zones and peripheral cells. Black asterisks indicate GUS outside IM (vascular tissues). (E) FDA/PI staining of IM from 1 WAB to 6 WAB. The top view of confocal images of FDA (green) and PI (red) signals is shown in the upper panel. The side view is shown in the lower panel. FDA-stained cells (in green) are alive, and PI-stained cells (in red) are dead. White dotted lines indicate SAM shapes. Scale bars = 50 μm.

**Table 2** The information of ROS homeostasis related DGEs

| Gene ID | Gene Name | $Log_2FC$ | Expression pattern | Adjusted *p*-value | GO term or KEGG pathway | Annotation |
|---|---|---|---|---|---|---|
| AT1G20620 | *CAT3* | 1.10 | Up | 4.82E-02 | GO:0004096 | catalase 3 |
| AT1G20630 | *CAT1* | 1.25 | Up | 3.14E-02 | GO:0004096 | catalase 1 |
| AT1G73680 | *DOX2* | 1.39 | Up | 2.65E-02 | GO:0004601 | alpha dioxygenase |
| AT4G11600 | *GPX6* | 1.32 | Up | 1.58E-02 | GO:0004601 | glutathione peroxidase 6 |
| AT4G16760 | *ACX1* | 1.45 | Up | 6.45E-03 | GO:0022857 | acyl-CoA oxidase 1 |
| AT4G37530 | *PRX51* | 3.99 | Up | 1.87E-02 | ko04146 | peroxidase superfamily protein |
| AT5G06720 | *PRX53* | 7.16 | Up | 3.53E-02 | ko04146 | peroxidase 2 |
| AT5G64110 | *PRX70* | 1.89 | Up | 2.41E-02 | ko04146 | peroxidase superfamily protein |

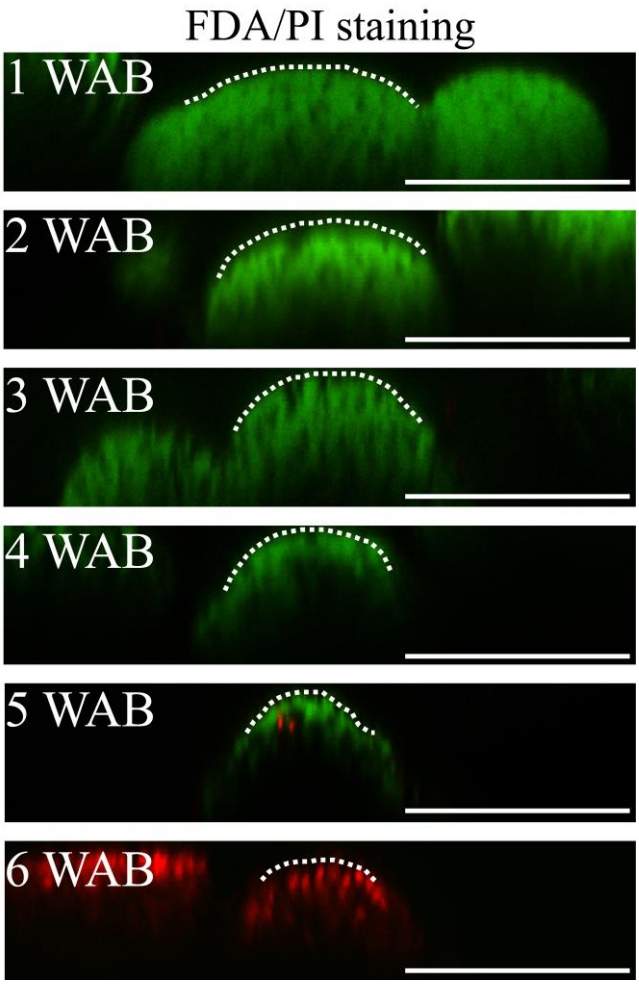


**Figure 13** Magnified images of side views of FDA/PI stained IMs. White dotted lines indicate SAM shapes. Scale bar = 50.

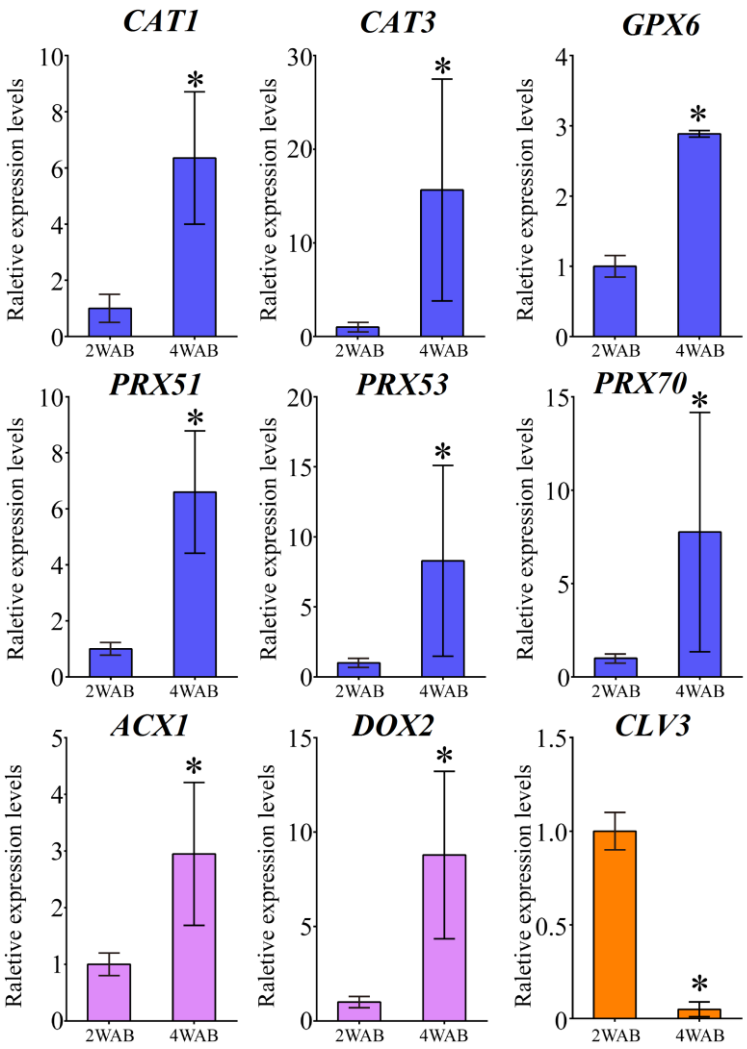


**Figure 14** Validation of ROS-related DEGs and stem cell marker gene *CLV3* in WT plants at 2 WAB and 4 WAB. Blue and pink colors indicate ROS clearance- and ROS production-related DEGs, respectively. Orange color shows the expression of *CLV3*. Error bars denote SD. Two-tailed Student's t-test was performed. *: $p < 0.05$.

It has been reported that ROS regulates programmed cell death (PCD) in both plants and animals. Therefore, I hypothesized that ROS-mediated PCD occurred after IM maturation at 4 WAB. To elucidate the spatiotemporal accumulation pattern of the ROS hydrogen peroxide ($H_2O_2$), I performed DAB staining in cross-sections of IM from 1 WAB to 6 WAB. I observed pronounced accumulation of hydrogen peroxide in the IM region at 5 WAB when IM cells were fully matured with a large vacuole (Figure 12C). Next, I examined the expression of a PCD marker gene, *BIFUNCTIONAL NUCLEASE 1* (*BFN1*), which mediates the degradation of nucleic acids (Figure 12D). In the stem cells, I found a notable expression peak of *BFN1* at 5 WAB, while vasculature expression started earlier at 3 WAB (Figure 12D). These results suggested that ROS and *BFN1* were involved in PCD of the stem cells. Next, I observed cell death in the IM region by using FDA/PI staining. At 5 WAB, some cells were dead and thus were stained by PI in the IM region; however, the majority of cells were alive (Figures 12E and Figure 13). In contrast, at 6 WAB, all cells were dead (Figures 12E and Figure 13). These results suggested that PCD in IM cells was initiated at 5 WAB and was completed before 6 WAB.

# Discussion

**Phase transition of stem cells of IM during aging in *Arabidopsis thaliana***

In this study, by using the *Arabidopsis* L*er* accession, I determined the morphological changes (Figures 6 and 7), intracellular ultrastructures (Figure 8), and changes in gene expression (Figures 9 and 12) of the IM during aging. From these results, I proposed three different phases in the aging of Arabidopsis, which are summarized in Figure 15. In the first phase (green in Figure 15; 1 WAB to 3 WAB), along with the reduction in *WUS* expression in the CZ of the IM (green line), the stem cell activity (blue line) and size of the IM domain (gray line) gradually decrease. At 3 WAB, the *WUS* promoter activity is fully terminated at the IM domain.

In the second phase (light green in Figure 15; 3 WAB to 4 WAB), the transition of the intracellular ultrastructure of IM cells progresses continuously, resulting in an increase in the number of cells with large vacuoles. These cells may be ready to be killed by PCD. At the same time, the expression level of *CLV3* (red line) remains high. Since CLV3 has a role in inhibiting *WUS* expression, CLV3 may function as a component of the putative safeguard system to prevent the re-activation of *WUS*. It would be interesting to determine which factor(s) promote *CLV3* expression after the loss of *WUS* at 3 WAB expression because WUS is a known critical activator for *CLV3*. Unknown transcriptional factor(s) may maintain the expression of *CLV3* after 3 WAB. However, I could not exclude the possibility that WUS proteins still exist until 4 WAB and promote the expression of *CLV3* directly. To investigate this possibility, confocal microscopy with ultrahigh sensitivity is needed because the WUS protein is unstable.

At the third phase (yellow in Figure 15; 4 WAB to 6 WAB), ROS accumulation (brown line) and the expression of the programmed cell death indicator *BFN1* (black line) were observed in IM at the middle of phase 3, that is, 5 WAB. ROS accumulation and *BFN1* expression may promote the death of cells with large vacuoles in the IM because almost all cells in the IM are stained by PI at 6 WAB. These phases may be useful to future research attempting to identify mutants with defects in the progression of aging.

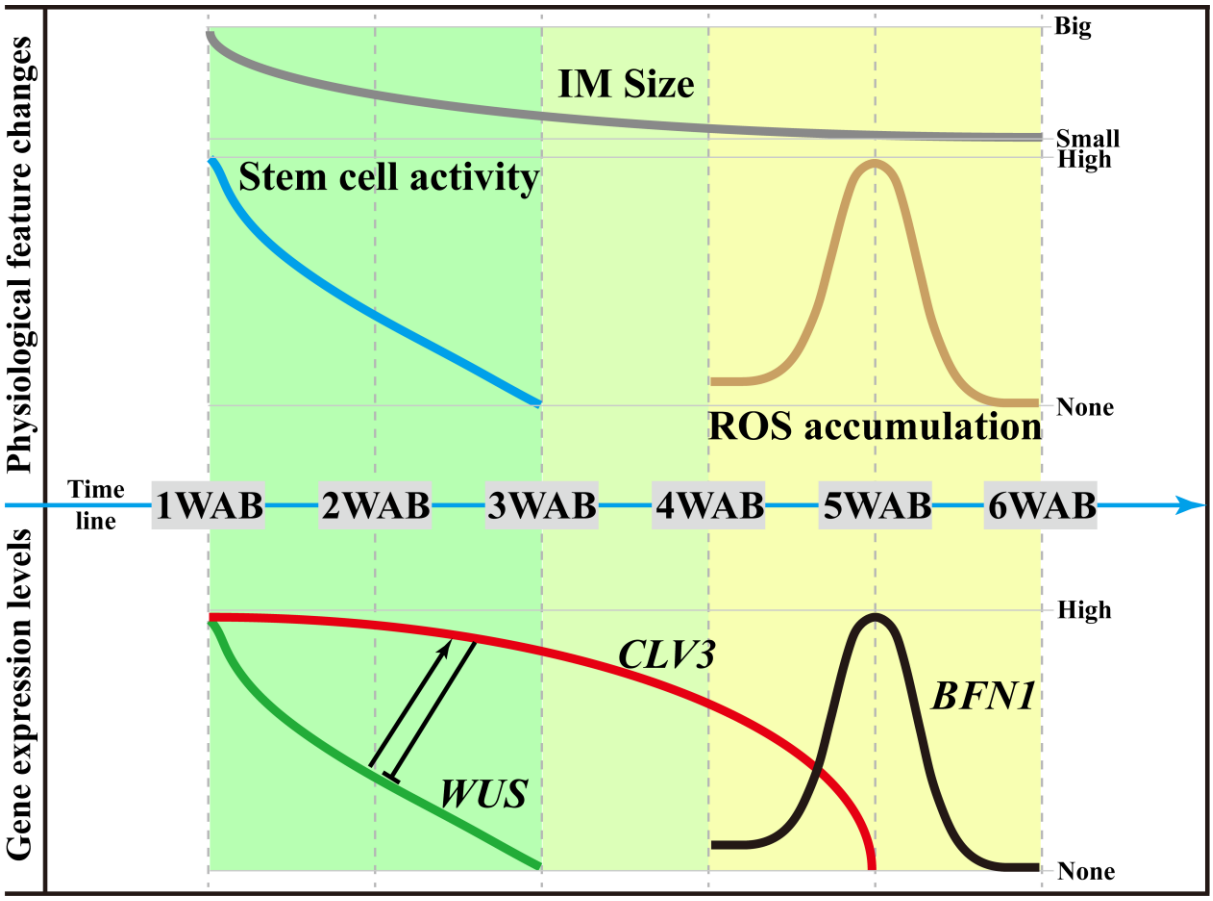


**Figure 15** Regulatory framework of the IM lifespan. Based on this study, I defined three phases of the IM lifespan. In the first phase (from 1 WAB to 3 WAB), along with the reduction in *WUS* expression in the CZ of the IM, the stem cell activity and size of the IM domain gradually decreased. At 3 WAB, *WUS* promoter activity is fully terminated. Next, from 3 WAB to 4 WAB (second phase), the transition of the intracellular ultrastructure of IM cells progresses, resulting in an increase in the number of cells with a large vacuole. These cells may be ready to be killed by PCD. At the same time, however, the expression level of *CLV3* is still maintained because *CLV3* may have a role in inhibiting the reactivation of *WUS*. In the third phase (from 4 WAB to 6 WAB), ROS accumulation and the expression of the programmed cell death indicator *BFN1* were observed in IM at 5 WAB. They may promote the death of cells with a large vacuole in IM, and almost all cells in IM are stained by PI at 6 WAB.

**In *Arabidopsis*, the final fate of stem cells in the IM may be PCD**

It is well-known that senescent cells often exhibit large vacuoles (Rhinn et al., 2019), that cell vacuolization means terminal differentiation, and that such cells have lost their proliferative and differentiated abilities (Shubin et al., 2016). Moreover, the vacuole is an executor of PCD (Hara-Nishimura and Hatsugai, 2011). In this study, I found that the number of stem cells with large vacuoles increased during the lifespan (Figure 8). In addition, I detected the expression peak of a PCD marker gene, *BFN1*, at 5 WAB (Figure 12D), and I observed and PI signals in stem cells in whole IM (including layers 1 and 2) at 6 WAB (Figure 12E). These results indicate that the final fate of stem cells is age-induced dPCD. In plants, age-induced dPCD is thought to trigger plant death and occur in various types of cells and organs for the remobilization of nutrients and secondary metabolites to the developing seeds (Rogers, 2013; Koyama, 2014; Daneva et al., 2016), but no direct evidence has shown that age-induced dPCD occurs in the stem cells of the IM. My data indicated that the last step of stem cell fate is dPCD, which is associated with vacuolation and *BFN1* induction. Future research employing mutants may serve to elucidate in detail the mechanisms of dPCD in the IM.

**$H_2O_2$ may be a molecular switch of stem cell death**

It has been reported that ROS levels are associated with dPCD (Daneva et al., 2016; Mhamdi and Van Breusegem, 2018). For instance, $H_2O_2$ accumulation triggers dPCD in the tapetal cells of rice (Yi et al., 2016). Similarly, the $H_2O_2$ burst was detected in the IM domain at 5 WAB (Figure 12C, and D). At 5 WAB, cell death was detected (Figure 12E). These results suggest that the dPCD process in the IM may be triggered by $H_2O_2$. Based on RNA-Seq results and the GO and KEGG enrichment analyses performed in this study, I also isolated a cluster of DEGs, such as peroxiredoxins (*PRXs*) and catalase 3 (*CAT3*), involved in ROS homeostasis (Figures 12A, B and Figure 14), suggesting that these genes might be involved in the dPCD of stem cells in the IM. However, more detailed work, including the analysis of mutants of these factors, is required. Taken together, the findings of previous studies (Mittler et al., 2004; Van Breusegem and Dat, 2006; Zeng et al., 2017) and this study indicate that $H_2O_2$ accumulation in stem cells may be a molecular switch of dPCD in stem cells.

## Chapter II Dynamic changes of reactive oxygen species in shoot apex is associated to stem cell death in *Arabidopsis thaliana*

### Results

#### *clv3-2* mutant exhibited a longer longevity phenotype than wild type

It is reported that *clv3-2* mutants produce an increased number of flowers (Clark et al., 1995), and the leaf longevity in *clv3-2* plants is 20-30 days longer than that in WT plants in short days- and long days- combined culture conditions (Nooden and Penney, 2001). However, the molecular basis of stem cell longevity underlying the lifespan of *clv3-2* remains unknown. In order to gain more information on the regulation of stem cell longevity, I examined the plant morphology and the longevity of *clv3-2* mutants until 12 WAB. As previously reported, *clv3-2* plants exhibited enlarged meristematic tissues, resulting in increased numbers of flowers and fruits (Figure 16). In addition to these phenotypes, *clv3-2* mutants lived up to 6 weeks longer than WT plants after bolting (Figure 16A). At 4 WAB, when some siliques started to turn yellow in WT plants, all siliques of *clv3-2* mutants kept the green color. At 5 WAB, when some mature siliques were opened in WT plants, some siliques of *clv3-2* mutants started to turn yellow. At 6 WAB, when whole WT inflorescences were dead, *clv3-2* mutants were still alive and exhibited green-colored IM. From 7 WAB to 11 WAB, brown regions were expanded in siliques and IM of *clv3-2* mutants. At 12 WAB, whole *clv3-2* mutant inflorescences were dead. Consistent with this finding, the expression window of *WUS* was also extended for 3 weeks longer than that of the WT (Figure 17). In addition, *clv3-2* mutants exhibited an increase in differentiated IM cells with large vacuoles until 10 WAB compared with those observed at 5 WAB (Figures 18 and 19). These results suggested that *clv3-2* plants possessed a longer longevity phenotype, and CLV3 may be a safeguard that inhibits the longer expression window of *WUS* at 3-5 WAB by shutting down *WUS* expression at the correct time.

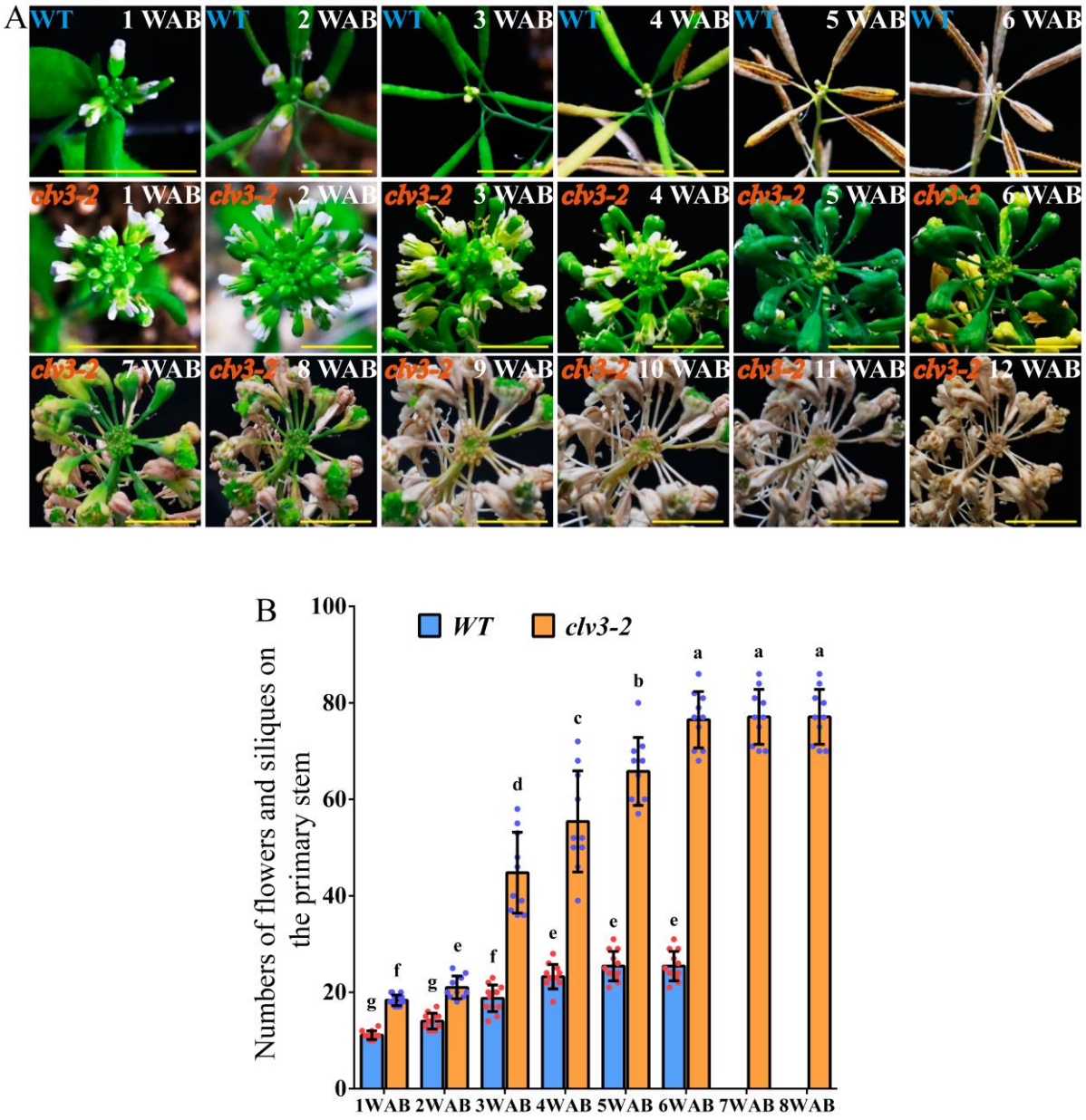


**Figure 16** *clv3-2* mutant showed a prolonged lifespan of IM. (A) Morphological changes in WT and *clv3-2* inflorescences. Scale bars = 1 cm. (B) The statistics of main shoot flowers and siliques numbers in WT and *clv3-2* mutant. One-way ANOVA post Tukey HSD test ($p < 0.05$) was carried out to calculate the differences among different groups. Over 10 individual seedlings of WT and *clv3-2* were observed. Different letters indicate significant differences, while the same letters indicate no significant differences.

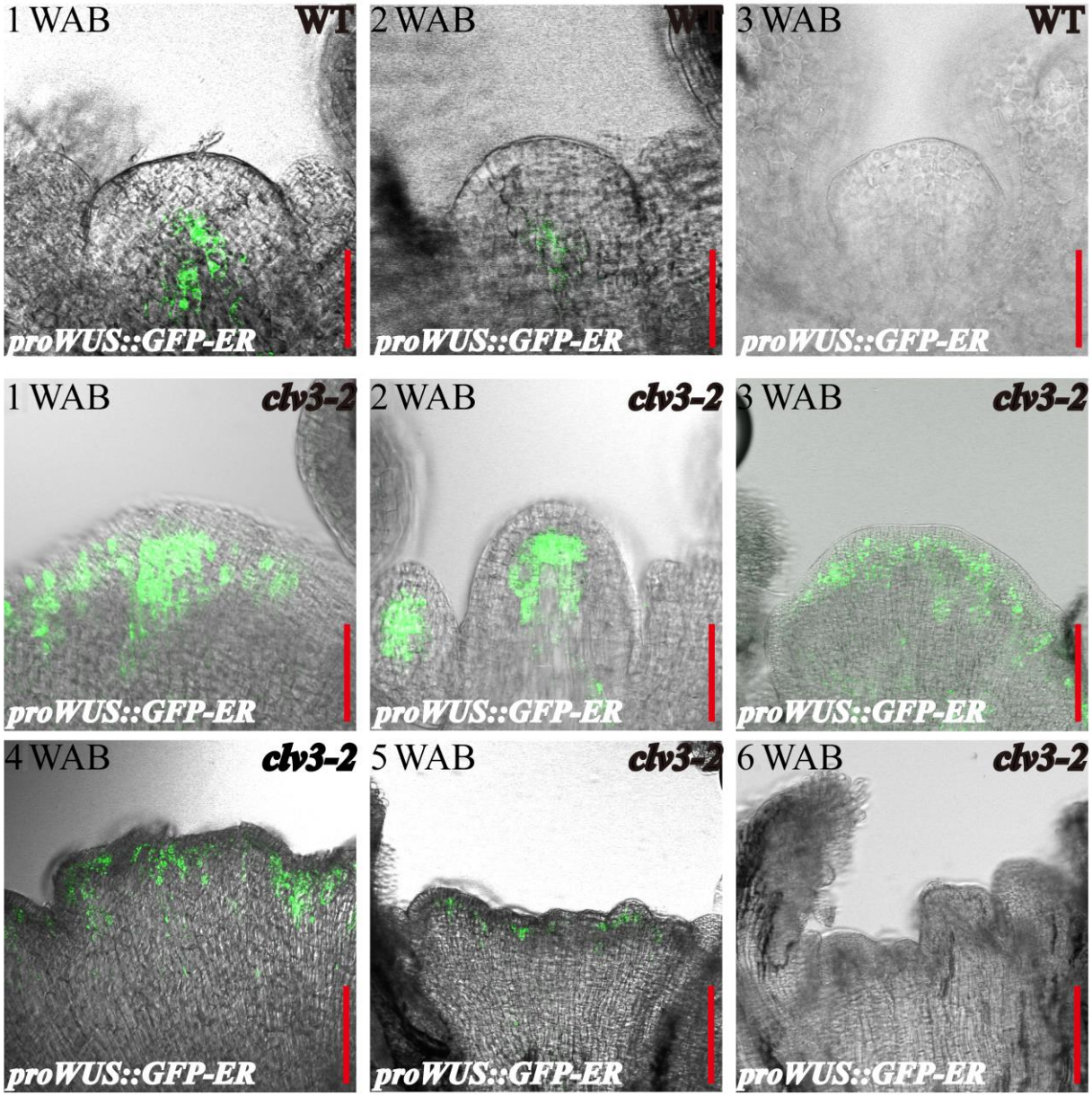


**Figure 17** Spatial-temporal expression patterns of *WUS* in IMs of WT and *clv3-2* mutants. The *proWUS::GFP-ER* reporter line (in WT and *clv3-2* mutant background) was used. Scale bars: 25 μm in WT and 100 μm in *clv3-2* mutant. At least five individual IMs were used for each experiment.

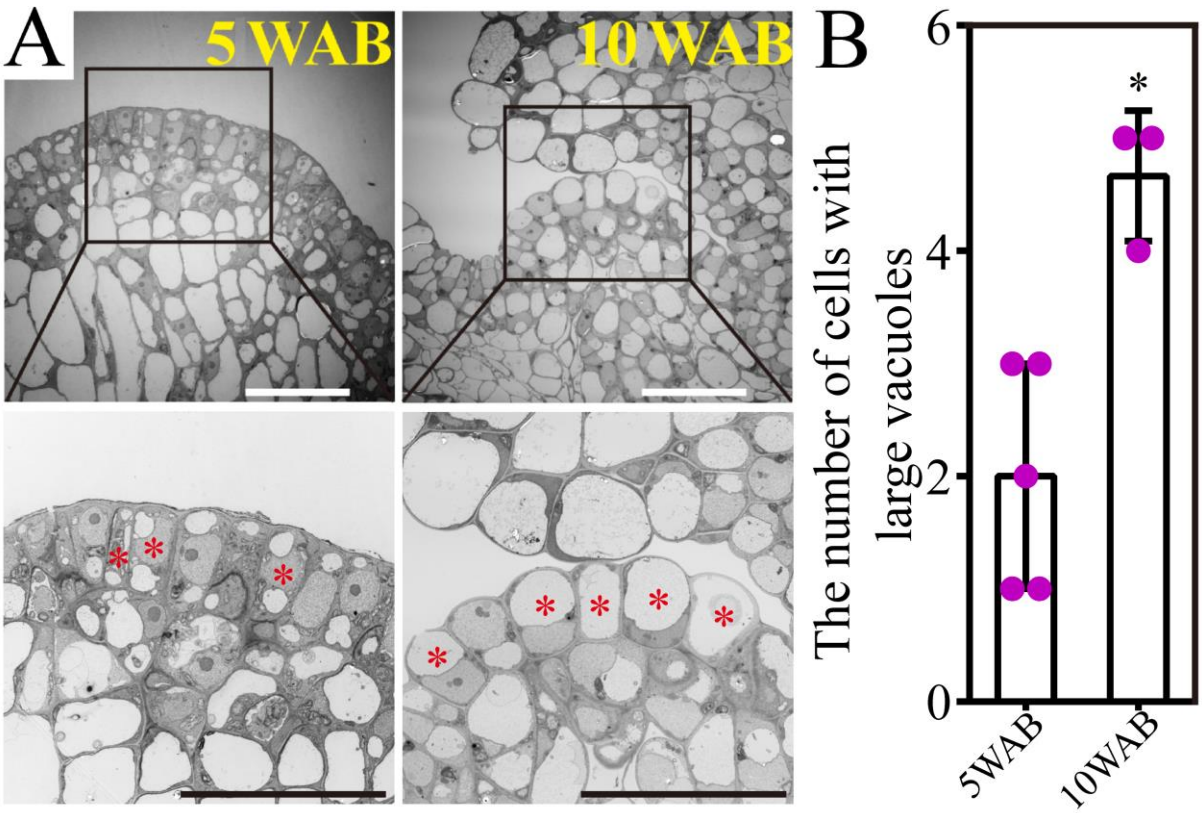


**Figure 18** The observation of vacuolated stem cells in *clv3-2* mutant. (A) The intracellular ultrastructures of stem cells in L1 of IM of *clv3-2* mutants at 5 WAB and 10 WAB by using transmission electron microscopy (TEM). Images in the lower panels indicate the magnified images of the black box area in the upper panels. Red stars indicate cells with total vacuole size that occupied over 40% of the cell size. Scale bars = 20 μm. (B) The number of cells with large vacuoles in *clv3-2* IM at 5 WAB and 10 WAB. Dots represent the vacuolated cell numbers at each time point. Error bars denote SD. Two-tailed Student's t-test was performed. *: $p < 0.05$.

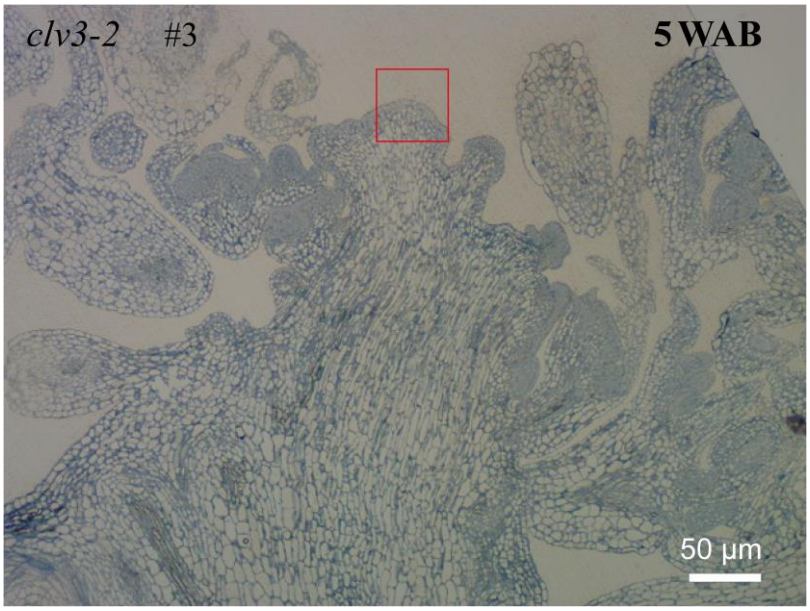


**Figure 19** Histological section shows the observed location of TEM in the *clv3-2* IM domain at 5 WAB. The red box shows the observed area. Scale bar = 50 μm.

**Dynamic changes of ROS components in wild type and *clv3-2* mutant**

It is well known that the mature CLV3 peptides can move to the organizing center (OC), in which *WUS* is initially expressed, and inhibits the *WUS* expression (Fletcher et al., 1999). However, the expression of *WUS* was still terminated at 6 WAB in *clv3-2* mutant (Figure 17), indicating that there must be other factors that inhibit *WUS* transcription. Recently, a study reported that two ROS components, $O_2^{\cdot-}$ and $H_2O_2$, are involved in regulating stem cell fate, and the balance between them is indispensable to stem cell maintenance and differentiation (Zeng et al., 2017). Moreover, $O_2^{\cdot-}$ can activate *WUS* expression and maintain stemness, and $H_2O_2$ accumulation in the peripheral zone (PZ) negatively regulates $O_2^{\cdot-}$ biosynthesis, resulting in stem cell termination (Zeng et al., 2017). These evidences strongly suggest that ROS homeostasis influences stem cell fate determination and $H_2O_2$ might be a regulator of *WUS* expression. Therefore, it is necessary to understand the spatial-temporal manner of ROS components in SAM domain.

Through NBT staining, a histological staining method, I examined the distribution and accumulation characteristics of $O_2^{\cdot-}$ in IM domains of WT and *clv3-2* mutants. In WT, $O_2^{\cdot-}$ displayed strong signal in IM domain, especially in stem cell layers, at 1 WAB and 2 WAB. At 3 WAB, the level of $O_2^{\cdot-}$ in stem cells was clearly decreased, while became undetectable from 4 WAB to 6 WAB (Figure 20). In *clv3-2* mutant, the detectable time window was 2 weeks longer than that in WT. Concretely, the clear $O_2^{\cdot-}$ signals were displayed in *clv3-2* IM domain from 1 WAB to 4 WAB. At 5 WAB, the level of $O_2^{\cdot-}$ in stem cell layers was reduced and fully disappeared in stem cells from 6 WAB (Figure 20).

The spatial-temporal distribution of $H_2O_2$ in *clv3-2* IM domain was observed as well. There were no detectable signals in *clv3-2* IM domains from 1 WAB to 5 WAB. $H_2O_2$ signals

were initially appeared in *clv3-2* IM domain from 6 WAB. Subsequently, clear and increased $H_2O_2$ signals were detected in *clv3-2* IM domain until 10 WAB. Notably, the level of $H_2O_2$ showed an accumulated peak at 10 WAB. At 11 and 12 WABs, there were no detectable $H_2O_2$ signals due to whole IM death (Figure 21). Comparing with WT, $H_2O_2$ signals appeared two weeks later in *clv3-2* IM domain (Figure 21).

Based on these findings, I found that the existence time of $O_2^{\cdot-}$ and $H_2O_2$ displayed a switched period. In WT, this switched period appeared from 3 WAB to 4 WAB, and the level of $O_2^{\cdot-}$ was decreased from 3WAB and fully disappeared from IM domain at 4 WAB. Meanwhile, very weak $H_2O_2$ signal was initially detected in stem cell layers from 3 WAB (Figures 20 and 21). Similarly, there were also a conversion period existed in *clv3-2* mutants from 6 WAB to 7 WAB, and showed a two-week's delay comparing with that in WT (Figures 20 and 21). These results indicated that dynamic changes of ROS components happened during the lifespan of IM in both WT and *clv3-2* mutants, and the deferred conversion period in *clv3-2* IM might result in the prolonged-expression window of *WUS*.

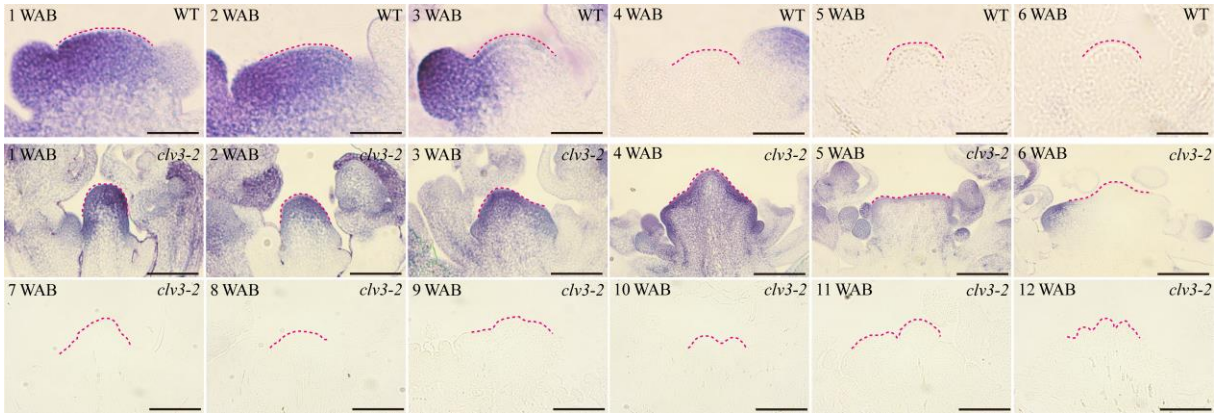


**Figure 20** NBT staining of WT and *clv3-2* IMs to show the $O_2^{\cdot-}$ signals (blue color). Dotted pink lines indicate IM shape. Scale bars: 25 μm in WT and 100 μm in *clv3-2*. At least five individual IMs were used for each experiment.

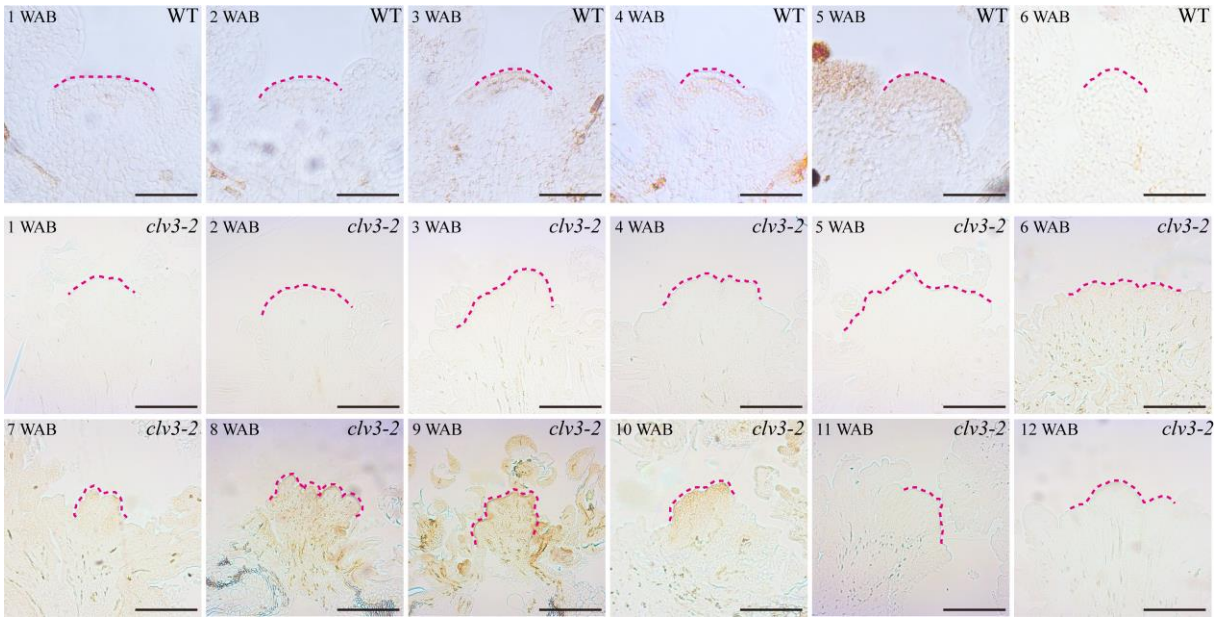


**Figure 21** DAB staining of WT and *clv3-2* IMs to show the $H_2O_2$ signals (brown color). Dotted pink lines indicate IM shape. Scale bars: 25 μm in WT and 100 μm in *clv3-2*. At least five individual IMs were used for each experiment.

**Features of programmed stem cell death in *clv3-2* mutant**

Whereas the stem cell death process has been studied in WT *Arabidopsis* (Wang et al., 2020), the entire landscape in *clv3-2* stem cells is still lacking. The FDA/PI staining results showed that stem cell death started from 7 WAB in *clv3-2* IM (Figure 22). In the stem cells, stronger PI signals could be detected from 7WAB to 10 WAB. All stem cells were stained by PI at 10 WAB and 11 WAB due to whole *clv3-2* IM was totally dead (Figure 22).

In order to understand which type of cell death was happened in the dead stem cells in *clv3-2* IM, I checked the spatial-temporal expression profiles of dPCD marker genes. The key dPCD marker gene *BFN1*, which encodes nuclease, was initially expressed in the bottom regions of *clv3-2* IM domain at 3 WAB. Then, the expression area of *BFN1* moved upwards but still did not enter into the stem cell layers until 6 WAB, when *WUS* started to be terminated (Figures 17 and 23). From 7 WAB to 10 WAB, *BFN1* was expressed in stem cells, resulting in stem cell death in *clv3-2* IM (Figures 22 and 23). Because the whole *clv3-2* IM was dead after 11 WAB, there were no *BFN1* signals found (Figure 23).

It has been reported that the NAC transcriptional factor ORESARA1 (ORE1) directly regulates *BFN1*, and the expression patterns of these two senescence-enhanced genes are largely overlapped during leaf senescence (Matallana-Ramirez et al., 2013). However, the spatial-temporal expression profiles of *ORE1* during IM senescence were still unknown. As shown in Figure 24, there were no *ORE1* expression signals (GUS signals) in IM domains in WT and *clv3-2* mutants from 1 WAB to 2 WAB. At 3 WAB, *ORE1* was expressed in the bottom area of IM domain in both WT and *clv3-2* mutants. In WT, the expression domain of *ORE1* moved upward from 4 WAB, and showed clear signals in stem cell layers at 5 WAB.

The expression signal of *ORE1* could not be detected at 6 WAB due to the whole WT IM was dead (Figures 22 and 24). In contrast, in *clv3-2* mutants, the expression region of *ORE1* started to be observed in upper layers from 4 WAB to 6 WAB. From 7 WAB to 10 WAB, *ORE1* expression signals could be detected in stem cell layers. Because the whole *clv3-2* IM was dead, there were no *ORE1* expression signals could be detected at 11 WAB and 12 WAB (Figure 24). These results proved that the spatial-temporal expression profiles of *BFN1* and *ORE1* were almost consistent during IM senescent period in WT and *clv3-2* mutants and suggested that *ORE1-BFN1* cascade might be involved in programmed stem cell death regulation.

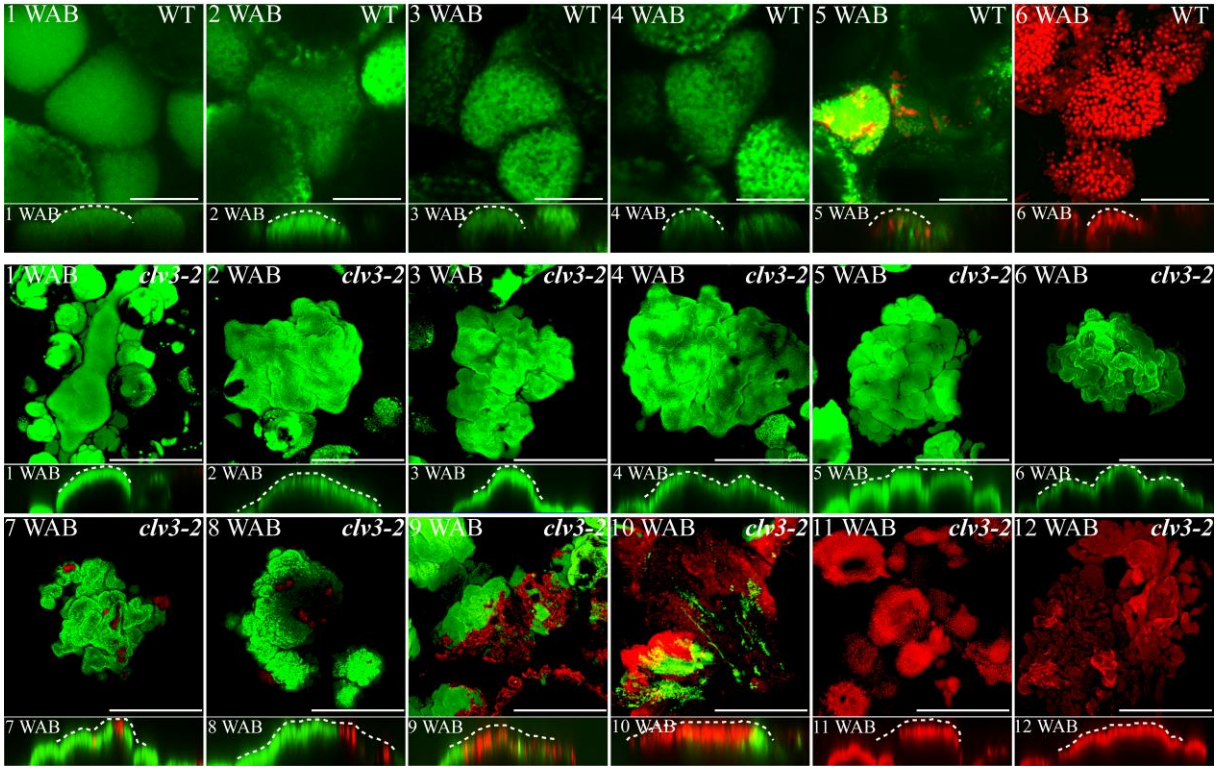


**Figure 22** FDA/PI staining of IMs in WT and *clv3-2* mutants. The top view of confocal images of FDA (green) and PI (red) signals are shown in the upper panel. The side view is shown in the lower panel. FDA-stained cells (in green) are alive, and PI-stained cells (in red) are dead. White dotted lines indicate IM shapes. Scale bars: 50 μm in WT and 100 μm in *clv3-2* mutants. At least five individual IMs were used for each experiment.

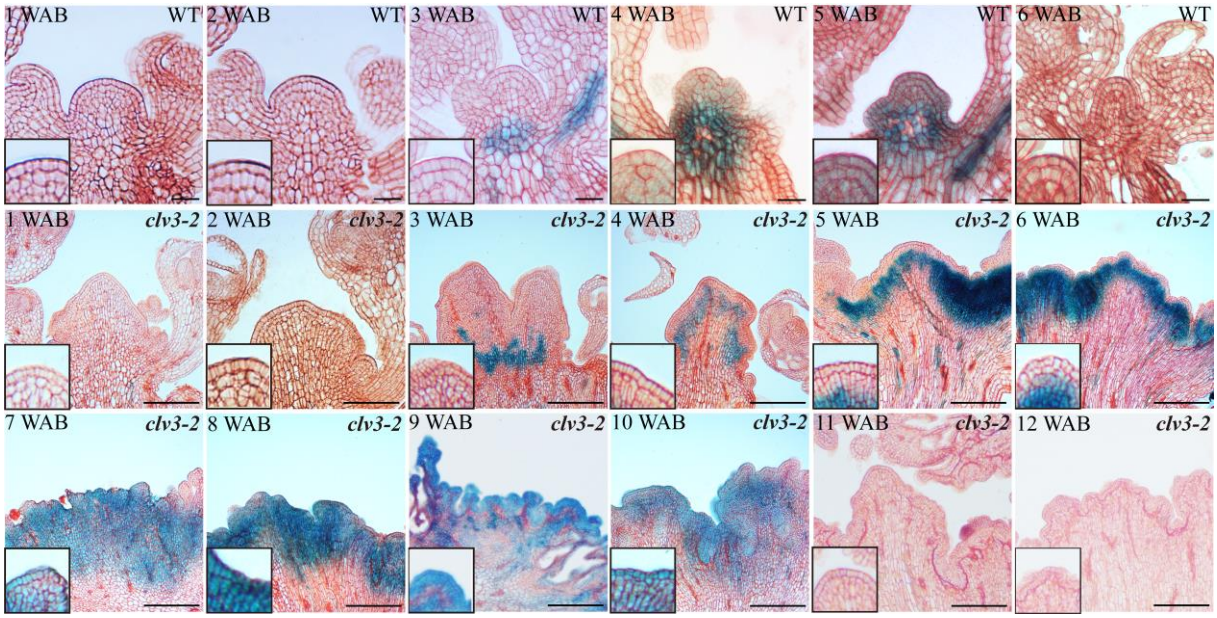


**Figure 23** The spatial-temporal expression patterns of *BFN1* in WT and *clv3-2* mutants. The magnified images at bottom left corner indicated the *BFN1* expression levels in stem cell layers. Scale bars: 15 μm in WT and 100 μm in *clv3-2*. At least five individual IMs were used for each experiment.

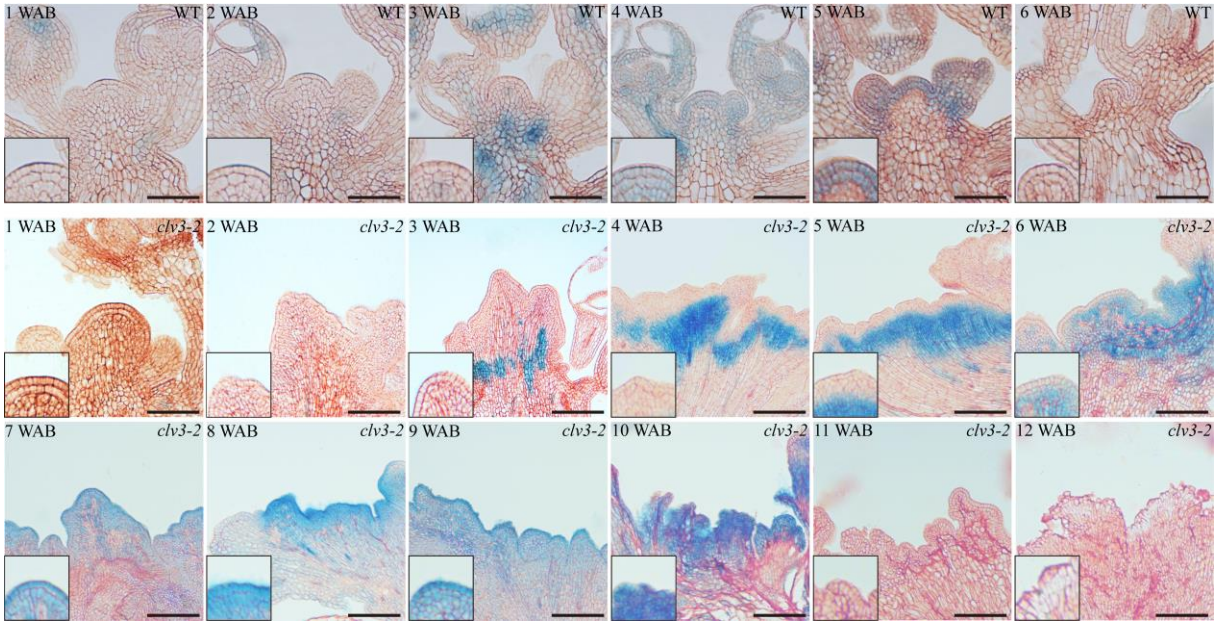


**Figure 24** The spatial-temporal expression patterns of *ORE1* in WT and *clv3-2* mutants. The magnified images at bottom left corner indicated the *ORE1* expression levels in stem cell layers. Scale bars: 50 μm in WT and 100 μm in *clv3-2*. At least five individual IMs were used for each experiment.

**Effects of exogenous $H_2O_2$ on *WUS*, *ORE1*, and *BFN1* expressions**

Based on the evidence mentioned above, it was highly possible that the conversion of ROS components in IM domain govern the stem cell activity termination and stem cell senescence and death. In order to verify this hypothesis, the exogenous $H_2O_2$ assay was performed in WT IMs. First, I studied the effects of exogenous $H_2O_2$ on *WUS* expression under different concentration and found that 5 mM, 10 mM, and 20 mM $H_2O_2$ could inhibit *WUS* expressions after one week of continuous treatments (Figures 25 and 26). This result indicated that 5 mM exogenous $H_2O_2$ treatment was sufficient to terminate *WUS* expression. Next, I studied how soon *WUS* expression responds to 5 mM exogenous $H_2O_2$ treatment. As shown in Figure 25, *WUS* could respond to exogenous $H_2O_2$ only after 1 day's treatment. These results revealed that *WUS* was sensitive to exogenous $H_2O_2$.

Besides, *proORE1::GUS* and *proBFN1::GUS* lines were treated by exogenous $H_2O_2$. Under one-week 5, 20, and 40 mM $H_2O_2$ treatments, the expression areas of *ORE1* and *BFN1* were similar as Mock, indicating that *ORE1* and *BFN1* could not respond to low concentration of $H_2O_2$ (Figures 27 and 28). Interestingly, the expression signals of *ORE1* and *BFN1* could be detected in stem cell layers after one-week 50 mM $H_2O_2$ treatment, suggesting that a relatively high concentration of $H_2O_2$ could induce dPCD marker gene expression (Figure 27).

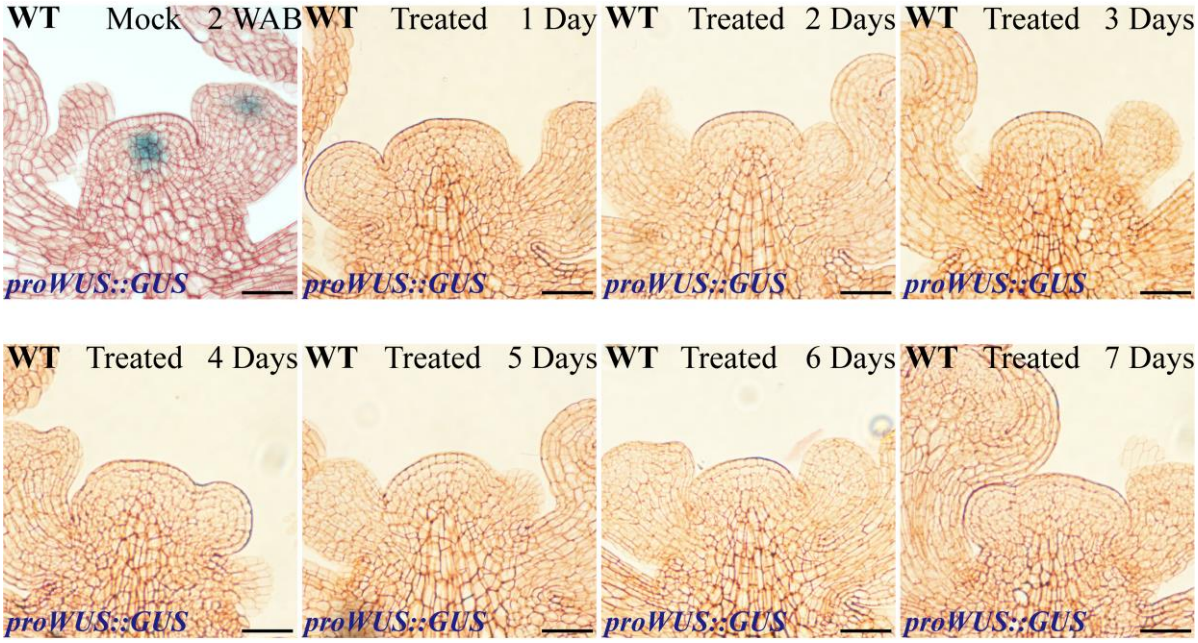


**Figure 25** Effects of exogenous $H_2O_2$ on *WUS* expressions. The IMs at 1 WAB were treated with 5 mM $H_2O_2$ until to 2 WAB. The *WUS* expression profile from 1 day to 7 days was shown. At least five individual IMs were treated in each experiment. Scale bars: 20 μm.

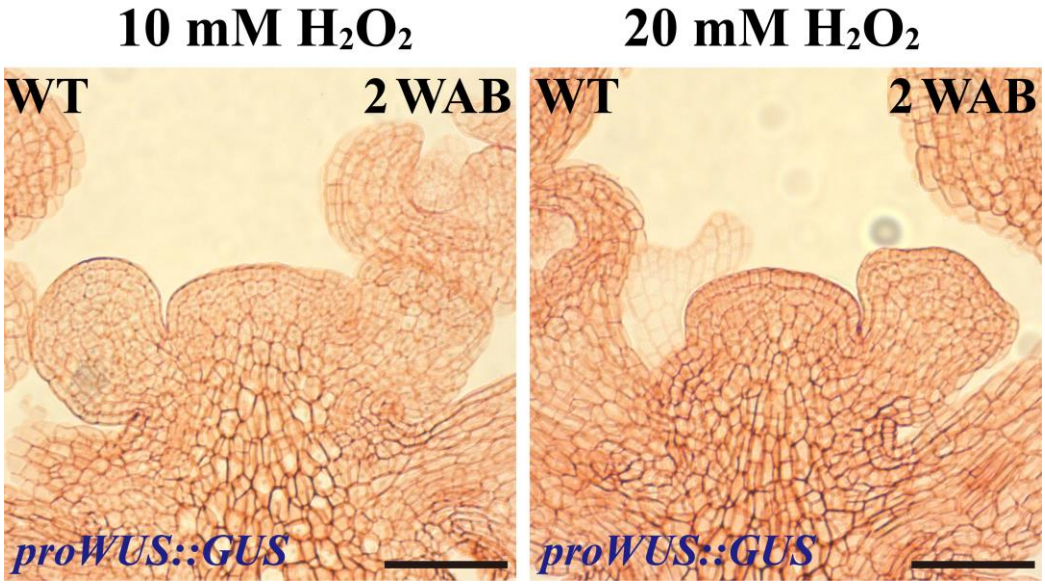


**Figure 26** Different concentration of exogenous $H_2O_2$ inhibited *WUS* expression in WT IMs after one-week continuous treatment. Scale bars = 30 μm.

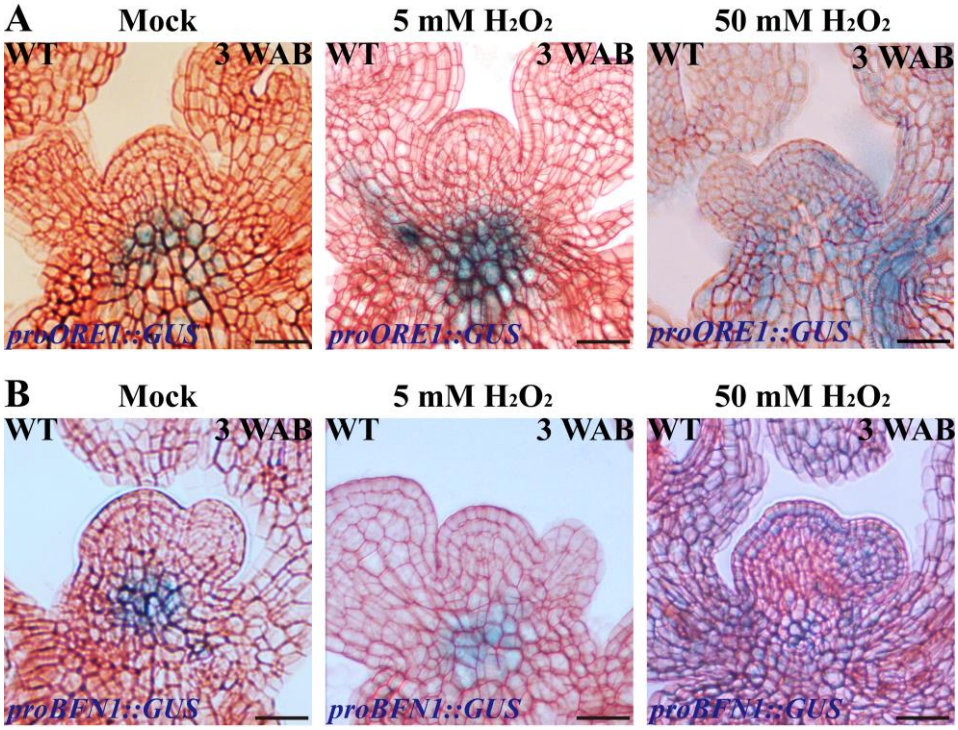


**Figure 27** Effects of exogenous $H_2O_2$ on dPCD marker genes *ORE1* and *BFN1* expressions. The IMs at 2 WAB were treated with 5 mM (negative control) and 50 mM $H_2O_2$ until to 3 WAB. At least five individual IMs were treated in each experiment. (A) Effects of 5 mM and 50 mM $H_2O_2$ on *ORE1* expression. Scale bars: 20 μm. (B) Effects of 5 mM and 50 mM $H_2O_2$ on *BFN1* expression. Scale bars: 20 μm.

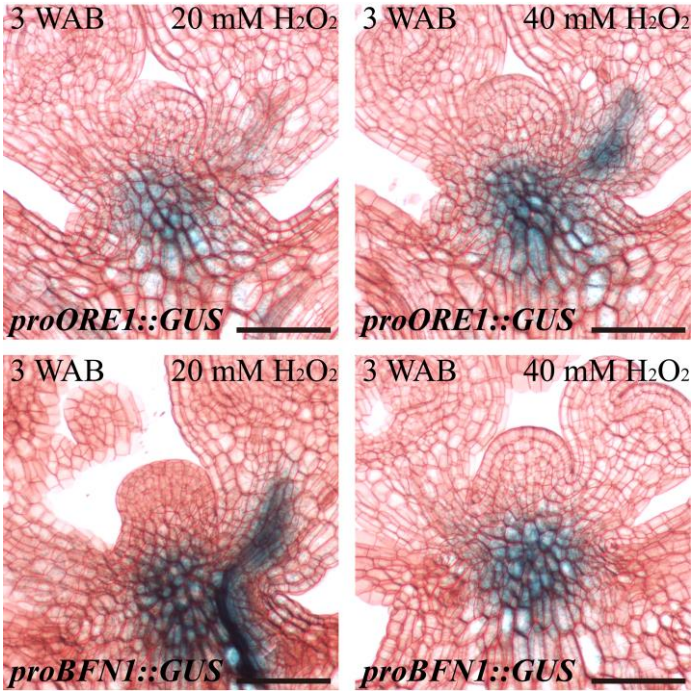


**Figure 28** 20 and 40 mM of exogenous $H_2O_2$ did not change *WUS* expression pattern in WT IMs after one-week continuous treatment. Scale bars = 30 μm.

**The expression profiles of ROS metabolism-related genes**

In the RNA-seq results, a total of eight ROS metabolism-related genes were identified (Table 2). I submitted these candidate genes in the BAR database to check their expression patterns in shoot apexes at vegetative, transition, and inflorescence stages. Among these 8 candidates, only *CAT3* and *ACX1*, which have opposite roles in $H_2O_2$ metabolism, were highly expressed in all three types of shoot apex tissues (Figure 29A), indicating that these genes might play roles in regulating shoot apex development. In addition, I compared my data with published transcriptome data (Wuest et al., 2016; Wang et al., 2020). In the published data, there are 75 DEGs, which are isolated through comparing data in grown and arrested meristem tissues, involved in ROS metabolic pathways (Wuest et al., 2016). In my RNA-seq data, eight DEGs that are involved in ROS metabolic pathways (Wang et al., 2020; Table 2). In these two datasets, only *CAT3* was screened out as a common gene, indicating that *CAT3* may be involved in ROS-mediated stem cell longevity regulation (Figure 29B). In order to understand the authentic expression profiles of *CAT3* and *ACX1* in WT and *clv3-2* IM tissues, I carried out qRT-PCR assay using IM tissues at 2 WAB and 4 WAB. *CAT3* was upregulated from 2 WAB to 4 WAB in both WT and *clv3-2* mutants, but the expression levels in *clv3-2* mutants were significantly increased at 4 WAB than that of WT. *ACX1* was significantly induced at 4 WAB in WT, while no change in *clv3-2* mutants at the same time point (Figure 29C). These results revealed that *clv3-2* mutants might have a higher ability of $H_2O_2$ clearance than WT.

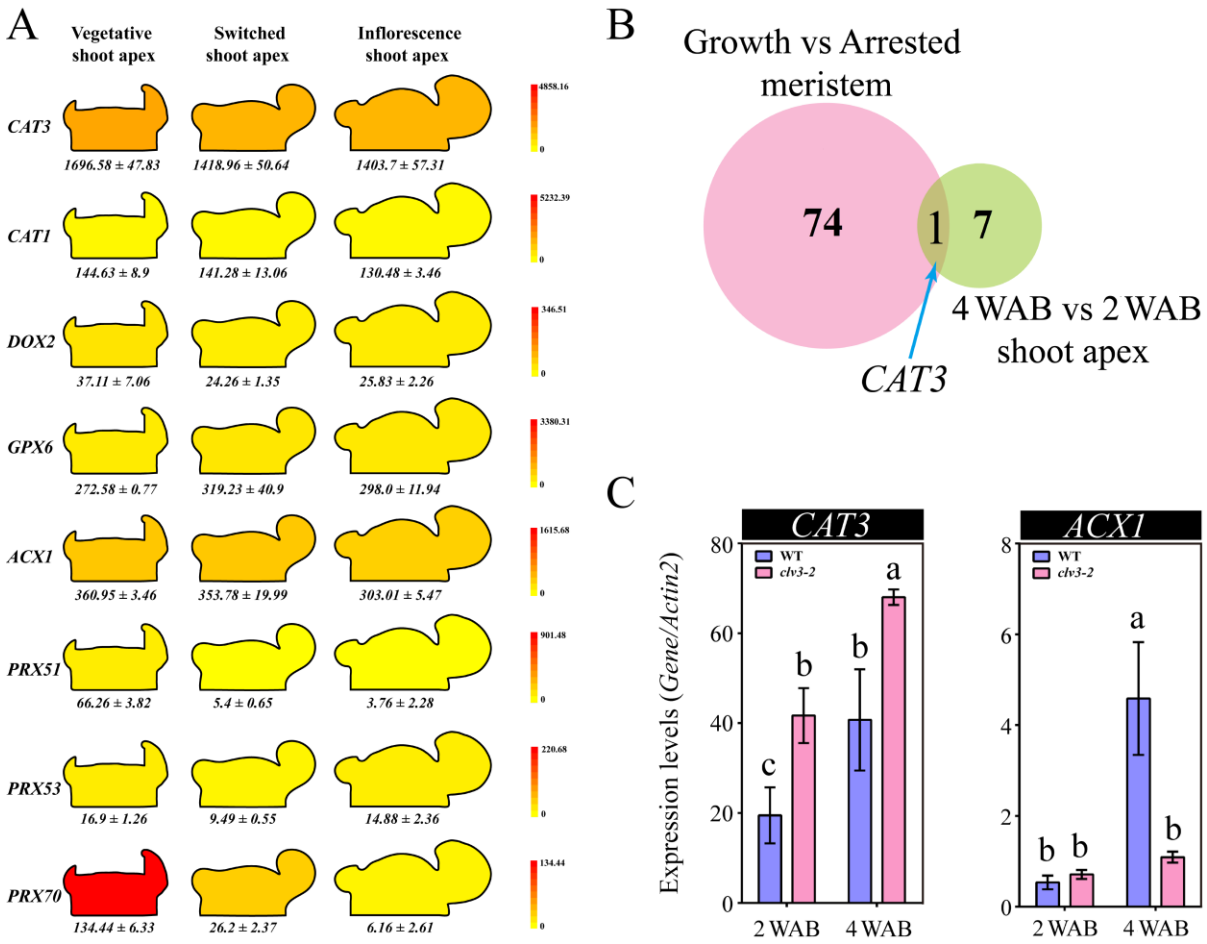


**Figure 29** The expression profiles of ROS metabolism related genes. (A) The expression patterns of eight ROS metabolism related genes in BAR database. The gene expression data in three types of shoot apex were shown. (B) Common gene isolation between published RNA-seq datasets and RNA-seq datasets in this study. (C) The expression profiles of ROS clearance related gene *CAT3* and ROS production related *ACX1* at 2WAB and 4WAB in WT and *clv3-2* IM tissues. qRT-PCR assay was performed. Each experiment was replicated three times, and error bars indicated SD. One-way ANOVA post Tukey HSD test ($p < 0.05$) was carried out to calculate the differences among different groups. Different letters indicate significant differences, while the same letters indicate no significant differences.

***ACX1* may be involved in regulating stem cell activity**

In order to understand the functions of *ACX1* in regulating stem cell activity, the *acx1-3* mutants, which is the Columbia background, were used. After comparing with WT (Col-0), I found that the numbers of flowers and siliques on the primary shoot in *acx1-3* mutants were significantly higher than that of WT at each time point (1 WAB-6 WAB) (Figure 30). This result demonstrated that loss-of-function of *ACX1* resulting in generating more lateral organs during the same lifetime with WT, thereby indicated that stem cells in *acx1-3* mutants maintained higher activities. On the other hand, this result also revealed that the RNA-seq data mentioned in chapter I was highly reliable.

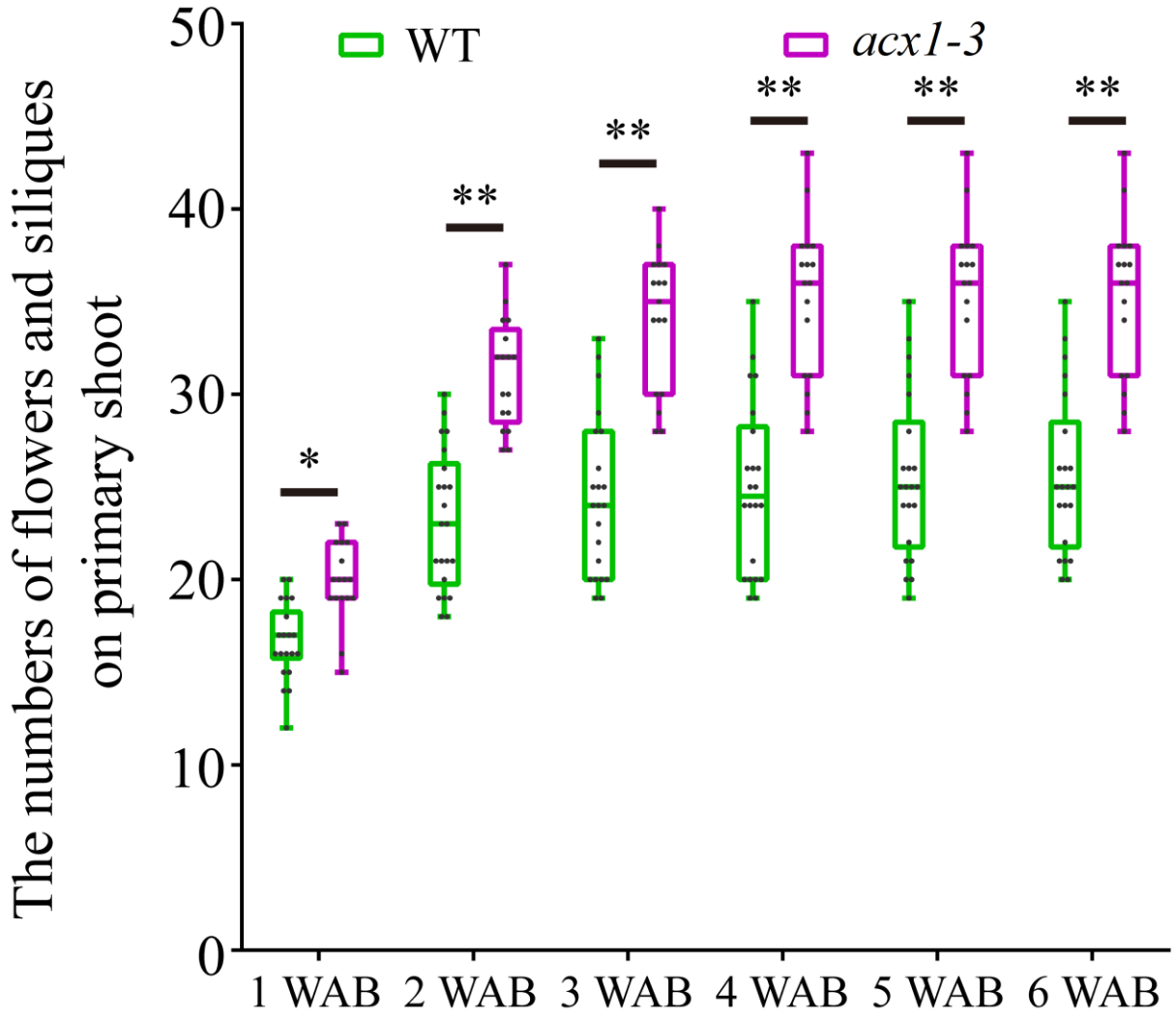


**Figure 30** The statistics of flower and silique numbers on WT (Col-0) and *acx1-3* mutants (Col-0). Student's *t*-test (two-tails) was performed to detect the differences between WT and *acx1-3* mutants. *: $p < 0.05$; **: $p < 0.01$. n = 22 in WT and 17 in *acx1-3* mutants.

## Discussion

### The possible functions of stem cell marker genes in regulating stem cell fate in *Arabidopsis*

So far, the functions of *WUS* in diverse signaling pathways are relatively clear (Jha et al., 2020). As a master regulator, WUS plays essential roles in governing shoot and floral meristem identity, reproductive organ development, embryogenesis, plant genetic transformation, and even antiviral immunity in plant stem cells (Jha et al., 2020; Wu et al., 2020). The functions of *CLV3* are still largely uncovered except for restricting *WUS* expression. Further, the relationships among stem cell marker genes, ROS components, and dPCD process during stem cell senescence and death processes are largely unknown.

In this part, my results reveal the possible network between stem cell marker genes and ROS metabolism. It has been reported that *ACX1* is involved in the production of $H_2O_2$ (Khan et al., 2012). On the contrary, *CAT3* catalyzes the decomposition of $H_2O_2$ and plays critical role in controlling the homeostasis of ROS in *Arabidopsis* (Du et al., 2008). When *WUS* was expressed in IM domain, there were no detectable $H_2O_2$ signals in IM domain, especially in stem cell layers in WT and *clv3-2* mutants. Interestingly, weak $H_2O_2$ signals started to be observed in stem layers of WT and IM domain of *clv3-2* mutants when *WUS* was terminated at 4 WAB in WT and 7 WAB in *clv3-2* mutants (Figure 21). These evidences indicate that *WUS* may inhibit $H_2O_2$ production through the regulation of the $H_2O_2$ biosynthetic gene *ACX1*. Consistent with this, the relative expression level of *ACX1* at 4 WAB, which was a *WUS*-missing stage, was maximal 6 folds compared to that at 2 WAB (*WUS*-existing stage) (Figure 29C). In *acx1-3* mutants, more lateral organs were generated during the same lifespan as WT (Figure 30), suggesting that *ACX1* might take part in stem cell activity regulation via a possible $H_2O_2$-dependent pathway. Besides, *WUS* may also promote *CAT3* to eliminate $H_2O_2$ as a homeostatic regulation, resulting in the low concentration of $H_2O_2$ in stem cells. Consistently, the relative expression level of *CAT3* at 4 WAB was significantly higher than that at 2 WAB due to the prolonged *WUS* expression period in *clv3-2* mutants (Figure 29C). However, I found that the relative expression intensity of *CAT3* at 4 WAB was also notably higher than that at 2 WAB in WT, but lower than that at 4 WAB in *clv3-2* mutants (Figure 29C), indicating that there may be some unknown signals inducing *CAT3* expression.

In addition, the expression domains and patterns of *WUS* and dPCD marker genes, *ORE1* and *BFN1*, reflect their potential regulatory relationship as well. In WT, *WUS* was expressed in OC at 1 WAB and 2 WAB, and was terminated at 3 WAB. dPCD marker genes *ORE1* and *BFN1* display quite similar expression profiles. Both genes were initially expressed in Rib zone, which is an area below the OC in WT and *clv3-2* mutants. The appearance of dPCD marker genes in stem cell layers was 1 week later than *WUS* termination in both WT and *clv3-2* mutants (Figures 17, 23, and 24). These results suggested that the expression of

*WUS* indirectly but strictly restricts the activities of dPCD marker genes in IM domain, thereby protects the stem cell niche to prevent the dPCD process activated untimely during the proliferative stage in *Arabidopsis*. Furthermore, the results indicate that the possible functions of another stem cell marker gene *CLV3* may restrict the production of $O_2^{\cdot-}$. Comparing with WT, the existence time of $O_2^{\cdot-}$ is prolonged in *clv3-2* mutants (Figure 20). Meanwhile, *CLV3* can repress *WUS* expression (Fletcher et al., 1999), but it is not shown how the CLV3 signal leads to *WUS* repression. In WT, the *CLV3* expression time was sustained until 4 WAB, while the expression of *WUS* was kept until 2 WAB (Figures 9 and 10). Meanwhile, loss-of-function of *CLV3* prolonged the expression time of *WUS* (Figure 16). Combining these findings, it is highly possible that *CLV3* may prevent *WUS* reactivation via the inhibition of $O_2^{\cdot-}$-mediated pathway.

**Dynamic changes of ROS components may play key roles in controlling stem cell longevity in *Arabidopsis thaliana***

It is well known that the WUS-CLV3 negative feedback loop regulates stem cell activity and maintenance (Mayer et al. 1998, Fletcher et al. 1999, Yadav et al. 2011, Daum et al. 2014, Perales et al. 2016). So far, several studies have proved that WUS-CLV3 negative feedback loop can be modulated by different factors. Among these factors, the ROS signaling pathway plays essential role in regulating the stem cell population (Kitagawa et al., 2019). Loss-of-function of a mitochondrial protease AtFTSH4 results in the abnormal accumulation of ROS in the shoot apex, therefore, induces SAM termination (Dolzblasz et al. 2016). Moreover, a recent study reported that $O_2^{\cdot-}$ is accumulated in shoot stem cells and promotes the expression of *WUS* during the vegetative stage of *Arabidopsis*, while $H_2O_2$ is accumulated in PZ to facilitate shoot stem cells differentiation (Zeng et al., 2017). These findings indicate the regulatory link between the WUS-CLV3 feedback loop and ROS homeostasis in controlling stem cell development during the very early growth stage of *Arabidopsis*.

During the proliferative, senescent, and dead stages of stem cells, I found that a dynamic conversion of ROS components $O_2^{\cdot-}$ and $H_2O_2$ is carried out in both WT and *clv3-2* mutants in a different timing (Figures 20 and 21). The *WUS* expression period was fully overlapped with the existence time window of $O_2^{\cdot-}$ in WT and *clv3-2* mutants (Figures 17 and 20). These results revealed that $O_2^{\cdot-}$ can promote *WUS* expression, and this phenomenon is also in line with the previous observation (Zeng et al., 2017). It has been reported that another ROS component $H_2O_2$ is accumulated in PZ and inhibits the production of $O_2^{\cdot-}$ during stem cell development (Zeng et al., 2017). Thus, I speculate that the accumulation of $H_2O_2$ in SAM domain inhibited the production of $O_2^{\cdot-}$ during the conversion stage. On the other hand, the exogenous $H_2O_2$ assay demonstrated that $H_2O_2$ can repress *WUS* expression with a very short-term manner (Figure 25), suggesting that the effect of $H_2O_2$ on *WUS* is controlled by an unknown straightforward pathway. In addition, the expression time window of *CLV3* was 1 week longer than *WUS* (Figures 9 and 10), and partially overlapped the $H_2O_2$ existent time

(Figure 21), suggesting that $H_2O_2$ accumulation may inhibit CLV3 expression after WUS termination. I also found that the exogenous $H_2O_2$ enhanced the expressions of dPCD marker genes *ORE1* and *BFN1* in stem cell layers, indicating that the accumulation and burst of endogenous $H_2O_2$ are most likely caused by the factor inducing dPCD in the stem cell population (Figures 21, 22, 23, 24, and 27).

**Other factors that possibly influence stem cell longevity in *Arabidopsis***

In all aerobic organisms, ROS are mainly produced during the respiratory and photosynthetic processes (Moller, 2001). Except for mitochondria and chloroplasts, the vacuole is also an organelle involved in ROS production (Peshev et al., 2013). During the senescent stage of stem cells, cell vacuolization was observed as an important intracellular feature (Figures 8 and 18). Thus, the development and expansion of vacuoles in stem cells may be an important factor in ROS, especially $H_2O_2$ accumulation.

Another possible factor in stem cell senescence is DNA damage. In animals, stem cells tend to be highly sensitive to DNA damage, and DNA damage-triggered PCD process is key to prevent harm (Rich et al., 2000; Schumacher et al., 2001). Plants cannot escape from environmental hazards, which always cause oxidative stress and DNA damage (Bray and West, 2005). ROS-induced DNA damage, which is also named oxidative DNA damage, has also been largely studied in plants (Roldán-Arjona and Ariza, 2009). In this study, the $H_2O_2$ burst was detected during dPCD in stem cells (Figures 21, 22, 23, and 24), indicating that $H_2O_2$-induced DNA damage may be caused. Besides, dPCD marker gene *BFN1* encodes a bifunctional nuclease that acts on DNA degradation (Pérez-Amador et al., 2000). Thus, the action of *BNF1* maybe belonging to a kind of DNA damage.

Overall, I examined the dynamic changes of ROS components $O_2^{\cdot-}$ and $H_2O_2$ in the stem cell population and uncovered their potential regulatory relationship between stem cell marker genes using morphological and physiological methods (Figure 31). Meanwhile, two ROS metabolism-related genes *CAT3* and *ACX1*, were screened out. *ACX1* might be involved in regulating stem cell activity. More molecular and genetic works should be performed in the future.

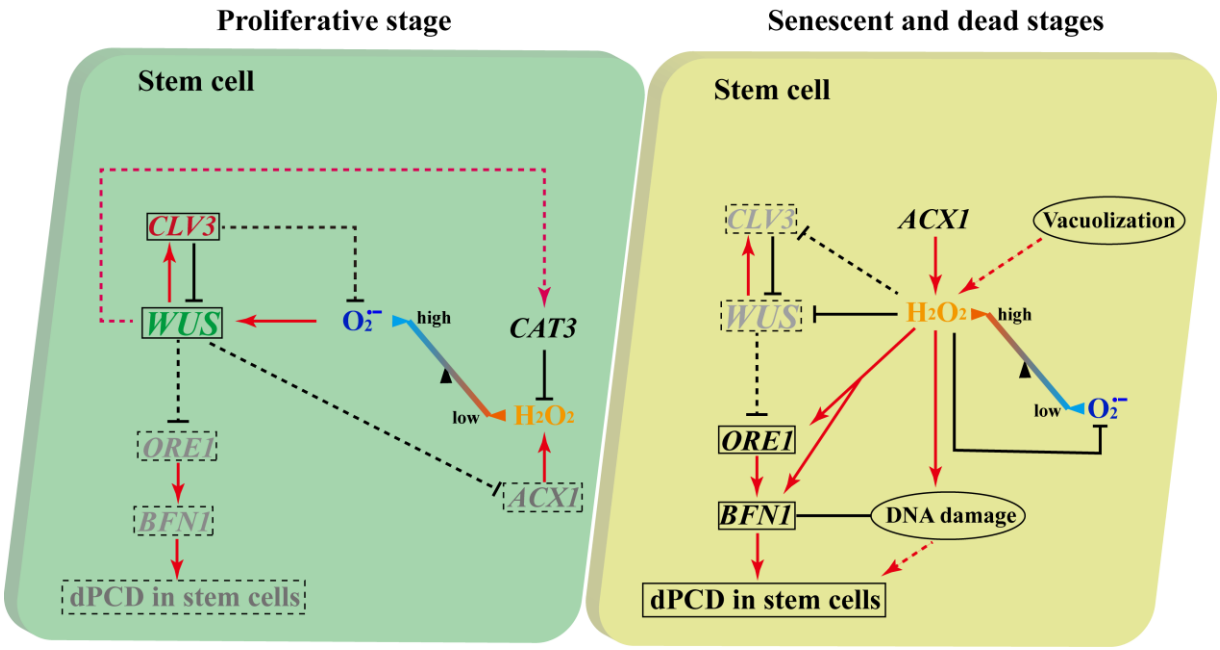


**Figure 31** The putative network of stem cell marker genes, ROS components, ROS metabolism related genes, and dPCD marker genes in regulating stem cell longevity. During proliferative stage, *WUS* is promoted by $O_2^{\cdot-}$ and inhibited by *CLV3* at same time. *WUS* may increase *CAT3* expression and repress *ACX1* expression to keep $O_2^{\cdot-}$ at the high level and $H_2O_2$ at low level in stem cells. Meanwhile, *WUS* may repress *ORE1* and *BFN1* expressions to prevent the dPCD happened at wrong time. In order to prevent *WUS* reactivation at wrong time, except the direct inhibition, *CLV3* may also inhibit $O_2^{\cdot-}$ production via unknown pathways to repress *WUS* indirectly. During senescent and dead stages, cell vacuolization may promote the $H_2O_2$ accumulation in stem cell population. Appropriate level of $H_2O_2$ can decrease $O_2^{\cdot-}$ production and terminate *WUS* directly. Besides, *ACX1* may be activated to induce $H_2O_2$ burst. High levels of $H_2O_2$ directly triggers dPCD process by activating *ORE1* and *BFN1*. In addition, ROS-induced DNA damage may be also involved in stem cell death. Lines and arrow lines indicate the known processes; Dotted lines and arrow lines denote the unconfirmed process.

## Acknowledgements

Upon completing this doctoral thesis, I am grateful to those who have offered me encouragement and support during the doctoral course of my study.

First of all, the profound gratitude should go to my supervisor Professor Ito Toshiro. He has given me great instructions and encouragement throughout selecting the research topic, writing the thesis, improving the outline and the argumentation, and correcting the grammatical errors. His insightful comments on every draft, which provide me with many enlightening ideas, have inspired me to a great extent. The thesis could not have been finished without his patient guidance. It is my glory that I can finish my doctoral study in the Laboratory of Plant Stem Cell Regulation and Floral Patterning.

Secondly, I would like to say thanks to my mentor, Assistant professor Shirakawa Makoto. He has given me direct training on academic works. He also supports me in doing more presentations in several conferences, letting me gain more academic experience. During the article writing and thesis organization, he also plays key roles in writing, discussion, and suggestions. He helps me a lot during my working period. It will difficult for my smooth graduation if no his supports.

Thirdly, I would like to say thanks to my advisors, Professor Demura Taku and Professor Umeda Masaaki. They have given me very constructive comments during my study and thesis writing. Their excellent help makes my work more skilled.

Besides, I would like to say thanks to lab members who gave me lots of help. Thanks to Assistant Professors Yamaguchi Nobutoshi and Wada Yuuko. They have given me lots of comments and assistants during my study. Thanks to Uemura Akira, Iimura Hideaki, Looi Liang Sheng (former Postdoctoral), Wu Jinfeng (former Doctor), Lee Ze Hong (former Doctor), Pelayo Margaret Anne, Moruoka Takashi, and Wang Yicong. They have given me lots of help in study and life. Thanks to all graduated and current masters and former and current technicians for their help. Especially thanks to my friends Dr. Cui songkui and Cui yihui. They make my life in NAST more colorful.

Thanks very much to my wife, Ms. Ye Hong. She is a very important part of my life and gives me lots of encourages. She makes me not feel lonely in Japan, in NAIST. It is an excellent thing that I can get the Doctoral degree with her at the same time.

Finally, I would appreciate my family. Thanks very much to my Dad and Mom. Thanks to their silence given and support back of me. Their love is always the source of my strength during the period of my study in Japan.

# References


Allu, A.D., Soja, A.M., Wu, A., Szymanski, J., Balazadeh, S. (2014). Salt stress and senescence: identification of cross-talk regulatory components. *J. Exp. Bot.* 65, 3993–4008.

Avci, U., Petzold, H.E., Ismail, I.O., Beers, E.P., Haigler, C.H. (2008). Cysteine proteases XCP1 and XCP2 aid micro-autolysis within the intact central vacuole during xylogenesis in *Arabidopsis roots*. *Plant J.* 56, 303–315.

Bailly, C., El-Maarouf-Bouteau, H., Corbineau, F. (2008). From intracellular signaling networks to cell death: the dual role of reactive oxygen species in seed physiology. *C. R. Biol.* 331, 806–814.

Balanzà, V., Martínez-Fernández, I., Sato, S., Yanofsky, M.F., Kaufmann, K., Angenent, G.C., Bemer, M., Ferrándiz, C. (2018). Genetic Control of Meristem Arrest and Life Span in Arabidopsis by a FRUITFULL-APETALA2 Pathway. *Nat. Commun.* 9, 565.

Balazadeh, S., Kwasniewski, M., Caldana, C., Mehrnia, M., Zanor, M.I., Xue, G.-P., Mueller-Roeber, B. (2011). ORS1, an $H_2O_2$-responsive NAC transcription factor, controls senescence in Arabidopsis thaliana. *Mol. Plant* 4, 346–360.

Balazadeh, S., Siddiqui, H., Allu, A.D., Matallana-Ramirez, L.P., Caldana, C., Mehrnia, M., Zanor, M.-I., Kö hler, B., Mueller-Roeber, B. (2010). Gene regulatory network controlled by NAC transcription factor ANAC092/AtNAC2/ORE1 during salt-promoted senescence. *Plant J.* 62, 250–264.

Baurle, I., Laux, T. (2003). Apical meristems: the plant's fountain of youth. *Bioessays* 25, 961–970.

Beers, E.P. (1997). Programmed cell death during plant growth and development. *Cell Death Differ.* 4, 649–661.

Bela, K., Horváth, E., Gallé, Á., Szabados, L., Tari, I., Csiszár, J. (2015). Plant glutathione peroxidases: emerging role of the antioxidant enzymes in plant development and stress responses. *J. Plant Physiol.* 176, 192–201.

Betsuyaku, S., Takahashi, F., Kinoshita, A., Miwa, H., Shinozaki, K., Fukuda, H., Sawa, S. (2010). Mitogen-activated protein kinase regulated by the CLAVATA receptors contributes to shoot apical meristem homeostasis. *Plant Cell Physiol*. 52, 14–29.

Bi, C., Ma, Y., Wu, Z., Yu, Y.T., Liang, S., Lu, K., Wang, X.F. (2017). Arabidopsis ABI5 plays a role in regulating ROS homeostasis by activating CATALASE 1 transcription in seed germination. *Plant Mol. Biol.* 94, 197–213.

Biswas, A.K., Choudhuri, M.A. (1980). Mechanism of monocarpic senescence in rice. *Plant Physiol.* 65, 340–345.

Bleckmann, A., Weidtkamp-Peters, S., Seidel, C.A., Simon, R. (2010). Stem cell signaling in Arabidopsis requires CRN to localize CLV2 to the plasma membrane. *Plant Physiol.* 152, 166–176.

Brand, U., Fletcher, J.C., Hobe, M., Meyerowitz, E.M., Simon, R. (2000). Dependence of stem cell fate in Arabidopsis on a feedback loop regulated by CLV3 activity. *Science* 289, 617–619.

Brand, U., Grünewald, M., Hobe, M., Simon, R. (2002). Regulation of CLV3 expression by two homeobox genes in Arabidopsis. *Plant physiol.* 129, 565–575.

Bray, C.M., West, C.E. (2005). DNA repair mechanisms in plants: Crucial sensors and effectors for the maintenance of genome integrity. *New Phytol.* 168, 511–528.

Breeze, E., Harrison, E., McHattie, S., Hughes, L., Hickman, R., Hill, C., Kiddle, S., Kim, Y.S., Penfold, C.A., Jenkins, D., Zhang, C., Morris, K., Jenner, C., Jackson, S., Thomas, B., Tabrett, A., Legaie, R., Moore, J.D., Wild, D.L., Ott, S., … Buchanan-Wollaston, V. (2011). High-resolution temporal profiling of transcripts during Arabidopsis leaf senescence reveals a distinct chronology of processes and regulation. (2011). High-resolution temporal profiling of transcripts during Arabidopsis leaf senescence reveals a distinct chronology of processes and regulation. *Plant Cell* 23, 873–894.

Busch, W., Miotk, A., Ariel, F.D., Zhao, Z., Forner, J., Daum, G., Suzaki, T., Schuster, C., Schultheiss, S.J., Leibfried, A., Haubeiss, S., Ha, N., Chan, R.L., Lohmann, J.U. (2010). Transcriptional control of a plant stem cell niche. *Developmental Cell* 18, 849–861.

Cai, C.-F., Zhu, J., Lou, Y., Guo, Z.-L., Xiong, S.-X., Wang, K., Yang, Z.-N. (2015). The functional analysis of OsTDF1 reveals a conserved genetic pathway for tapetal development between rice and Arabidopsis. *Science Bulletin* 60, 1073–1082.

Cao, X., He, Z., Guo, L., Liu, X. (2015), Epigenetic mechanisms are critical for the regulation

of WUSCHEL expression in foral meristems. *Plant physiol.* 168, 1189–1196.

Chen, C., Letnik, I., Hacham, Y., Dobrev, P., Ben-Daniel, B.-H., Vanková, R., Amir, R., Miller, G. (2014). ASCORBATE PEROXIDASE6 protects Arabidopsis desiccating and germinating seeds from stress and mediates cross talk between reactive oxygen species, abscisic acid, and auxin. *Plant Physiol.* 166, 370–383.

Chen, P., Umeda, M. (2015). DNA double-strand breaks induce the expression of flavin-containing monooxygenase and reduce root meristem size in *Arabidopsis thaliana*. *Genes Cells* 20, 636–646.

Clark, S.E., Running, M.P., Meyerowitz, E.M. (1995). CLAVATA3 is a specific regulator of shoot and floral meristem development affecting the same processes as CLAVATA1. *Development* 121, 2057–2067.

Clark, S.E., Williams, R.W, Meyerowitz, E.M. (1997). The CLAVATA1 gene encodes a putative receptor kinase that controls shoot and floral meristem size in Arabidopsis. *Cell* 89, 575–585.

Cock, J.M., McCormick, S. (2001) A large family of genes that share homology with CLAVATA3. *Plant Physiol.* 126, 939– 942.

Considine, M.J., Foyer, C.H. (2014). Redox regulation of plant development. Antioxid. *Redox Signal.* 21, 1305–1326.

Daneva, A., Gao, Z., Van Durme, M., Nowack, M.K. (2016). Functions and regulation of programmed cell death in plant development. *Annu. Rev. Cell Dev. Biol.* 32, 441–468.

Daum, G., Medzihradszky, A., Suzaki, T., Lohmann, J.U. (2014). A mechanistic framework for noncell autonomous stem cell induction in Arabidopsis. *Proc. Natl. Acad. Sci. USA*. 111, 14619–14624.

Denay, G., Creff, A., Moussu, S., Wagnon, P., Thévenin, J., Gérentes, M.F., Chambrier, P., Dubreucq, B., Ingram, G. (2014). Endosperm breakdown in Arabidopsis requires heterodimers of the basic helix-loop-helix proteins ZHOUPI and INDUCER OF CBP EXPRESSION 1. *Development*, 141, 1222–1227.

Deyhle, F., Sarkar, A.K., Tucker, E.J., Laux, T. (2007). WUSCHEL regulates cell differentiation during anther development. *Dev. Biol.* 302, 154–159.

DeYoung, B.J., Bickle, K.L., Schrage, K.J., Muskett, P., Patel, K., Clark, S.E. (2006). The CLAVATA1-related BAM1, BAM2 and BAM3 receptor kinase-like proteins are required for meristem function in Arabidopsis. *Plant J.* 45, 1–16.

Diaz-Vivancos, P., De Simone, A., Kiddle, G., Foyer, C.H. (2015). Glutathione- linking cell proliferation to oxidative stress. *Free Radic. Biol. Med.* 89, 1154–1104.

Dietrich, R.A., Richberg, M.H., Schmidt, R., Dean, C., Dangl, J.L. (1997). A novel zinc finger protein is encoded by the Arabidopsis LSD1 gene and functions as a negative regulator of plant cell death. *Cell* 88, 685–694.

Dietz, K.-J. (2011). Peroxiredoxins in plants and cyanobacteria. *Antioxid. Redox Signal.* 15, 1129–1159.

Dijkwel, P.P., Lai, A.G. (2019). Hypothesis: Plant stem cells hold the key to extreme longevity. *Translational Medicine of Aging* 3, 14–16.

Dixon, D.P., Edwards, R. (2010). Glutathione S-transferases. *Arabidopsis Book* 8, e0131.

Dolzblasz, A., Smakowska, E., Gola, E.M., Sokolowska, K., Kicia, M., Janska, H. (2016). The mitochondrial protease AtFTSH4 safeguards *Arabidopsis* shoot apical meristem function. *Sci. Rep.* 6, 28315.

Du, Y.Y., Wang, P.C., Chen, J., Song, C.P. (2008). Comprehensive functional analysis of the catalase gene family in *Arabidopsis thaliana*. *J. Integrative Plant Biol.* 50, 1318–1326.

Duan, Q., Kita, D., Johnson, E.A., Aggarwal, M., Gates, L., Wu, H.-M., Cheung, A.Y. (2014). Reactive oxygen species mediate pollen tube rupture to release sperm for fertilization in Arabidopsis. *Nat Commun.* 5, 3129.

Emery, J.F., Floyd, S.K., Alvarez, J., Eshed, Y., Hawker, N.P., Izhaki, A., Baum, S.F., Bowman, J.L. (2003). Radial patterning of Arabidopsis shoots by class III HD-ZIP and KANADI genes. *Curr. Biol.* 13, 1768–1774.

Endo, H., Yamaguchi, M., Tamura, T., Nakano, Y., Nishikubo, N., Yoneda, A., Kato, K., Kubo, M., Kajita, S., Katayama, Y., Ohtani, M., Demura, T. (2015). Multiple classes of transcription factors regulate the expression of VASCULAR-RELATED NAC-DOMAIN7, a master switch of xylem vessel differentiation. *Plant Cell Physiol.* 56, 242–254.

Endrizzi, K, Moussian, B., Haecker, A., Levin, J.Z., Laux, T. (1996). The SHOOT MERISTEMLESS gene is required for maintenance of undifferentiated cells in Arabidopsis shoot and floral meristems and acts at a different regulatory level than the meristem genes WUSCHEL and ZWILLE. *Plant J.* 10, 967–979.

Epple, P., Mack, A.A., Morris, V.R.F., Dangl, J.L. (2003). Antagonistic control of oxidative stress-induced cell death in Arabidopsis by two related, plantspecific zinc finger proteins. *Proc. Natl. Acad. Sci. USA* 100, 6831–6836.

Escamez, S., André, D., Zhang, B., Bollhoner, B., Pesquet, E., Tuominen, H. (2016). METACASPASE9 modulates autophagy to confine cell death to the target cells during *Arabidopsis* vascular xylem differentiation. *Biol. Open* 5, 122–129.

Farage-Barhom, S., Burd, S., Sonego, L., Perl-Treves, R., Lers, A. (2008). Expression analysis of the BFN1 nuclease gene promoter during senescence, abscission, and programmed cell death–related processes. *J. Exp. Bot.* 59, 3247–3258.

Fendrych, M., Van Hautegem, T., Van Durme, M., Olvera-Carrillo, Y., Huysmans, M., Karimi, M., Lippens, S., Guérin, C.J., Krebs, M., Schumacher, K., Nowack, M.K. (2014). Programmed cell death controlled by ANAC033/SOMBRERO determines root cap organ size in Arabidopsis. *Curr. Biol.* 24, 931–940.

Fletcher, J.C. (2002). Shoot and floral meristem maintenance in Arabidopsis. *Annu. Rev. Plant Biol.* 53, 45–66.

Fletcher, J.C., Brand, U., Running, M.P., Simon, R., Meyerowitz, E.M. (1999) Signaling of cell fate decisions by *CLAVATA3* in *Arabidopsis* shoot meristems. *Science* 283, 1911–1914.

Foreman, J., Demidchik, V., Bothwell, J.H., Mylona, P., Miedema, H., Torres, M.A., Linstead, P., Costa, S., Brownlee, C., Jones, J.D., Davies, J.M., Dolan, L. (2003). Reactive oxygen species produced by NADPH oxidase regulate plant cell growth. *Nature* 422, 442–446.

Fouracre, J.P., Poethig, R.S. (2019). Role for the shoot apical meristem in the specification of juvenile leaf identity in *Arabidopsis*. *Proc. Natl. Acad. Sci. USA* 116, 10168–10177.

Fourquin, C., Beauzamy, L., Chamot, S., Creff, A., Goodrich, J., Boudaoud, A., Ingram, G. (2016). Mechanical stress mediated by both endosperm softening and embryo growth underlies endosperm elimination in Arabidopsis seeds. *Development* 143, 3300–3305.

Foyer, C.H., Noctor, G. (2005). Redox homeostasis and antioxidant signaling: a metabolic interface between stress perception and physiological responses. *Plant Cell* 17, 1866–1875.

Foyer, C.H., Noctor, G. (2009). Redox regulation in photosynthetic organisms: signaling, acclimation, and practical implications. *Antioxid. Redox Signal.* 11, 861–905.

Fridovich, I. (1997). Superoxide anion radical ($O_2^{\cdot -}$), superoxide dismuatases, and related matters. *J. Biol. Chem.* 272, 18515–18517.

Gaillochet, C., Stiehl, T., Wenzl, C., Ripoll, J.J., Bailey-Steinitz, L.J., Li, L., Pfeiffer, A., Miotk, A., Hakenjos, J.P., Forner, J., Yanofsky, M.F., Marciniak-Czochra, A., Lohmann, J.U. (2017). Control of plant cell fate transitions by transcriptional and hormonal signals. *eLife* 6, e30135.

Gao, Z., Daneva, A., Salanenka, Y., Van Durme, M., Huysmans, M., Lin, Z., De Winter, F., Vanneste, S., Karimi, M., Van de Velde, J., Vandepoele, K., Van de Walle, D., Dewettinck, K., Lambrecht, B.N., Nowack, M.K. (2018). KIRA1 and ORESARA1 terminate flower receptivity by promoting cell death in the stigma of Arabidopsis. *Nat Plants* 4, 365–375.

Gordon, S.P., Chickarmane, V.S., Ohno, C., Meyerowitz, E.M. (2009). Multiple feedback loops through cytokinin signaling control stem cell number within the Arabidopsis shoot meristem. *Proc. Natl. Acad. Sci. USA* 106, 16529–16534.

Gordon, S.P., Heisler, M.G., Reddy, G.V., Ohno, C., Das, P., Meyerowitz, E.M. (2007). Pattern formation during de novo assembly of Arabidopsis shoot meristem. *Development* 134, 3539–3548.

Green, K.A., Prigge, M.J., Katzman, R.B., Clark, S.E. (2005). *CORONA*, a member of the class Ⅲ homeodomain leucine zipper gene family in Arabidopsis, regulates stem cell specification and organogenesis. *Plant Cell* 17, 691–704.

Gu, J.N., Zhu, J., Yu, Y., Teng, X.D., Lou, Y., Xu, X.F., Liu, J.L., Yang, Z.N. (2014). DYT1 directly regulates the expression of TDF1 for tapetum development and pollen wall formation in Arabidopsis. *Plant Journal* 80, 1005–1013.

Guo, P., Li, Z., Huang, P., Li, B., Fang, S., Chu, J., Guo, H. (2017). A tripartite amplification loop involving the transcription factor WRKY75, salicylic acid, and reactive oxygen species accelerates leaf senescence. *Plant Cell* 29, 2854–2870.

Guo, Y., Gan, S.S. (2012). Convergence and divergence in gene expression profiles induced by leaf senescence and 27 senescence-promoting hormonal, pathological and environmental stress treatments. *Plant Cell Environ.* 35, 644–655.

Gutsche, N., Thurow, C., Zachgo, S., Gatz, C. (2015). Plant-specific CC-type glutaredoxins: functions in developmental processes and stress responses. *Biol. Chem.* 396, 495–509.

Hara-Nishimura, I., Hatsugai, N. (2011). The role of vacuole in plant cell death. *Cell Death Differ.* 18, 1298–1304.

Hensel, L.L., Grbić, V., Baumgarten, D.A., Bleecker, A.B. (1993). Developmental and Age-Related Processes That lnfluence the Longevity and Senescence of Photosynthetic Tissues in Arabidopsis. *Plant Cell* 5, 553–564.

Hensel, L.L., Nelson, M.A., Richmond, T.A., Bleeker, A.B. (1994). The fate of inflorescence meristems is controlled by developing fruits in *Arabidopsis*. *Plant Physiol.* 106, 863–876.

Holt, A.L., Van Haperen, J.M.A., Groot, E.P., Laux, T. (2014). Signaling in shoot and flower meristems of *Arabidopsis thaliana*. *Curr. Opin. Plant Biol.* 17, 96–102.

Hu, C., Zhu, Y., Cui, Y., Cheng, K., Liang, W., Wei, Z., Zhu, M., Yin, H., Zeng, L., Xiao, Y., Lv, M., Yi, J., Hou, S., He, K., Li, J., Gou, X. (2018). A group of receptor kinases are essential for CLAVATA signalling to maintain stem cell homeostasis. *Nat Plants* 4, 205–211.

Hu, L., Liang, W., Yin, C., Cui, X., Zong, J., Wang, X., Hu, J., Zhang, D. (2011). Rice MADS3 regulates ROS homeostasis during late anther development. *Plant Cell* 23, 515–533.

Huang, H., Ullah, F., Zhou, D.X., Yi, M., Zhao, Y. (2019). Mechanisms of ROS regulation of plant development and stress responses. *Front. Plant Sci.* 10, 1–10.

Huysmans, M., Buono, R.A., Skorzinski, N., Radio, M.C., De Winter, F., Parizot, B., Mertens, J., Karimi, M., Fendrych, M., Nowack, M.K. (2018). NAC Transcription Factors ANAC087 and ANAC046 control distinct aspects of programmed cell death in the Arabidopsis columella and lateral root cap. *Plant Cell* 30, 2197–2213.

Iqbal, A., Yabuta, Y., Takeda, T., Nakano, Y., Shigeoka, S. (2006). Hydroperoxide reduction by thioredoxin-specific glutathione peroxidase isoenzymes of *Arabidopsis thaliana*. *FEBS J.* 273, 5589–5597.

Ito, Y., Nakanomyo, I., Motose, H., Iwamoto, K., Sawa, S., Dohmae, N., Fukuda, H. (2006). Dodeca-CLE peptides as suppressors of plant stem cell differentiation. *Science* 31, 842–845.

Jabs, T., Dietrich, R.A., Dangl, J.L. (1996). Initiation of runaway cell death in an *Arabidopsis* mutant by extracellular superoxide. *Science* 273, 1853–1856.

Jasinski, S., Piazza, P., Craft, J., Hay, A., Woolley, L., Rieu, I., Phillips, A., Hedden, P., Tsiantis, M. (2005). KNOX action in Arabidopsis is mediated by coordinate regulation of cytokinin and gibberellin activities. *Curr. Biol.* 15, 1560–1565.

Jeong, S., Trotochaud, A.E., Clark, S.E. (1999). The Arabidopsis CLAVATA2 gene encodes a receptor-like protein required for the stability of the CLAVATA1 receptor-like kinase. *Plant Cell* 11, 1925–1933.

Jha, P., Ochatt, S.J., Kumar, V. (2020). *WUSCHEL*: a master regulator in plant growth signaling. *Plant Cell Rep.* 39, 431–444.

Jones, A.M. (2001). Programmed cell death in development and defense. *Plant Physiol.* 125, 94–97.

Kamdee, C., Kirasak, K., Ketsa, S., van Doorn, W.G. (2015). Vesicles between plasma membrane and cell wall prior to visible senescence of Iris and Dendrobium flowers. *J. Plant Physiol.* 188, 37–43.

Karami, O., Rahimi, A., Khan, M., Bemer, M., Hazarika, R.R., Mak, P., Compier, M., van Noort, V., Offringa, R. (2020). A suppressor of axillary meristem maturation promotes longevity in flowering plants. *Nat Plants* 6, 368–376.

Katsir, L., Davies, K.A., Bergmann, D.C., Laux T. (2011). Peptide signaling in plant development. *Curr. Biol.* 21, 356–364.

Kerr, J.F., Wyllie, A.H., Currie, A.R. (1972). Apoptosis: a basic biological phenomenon with wide-ranging implications in tissue kinetics. *Br. J. Cancer* 26, 239–257.

Khan, B.R., Adham, A.R., Zolman, B.K. (2012). Peroxisomal Acyl-CoA oxidase 4 activity differs between Arabidopsis accessions. *Plant Mol. Biol.* 78, 45–58

Kim, H.J., Hong, S.H., Kim, Y.W., Lee, I.H., Jun, J.H., Phee, B.K., Rupak, T., Jeong, H., Lee, Y., Hong, B.S., Nam, H.G., Woo, H.R., Lim, P.O. (2014). Gene regulatory cascade of

senescence-associated NAC transcription factors activated by ETHYLENE-INSENSITIVE2-mediated leaf senescence signalling in Arabidopsis. *J. Exp. Bot.* 65, 4023–4036.

Kinoshita, A., Betsuyaku, S., Osakabe, Y., Mizuno, S., Nagawa, S., Stahl, Y., Simon, R., Yamaguchi-Shinozaki, K., Fukuda, H., Sawa, S. (2010). RPK2 is an essential receptor-like kinase that transmits the CLV3 signal in Arabidopsis. *Development* 137, 3911–3920.

Kitagawa, M., Balkunde, R., Bui, H., Jackson, D. (2019). An Aminoacyl tRNA Synthetase, OKI1, Is Required for Proper Shoot Meristem Size in *Arabidopsis*. *Plant Cell Physiol*. 60, 2597–2608.

Klimešová, J., Nobis, M., Herben, T. (2015). Senescence, ageing and death of the whole plant: morphological prerequisites and constraints of plant immortality. *New Phytol.* 206, 14–18.

Knauer, S., Holt, A.L., Rubio-Somoza, I., Tucker, E.J., Hinze, A., Pisch, M., Javelle, M., Timmermans, M.C., Tucker, M.R., Laux, T. (2013). A protodermal miR394 signal defines a region of stem cell competence in the Arabidopsis shoot meristem. *Dev. Cell* 24, 125–132.

Kondo, T., Sawa, S., Kinoshita, A., Mizuno, S., Kakimoto, T., Fukuda, H., Sakagami, Y. (2006). A plant peptide encoded by CLV3 identified by in situ MALDI-TOF MS analysis. *Science* 313, 845–848.

Kondou, Y., Nakazawa, M., Kawashima, M., Ichikawa, T., Yoshizumi, T., Suzuki, K., Ishikawa, A., Koshi, T., Matsui, R., Muto, S., Matsui, M. (2008). RETARDED GROWTH OF EMBRYO1, a new basic helix-loop-helix protein, expresses in endosperm to control embryo growth. *Plant Physiol.* 147, 1924–1935.

Koyama, T. (2014). The roles of ethylene and transcription factors in the regulation of onset of leaf senescence. *Front. Plant Sci.* 5, 650.

Kubo, M., Udagawa, M., Nishikubo, N., Horiguchi, G., Yamaguchi, M., Ito, J., Mimura, T., Fukuda, H., Demura, T. (2005). Transcription switches for protoxylem and metaxylem vessel formation. *Genes Dev.* 19, 1855–1860.

Landrein, B., Formosa-Jordan, P., Malivert, A., Schuster, C., Melnyk, C.W., Yang, W., Turnbull, C., Meyerowitz, E.M., Locke, J., Jönsson, H. (2018). Nitrate modulates stem cell dynamics in Arabidopsis shoot meristems through cytokinins. *Proc. Natl. Acad. Sci. USA* 115, 1382–1387.

Laux, T., Mayer, K.F., Berger, J., Jurgens, G. (1996). The WUSCHEL gene is required for shoot and floral meristem integrity in Arabidopsis. *Development* 122, 87–96.

Lee, H., Jun, Y.S., Cha, O.-K., Sheen, J. (2019). Mitogen-activated protein kinases MPK3 and MPK6 are required for stem cell maintenance in the Arabidopsis shoot apical meristem. Plant *Cell Rep.* 38, 311–319.

Leibfried, A., To, J.P., Busch, W., Stehling, S., Kehle, A., Demar, M., Kieber, J.J., Lohmann, J.U. (2005). WUSCHEL controls meristem function by direct regulation of cytokinin-inducible response regulators. *Nature* 438, 1172.

Lenhard, M., Jürgens, G., Laux, T. (2002). The WUSCHEL and SHOOTMERISTEMLESS genes fulfil complementary roles in Arabidopsis shoot meristem regulation. *Development* 129, 3195–3206.

Lenhard, M., Laux, T. (2003). Stem cell homeostasis in the Arabidopsis shoot meristem is regulated by intercellular movement of CLAVATA3 and its sequestration by CLAVATA1. *Development* 130, 3163–3173.

Lesgemy, Y. (1981). Oxygen free radicals and plant senescence. *Wheats New in Plant Physiol.* 12, 124.

Leydon, A.R., Beale, K.M., Woroniecka, K., Castner, E., Chen, J., Horgan, C., Palanivelu, R., Johnson, M.A. (2013). Three MYB transcription factors control pollen tube differentiation required for sperm release. *Curr. Biol.* 23, 1209–1214.

Li, N., Sun, L., Zhang, L., Song, Y., Hu, P., Li, C., Hao, F.S. (2015). AtrbohD and AtrbohF negatively regulate lateral root development by changing the localized accumulation of superoxide in primary roots of Arabidopsis. *Planta* 241, 591–602.

Liang, Y., Tan, Z.M., Zhu, L., Niu, Q.K., Zhou, J.J., Li, M., Chen, L.Q., Zhang, X.Q., Ye, D. (2013). MYB97, MYB101 and MYB120 function as male factors that control pollen tube-synergid interaction in *Arabidopsis thaliana* fertilization. *PLoS Genet.* 9, e1003933.

Liu, Q., Yao, X., Pi, L., Wang, H., Cui, X., Huang, H. (2009). The ARGONAUTE10 gene modulates shoot apical meristem maintenance and establishment of leaf polarity by repressing miR165/166 in Arabidopsis. *Plant J.* 58, 27–40.

Livak, K.J., Schmittgen, T.D. (2001). Analysis of Relative Gene Expression Data Using Real-Time Quantitative PCR and the $2^{-\Delta\Delta CT}$ Method. *Methods* 25, 402–408.

Locato, V., De Gara, L. (2018). Programmed Cell Death in Plants: An Overview. *Methods in molecular biology* (Clifton, N.J.) 1743, 1–8.

Luo, D., Xu, H., Liu, Z., Guo, J., Li, H., Chen, L., Fang, C., Zhang, Q., Bai, M., Yao, N., Wu, H., Wu, H., Ji, C., Zheng, H., Chen, Y., Ye, S., Li, X., Zhao, X., Li, R., Liu, Y.G. (2013). A detrimental mitochondrial-nuclear interaction causes cytoplasmic male sterility in rice. *Nat Genet.* 45, 573–577.

Luo, L., Zeng, J., Wu, H., Tian, Z., Zhao, Z. (2018). A molecular framework for auxin-controlled homeostasis of shoot stem cells in Arabidopsis. *Mol. Plant* 11, 899–913.

Lynn, K., Fernandez, A., Aida, M., Sedbrook, J., Tasaka, M., Masson, P., Barton, M.K. (1999). The *PINHEAD/ZWILLE* gene acts pleiotropically in Arabidopsis development and has overlapping functions with the *ARGONAUTE1* gene. *Development* 126, 469–481.

Ma, Y., Miotk, A., Šutiković, Z., Ermakova, O., Wenzl, C., Medzihradszky, A., Gaillochet, C., Forner, J., Utan, G., Brackmann, K., Galván-Ampudia, C.S., Vernoux, T., Greb, T., Lohmann, J.U. (2019). WUSCHEL acts as an auxin response rheostat to maintain apical stem cells in Arabidopsis. *Nat Commun*. 10, 5093.

Mangano, S., Denita-Juarez, S.P., Choi, H.S., Marzol, E., Hwang, Y., Ranocha, P., Velasquez, S.M., Borassi, C., Barberini, M.L., Aptekmann, A.A., Muschietti, J.P., Nadra, A.D., Dunand, C., Cho, H.T., Estevez, J.M. (2017). Molecular link between auxin and ROS-mediated polar growth. *Proc. Natl. Acad. Sci. USA* 114, 5289–5294.

Martin, C., Thimann, K.N. (1972). The role of protein synthesis in the senescence of leaves. *Plant Physiol.* 49, 64–71.

Marty, F. (1997). The biogenesis of vacuoles: insights from microscopy. In: Leigh RA, Sanders D, eds. The plant vacuole. *Advances in Botanical Research*, Vol. 25. San Diego, CA: Academic Press, 1–42.

Marty, F. (1999). Plant vacuoles. *Plant Cell* 11, 587–600.

Matallana-Ramirez, L.P., Rauf, M., Farage-Barhom, S., Dortay, H., Xue, G.P., Dröge-Laser, W., Lers, A., Balazadeh, S., Mueller-Roeber, B. (2013). NAC transcription factor ORE1 and

senescence-induced *BIFUNCTIONAL NUCLEASE1* (*BFN1*) constitute a regulatory cascade in *Arabidopsis*. *Mol. Plant* 6, 1432–1452.

Matile, P., Winkenbach, F. (1971). Function of lysosomal enzymes in the senescing corolla of the morning glory (*Ipomoea purpua*). *J. Exp. Bot.* 22, 759–771.

Mayer, K.F., Schoof, H., Haecker, A., Lenhard, M., Jürgens, G., Laux, T. (1998) Role of *WUSCHEL* in regulating stem cell fate in the *Arabidopsis* shoot meristem. *Cell* 95, 805–815.

McConnell, J.R., Barton, M.K. (1995). Effects of mutations in the PINHEAD gene of Arabidopsis on the formation of shoot apical meristems. *Dev. Genet.* 16, 358–366.

McConnell, J.R., Emery, J., Eshed, Y., Bao, N., Bowman, J., Barton, M.K. (2001). Role of PHABULOSA and PHAVOLUTA in determining radial patterning in shoots. *Nature* 411, 709–713.

Meng, W.J., Cheng, Z.J., Sang, Y.L., Zhang, M.M., Rong, X.F., Wang, Z.W., Tang, Y.Y., Zhang, X.S. (2017). Type-B ARABIDOPSIS RESPONSE REGULATORs specify the shoot stem cell niche by dual regulation of WUSCHEL. *Plant Cell* 29, 1357–1372.

Meyerowitz, E.M. (1997). Genetic control of cell division patterns in developing plants. *Cell* 88, 299–308.

Mhamdi, A., Van Breusegem, F. (2018). Reactive oxygen species in plant development. *Development* 145, dev164376.

Mittler, R. (2017). ROS are good. *Trends Plant Sci.* 22, 11–19.

Mittler, R., Vanderauwera, S., Gollery, M., Van Breusegem, F. (2004). The reactive oxygen gene network in plants. *Trends Plant Sci.* 9, 490–498.

Moll, C., von Lyncker, L., Zimmermann, S., Kägi, C., Baumann, N., Twell, D., Grossniklaus, U., Gross-Hardt, R. (2008). CLO/GFA1 and ATO are novel regulators of gametic cell fate in plants. *Plant J.* 56, 913–921.

Moller, I.M. (2001). Plant mitochondria and oxidative stress: electron transport, NADPH turnover, and metabolism of reactive oxygen species. *Annu. Rev. Plant Physiol. Plant Mol. Biol.* 52, 561–591.

Moussian, B., Schoof, H., Haecker, A., Jurgens, G., Laux, T. (1998). Role of the ZWILLE gene in the regulation of central shoot meristem cell fate during Arabidopsis embryogenesis. *EMBO J.* 17, 1799–1809.

Müller, R., Bleckmann, A., Simon, R. (2008). The receptor kinase CORYNE of Arabidopsis transmits the stem cell–limiting signal CLAVATA3 independently of CLAVATA1. *Plant Cell* 20, 934–946.

Munné-Bosch, S., Queval, G., Foyer, C.H. (2013). The impact of global change factors on redox signaling underpinning stress tolerance. *Plant Physiol.* 161, 5–19.

Murmu, J., Bush, M.J., DeLong, C., Li, S., Xu, M., Khan, M., Malcolmson, C., Fobert, P.R., Zachgo, S., Hepworth, S.R. (2010). Arabidopsis basic leucinezipper transcription factors TGA9 and TGA10 interact with floral glutaredoxins ROXY1 and ROXY2 and are redundantly required for anther development. *Plant Physiol.* 154, 1492–1504.

Nakagami, H., Kiegerl, S., Hirt, H. (2004). OMTK1, a novel MAPKKK, channels oxidative stress signaling through direct MAPK interaction. *J. Biol. Chem.* 279, 26959–26966.

Noctor, G., Lelarge-Trouverie, C., Mhamdi, A. (2015). The metabolomics of oxidative stress. *Phytochemistry* 112, 33–53.

Noctor, G., Mhamdi, A., Chaouch, S., Han, Y., Neukermans, J., Marquez-Garcia, B., Queval, G., Foyer, C.H. (2012). Glutathione in plants: an integrated overview. *Plant Cell Environ*. 35, 454–484.

Noodén, L.D., Penney, J.P. (2001). Correlative controls of senescence and plant death in *Arabidopsis thaliana* (*Brassicaceae*). *J. Exp. Bot.* 52, 2151–2159.

Ogawa, M., Shinohara, H., Sakagami, Y., Matsubayashi, Y. (2008). Arabidopsis CLV3 peptide directly binds CLV1 ectodomain. *Science* 319, 294.

Ohyama, K., Shinohara, H., Ogawa-Ohnishi, M., Matsubayashi, Y. (2009). A glycopeptide regulating stem cell fate in *Arabidopsis thaliana*. *Nat. Chem. Biol.* 5, 578–580.

Olvera-Carrillo, Y., Van Bel, M., Van Hautegem, T., Fendrych, M., Huysmans, M., Simaskova, M., van Durme, M., Buscaill, P., Rivas, S., Coll, N.S., Coppens, F., Maere, S., Nowack, M.K. (2015). A conserved core of programmed cell death indicator genes discriminates developmentally and environmentally induced programmed cell death in plants. *Plant Physiol.*

169, 2684–2699.

Orman-Ligeza, B., Parizot, B., de Rycke, R., Fernandez, A., Himschoot, E., Van Breusegem, F., Bennett, M.J., Périlleux, C., Beeckman, T., Draye, X. (2016). RBOH-mediated ROS production facilitates lateral root emergence in *Arabidopsis*. *Development* 143, 3328–3339.

Ortiz-Espín, A., Iglesias-Fernandez, R., Calderón, A., Carbonero, P., Sevilla, F., Jiménez, A. (2017). Mitochondrial AtTrxo1 is transcriptionally regulated by AtbZIP9 and AtAZF2 and affects seed germination under saline conditions. *J. Exp. Bot.* 68, 1025–1038.

Pagnussat, G.C., Yu, H.-J., Ngo, Q.A., Rajani, S., Mayalagu, S., Johnson, C.S., Capron, A., Xie, L.F., Ye, D., Sundaresan, V. (2005). Genetic and molecular identification of genes required for female gametophyte development and function in *Arabidopsis*. *Development* 132, 603–614.

Passaia, G., Queval, G., Bai, J., Margis-Pinheiro, M., Foyer, C.H. (2014). The effects of redox controls mediated by glutathione peroxidases on root architecture in *Arabidopsis thaliana*. *J. Exp. Bot.* 65, 1403–1413.

Perales, M., Rodriguez, K., Snipes, S., Yadav, R.K., Diaz-Mendoza, M., Reddy, G.V. (2016). Threshold-dependent transcriptional discrimination underlies stem cell homeostasis. *Proc. Natl. Acad. Sci. USA* 113, E6298–E6306.

Pérez-Amador, M.A., Abler, M.L., Rocher, E.J.D., Thompson, D.M., van Hoof, A., LeBrasseur, N.D., Lers, A., Green, P.J. (2000). Identification of BFN1, a bifunctional nuclease induced during leaf and stem senescence in Arabidopsis. *Plant Physiol.* 122, 169–179.

Peshev, D., Vergauwen, R., Moglia, A., Hideg, E., van den Ende, W. (2013). Towards understanding vacuolar antioxidant mechanisms: a role for fructans? *J. Exp. Bot.* 64, 1025–1038.

Petrov, V., Hille, J., Mueller-Roeber, B., Gechev, T. (2015). ROS-mediated abiotic stress-induced programmed cell death in plants. *Front. Plant Sci.* 6, 69.

Pfeiffer, A., Janocha, D., Dong, Y., Medzihradszky, A., Schöne, S., Daum, G., Suzaki, T., Forner, J., Langenecker, T., Rempel, E., Schmid, M., Wirtz, M., Hell, R., Lohmann, J.U. (2016). Integration of light and metabolic signals for stem cell activation at the shoot apical meristem. *eLife* 5, e17023.

Potocký, M., Pejchar, P., Gutkowska, M., Jiménez-Quesada, M.J., Potocká, A., Alché Jde, D., Kost, B., Žárský, V. (2012). NADPH oxidase activity in pollen tubes is affected by calcium ions, signaling phospholipids and Rac/Rop GTPases. *J. Plant Physiol.* 169, 1654–1663.

Prigge, M.J., Otsuga, D., Alonso, J.M., Ecker, J.R., Drews, G.N., Clark, S.E. (2005). Class III homeodomain-leucine zipper gene family members have overlapping, antagonistic, and distinct roles in Arabidopsis development. *Plant Cell* 17, 61–76.

Putcha, G.V., Johnson Jr., E.M. (2004). Men are but worms: neuronal cell death in *C elegans* and vertebrates. *Cell Death Differ.* 11, 38–48.

Queval, G., Issakidis-Bourguet, E., Hoeberichts, F.A., Vandorpe, M., Gakiere, B., Vanacker, H., Miginiac-Maslow, M., Van Breusegem, F., Noctor, G. (2007). Conditional oxidative stress responses in the *Arabidopsis* photorespiratory mutant cat2 demonstrate that redox state is a key modulator of daylength-dependent gene expression, and define photoperiod as a crucial factor in the regulation of $H_2O_2$-induced cell death. *Plant J.* 52, 640–657.

Quon, T., Lampugnani, E.R., Smyth, D.R. (2017). PETAL LOSS and ROXY1 interact to limit growth within and between sepals but to promote petal initiation in *Arabidopsis thaliana*. *Front. Plant Sci.* 8, 152.

Ray, S., Choudhuri, M.A. (1980). Flag leaf senescence in intact rice plant: Effects of hormones on the activities of “senescence-enzymes” during leaf age at the reproductive development. *Biochem. Physiol. Pflanz.* 175, 346–353.

Reddy, V., Meyerowitz, E.M. (2005). Stem-cell homoeostasis and growth dynamics can be uncoupled in the Arabidopsis shoot apex. *Science* 310, 663–667.

Reichheld, J.-P., Khafif, M., Riondet, C., Droux, M., Bonnard, G., Meyer, Y. (2007). Inactivation of thioredoxin reductases reveals a complex interplay between thioredoxin and glutathione pathways in Arabidopsis development. *Plant Cell* 19, 1851–1865.

Ren, D., Yang, H., Zhang, S. (2002). Cell death mediated by MAPK is associated with hydrogen peroxide production in Arabidopsis. *J. Biol. Chem.* 277, 559–565.

Rhinn, M., Ritschka, B., Keyes, W.M. (2019). Cellular senescence in development, regeneration and disease. *Development* 146, dev151837.

Rich, T., Allen, R.L., Wyllie, A.H. (2000). Defying death after DNA damage. *Nature* 407,

777–783.

Richards, S.L., Wilkins, K.A., Swarbreck, S.M., Anderson, A.A., Habib, N., Smith, A.G., McAinsh, M., Davies, J.M. (2015). The hydroxyl radical in plants: from seed to seed. *J. Exp. Bot.* 66, 37–46.

Rodriguez, K., Perales, M., Snipes, S., Yadav, R.K., Diaz-Mendoza, M., Reddy, G.V. (2016). DNA-dependent homodimerization, sub-cellular partitioning, and protein destabilization control WUSCHEL levels and spatial patterning. *Proc. Natl. Acad. Sci. USA.* 113, E6307–E6315.

Rogers, H., Munné-Bosch, S. (2016). Production and scavenging of reactive oxygen species and redox signaling during leaf and flower senescence: similar but different. *Plant Physiol.* 171, 1560–1568.

Rogers, H.J. (2013). From models to ornamentals: How is flower senescence regulated? *Plant Mol. Biol. Rep.* 82, 563–574.

Roldán-Arjona, T., Ariza, R.R. (2009). Repair and tolerance of oxidative DNA damage in plants. *Mutation Res.* 681, 169–179.

Rosenwasser, S., Rot, I., Sollner, E., Meyer, A.J., Smith, Y., Leviatan, N., Fluhr, R., Friedman, H. (2011). Organelles contribute differentially to reactive oxygen species-related events during extended darkness. *Plant Physiol.* 156, 185–201.

Ryan, C.A. (1973). Proteolytic enzymes and their inhibitors in plants. *Ann. Rev. Plant Physiol.* 24, 173–196.

Samuel, M.A., Ellis, B.E. (2002). Double jeopardy: both overexpression and suppression of a redox-activated plant-mitogen-activated protein kinase render tobacco plants ozone sensitive. *Plant Cell* 14, 2059–2069.

Samuel, M.A., Hall, H., Krzymowska, M., Drzewiecka, K., Hennig, J., Ellis, B.E. (2005). SIPK signaling controls multiple components of harpin-induced cell death in tobacco. *Plant J.* 42: 406–416.

Schindelin, J., Arganda-Carreras, I., Frise, E., Kaynig, V., Longair, M., Pietzsch, T., Preibisch, S., Rueden, C., Saalfeld, S., Schmid, B., Tinevez, J.Y., White, D.J., Hartenstein, V., Eliceiri, K., Tomancak, P., Cardona, A. (2012). Fiji: an open-source platform for biological-image

analysis. *Nat Methods* 9, 676–682.

Schippers, J.H.M., Foyer, C.H., van Dongen, J.T. (2016). Redox regulation in shoot growth, SAM maintenance and flowering. *Curr. Opin. Plant Biol.* 29, 121–128.

Schoof, H., Lenhard, M., Haecker, A., Mayer, K.F., Jürgens, G., Laux, T. (2000). The stem cell population of Arabidopsis shoot meristems is maintained by a regulatory loop between the *CLAVATA* and *WUSCHEL* genes. *Cell* 100, 635–644.

Schulze, S., Schäfer, B.N., Parizotto, E.A., Voinnet, O., Theres, K. (2010). LOST MERISTEMS genes regulate cell differentiation of central zone descendants in Arabidopsis shoot meristems. *Plant J.* 64, 668–678.

Schumacher, B., Hofmann, K., Boulton, S., Gartner, A. (2001). The *C. elegans* homolog of the p53 tumor suppressor is required for DNA damage-induced apoptosis. *Curr. Biol.* 11, 1722–1727.

Schuster, C., Gaillochet, C., Medzihradszky, A., Busch, W., Daum, G., Krebs, M., Kehle, A., Lohmann, J.U. (2014). A regulatory framework for shoot stem cell control integrating metabolic, transcriptional, and phytohormone signals. *Dev. Cell* 28, 438–449.

Shi, B.H., Guo, X.L., Wang,Y., Xiong, Y.Y., Wang, J., Hayashi, K.I., Lei, J.Z., Zhang, L., Jiao, Y.L. (2018). Feedback from Lateral Organs Controls Shoot Apical Meristem Growth by Modulating Auxin Transport. *Dev. Cell* 44, 204–216.

Shibuya, K. (2018). Molecular aspects of flower senescence and strategies to improve flower longevity. *Breeding Sci.* 68, 99–108.

Shibuya, K., Yamada, T., Ichimura, K. (2016). Morphological changes in senescing petal cells and the regulatory mechanism of petal senescence. *J. Exp. Bot.* 67, 5909–5918.

Shirakawa, M., Ueda, H., Nagano, A. J., Shimada, T., Kohchi, T., Hara-Nishimura, I. (2014). FAMA is an essential component for the differentiation of two distinct cell types, myrosin cells and guard cells, in Arabidopsis. *Plant Cell* 26, 4039–4052.

Shubin, A.V., Demidyuk, I.V., Komissarov, A.A., Rafieva, L.M., Kostrov, S.V. (2016). Cytoplasmic vacuolization in cell death and survival. *Oncotarget* 7, 55863–55889.

Singh, M.B., Bhalla, P.L. (2006). Plant stem cells carve their own niche. *Trends Plant Sci.* 11,

241–246.

Skubacz, A., Daszkowska-Golec, A., Szarejko, I. (2016). The role and regulation of ABI5 (ABA-Insensitive 5) in plant development, abiotic stress responses and phytohormone crosstalk. *Front. Plant Sci.* 16, 1884.

Sloan, J., Hakenjos, J.P., Gebert, M., Ermakova, O., Gumiero, A., Stier, G., Wild, K., Sinning, I., Lohmann, J.U. (2020). Structural basis for the complex DNA binding behavior of the plant stem cell regulator WUSCHEL. *Nat Commun.* 11, 2223.

Smyth, D.R., Bowman, J.L., Meyerowitz, E.M. (1990). Early flower development in Arabidopsis. *Plant Cell* 2, 755–767.

Snipes, S.A., Rodriguez, K., DeVries, A.E., Miyawaki, K.N., Perales, M., Xie, M., Reddy, G.V. (2018). Cytokinin stabilizes WUSCHEL by acting on the protein domains required for nuclear enrichment and transcription. *PLoS Genet.* 14, e1007351.

Stacey, M.G., Osawa, H., Patel, A., Gassmann, W., Stacey, G. (2006). Expression analyses of Arabidopsis oligopeptide transporters during seed germination, vegetative growth and reproduction. *Planta* 223, 291–305.

Steeves, T.A., Sussex, I.M. (1989). Patterns in Plant Development, 2nd edn. Cambridge: Cambridge University Press.

Stuurman, J., Jäggi, F., Kuhlemeier, C. (2002). Shoot meristem maintenance is controlled by a GRAS-gene mediated signal from differentiating cells. *Genes Dev.* 16, 2213–2218.

Su, Y.H., Zhou, C., Li, Y.J., Yu, Y., Tang, L.P., Zhang, W.J., Yao, W.J., Huang, R., Laux, T., Zhang, X.S. (2020). Integration of pluripotency pathways regulates stem cell maintenance in the Arabidopsis shoot meristem. *Proc. Natl. Acad. Sci. USA* 117, 22561–22571.

Sun, B., Zhou, Y., Cai, J., Shang, E., Yamaguchi, N., Xiao, J., Looi, L.S., Wee, W.Y., Gao, X., Wagner, D., Ito, T. (2019). Integration of transcriptional repression and polycomb-mediated silencing of WUSCHEL in floral meristems. *Plant Cell* 31, 1488–1505.

Sundaravelpandian, K., Chandrika, N.N.P., Schmidt, W. (2013). PFT1, a transcriptional Mediator complex subunit, controls root hair differentiation through reactive oxygen species (ROS) distribution in Arabidopsis. *New Phytol.* 197, 151–161.

Tan, T.T., Endo, H., Sano, R., Kurata, T., Yamaguchi, M., Ohtani, M., Demura, T. (2018). Transcription Factors VND1-VND3 Contribute to Cotyledon Xylem Vessel Formation. *Plant physiol.* 176, 773–789.

Tata, J.R. (1966). Requirement for RNA and protein synthesis for induced regression of the tadpole tail in organ culture. *Dev. Biol.* 13, 77–94.

Thomas, H. (2013). Senescence, Ageing and Death of the Whole Plant. *New Phytol.* 197, 696–711.

Tognetti, V.B., Bielach, A., Hrtyan, M. (2017). Redox regulation at the site of primary growth: auxin, cytokinin and ROS crosstalk. *Plant Cell Environ.* 40, 2586–2605.

Triantaphylidès, C., Havaux, M. (2009). Singlet oxygen in plants: production, detoxification and signaling. *Trends Plant Sci.* 14, 219–228.

Tsukagoshi, H., Busch, W., Benfey, P.N. (2010). Transcriptional regulation of ROS controls transition from proliferation to differentiation in the root. *Cell* 143, 606–616.

Uemura, A., Yamaguchi, N., Xu, Y., Wee, W., Ichihashi, Y., Suzuki, T., Shibata, A., Shirasu, K., Ito, T. (2018). Regulation of floral meristem activity through the interaction of AGAMOUS, SUPERMAN, and CLAVATA3 in Arabidopsis. *Plant Reprod.* 31, 89–105.

Van Breusegem, F., Dat J.F. (2006). Reactive Oxygen Species in Plant Cell Death. *Plant Physiol.* 141, 384–390.

van der Graaff, E., Laux, T., Rensing, S.A. (2009). The WUS homeobox-containing (WOX) protein family. *Genome Biol.* 10, 248.

van Doorn, W.G. (2011). Classes of programmed cell death in plants, compared to those in animals. *J. Exp. Bot.* 62, 4749–4761.

van Doorn, W.G., Balk, P.A., van Houwelingen, A.M., Hoeberichts, F.A., Hall, R.D., Vorst, O., van der Schoot, C., van Wordragen, M.F. (2003). Gene expression during anthesis and senescence in Iris flowers. *Plant Mole. Biol.* 53, 845–863.

Van Hautegem, T., Waters, A.J., Goodrich, J., Nowack, M.K. (2015). Only in dying, life: programmed cell death during plant development. *Trends Plant Sci.* 20, 102–113.

Wagner, D., Przybyla, D., Op den Camp, R., Kim, C., Landgraf, F., Lee, K.P., Würsch, M., Laloi, C., Nater, M., Hideg, E., Apel, K. (2004). The genetic basis of singlet oxygen-induced stress responses of *Arabidopsis thaliana*. *Science* 306, 1183–1185.

Wang, Y., Bai, J., Wang, P., Duan, W., Yuan, S., Zhang, F., Gao, S., Liu, L., Pang, B., Zhang, L., Zhao, C. (2018). Comparative transcriptome analysis identifies genes involved in the regulation of the pollen cytoskeleton in a genic male sterile wheat line. *Plant Growth Regul.* 86, 133–147.

Wang, Y., Kumaishi, K., Suzuki, T., Ichihashi, Y., Yamaguchi, N., Shirakawa, M., Ito, T. (2020). Morphological and Physiological Framework Underlying Plant Longevity in *Arabidopsis thaliana*. *Front. Plant Sci.* 11, 600726.

Ware, A., Walker, C., Simura, J., González-Suárez, P., Ljung, K., Bishopp, A., Wilson, Z., Bennett, T. (2020). Auxin export from proximal fruits drives arrest in competent inflorescences. *Na. Plants* 6, 699–707.

Weigel, D., Jürgens, G. (2002). Stem cells that make stems. *Nature* 415, 751.

Wiemken-Gehrig, V., Wiemken, A., Matile, P. (1974). Mobilisation der Zellwandstoffen in der welkenden Blüte von Ipomoea tricolor (Cav.). *Planta* 115, 297–307.

Williams, L., Fletcher, J.C. (2005). Stem cell regulation in the Arabidopsis shoot apical meristem. *Curr. Opin. Plant. Biol.* 8, 582–586.

Wojciechowska, M., Olszewska, M.J. (2003). Endosperm degradation during seed development of *Echinocystis lobata* (Cucurbitaceae) as a manifestation of programmed cell death (PCD) in plants. *Folia Histochem. Cytobiol.* 41, 41–50.

Wu, A., Allu, A.D., Garapati, P., Siddiqui, H., Dortay, H., Zanor, M.I., Asensi-Fabado, M.A., Munné-Bosch, S., Antonio, C., Tohge, T., Fernie, A.R., Kaufmann, K., Xue, G.P., Mueller-Roeber, B., Balazadeh, S. (2012). JUNGBRUNNEN1, a reactive oxygen species-responsive NAC transcription factor, regulates longevity in Arabidopsis. *Plant Cell* 24, 482–506.

Wu, H., Qu, X., Dong, Z., Luo, L., Shao, C., Forner, J., Lohmann, J.U., Su, M., Xu, M., Liu, X., Zhu, L., Zeng, J., Liu, S., Tian, Z., Zhao, Z. (2020). WUSCHEL triggers innate antiviral immunity in plant stem cells. *Science* 370, 227–231.

Wu, J., Ichihashi, Y., Suzuki, T., Shibata, A., Shirasu, K., Yamaguchi, N., Ito, T. (2019). Abscisic acid-dependent histone demethylation during postgermination growth arrest in Arabidopsis. *Plant Cell Environ.* 42, 2198–2214.

Wu, L., Chen, H., Curtis, C., Fu, Z.Q. (2014). Go in for the kill: how plants deploy effector-triggered immunity to combat pathogens. *Virulence* 5, 710–721.

Wuest, S.E., Philipp, M. A., Guthörl, D., Schmid, B., Grossniklaus, U. (2016). Seed production affects maternal growth and senescence in *Arabidopsis*. *Plant Physiol.* 171, 392–404.

Wuest, S.E., Philipp, M.A., Guthorl, D., Schmid, B., Grossniklaus, U. (2016). Seed production affects maternal growth and senescence in Arabidopsis. *Plant Physiol.* 171, 392–404.

Xie, M., Chen, H., Huang, L., O'Neil, R.C., Shokhirev, M.N., Ecker, J.R. (2018). A BARR-mediated cytokinin transcriptional network directs hormone cross-regulation and shoot development. *Nat. Commun.* 9, 1604.

Xing, S., Zachgo, S. (2008). ROXY1 and ROXY2, two Arabidopsis glutaredoxin genes, are required for anther development. *Plant J.* 53, 790–801.

Xing, S., Rosso, M. G., Zachgo, S. (2005). ROXY1, a member of the plant glutaredoxin family, is required for petal development in *Arabidopsis thaliana*. *Development* 132, 1555–1565.

Yadav, R.K., Girke, T., Pasala, S., Xie, M., Reddy, G.V. (2009). Gene expression map of the Arabidopsis shoot apical meristem stem cell niche. *Proc. Natl. Acad. Sci. USA.* 106, 4941–4946.

Yadav, R.K., Perales, M., Gruel, J., Girke, T., Jönsson, H., Reddy, G.V. (2011). WUSCHEL protein movement mediates stem cell homeostasis in the Arabidopsis shoot apex. *Genes Dev.* 25, 2025–2030.

Yadav, R.K., Tavakkoli, M., Reddy, G.V. (2010). WUSCHEL mediates stem cell homeostasis by regulating stem cell number and patterns of cell division and differentiation of stem cell progenitors. *Development* 137, 3581–3589.

Yamada, T., Ichimura, K., van Doorn, W.G. (2006a). DNA degradation and nuclear degeneration during programmed cell death in petals of Antirrhinum, Argyranthemum, and

Petunia. *J. Exp. Bot.* 57, 3543–3552.
Yamada, T., Takatsu, Y., Kasumi, M., Ichimura, K., van Doorn, W.G. (2006b). Nuclear fragmentation and DNA degradation during programmed cell death in petals of morning glory (*Ipomoea nil*). *Planta* 224, 1279–1290.

Yamaguchi, M., Goué, N., Igarashi, H., Ohtani, M., Nakano, Y., Mortimer, J.C., Nishikubo, N., Kubo, M., Katayama, Y., Kakegawa, K., Dupree, P., Demura, T. (2010a). VASCULAR-RELATED NAC-DOMAIN6 and VASCULAR-RELATED NAC-DOMAIN7 effectively induce transdifferentiation into xylem vessel elements under control of an induction system. *Plant Physiol.* 153, 906–914.

Yamaguchi, M., Ohtani, M., Mitsuda, N., Kubo, M., Ohme-Takagi, M., Fukuda, H., Demura, T. (2010b). VND-INTERACTING2, a NAC domain transcription factor, negatively regulates xylem vessel formation in Arabidopsis. *Plant Cell* 22, 1249–1263.

Yamaguchi, N., Huang, J., Tatsumi, Y., Abe, M., Sugano, S.S., Kojima, M., Takebayashi, Y., Kiba, T., Yokoyama, R., Nishitani, K., Sakakibara, H., Ito, T. (2018). Chromatin-mediated feed-forward auxin biosynthesis in floral meristem determinacy. *Nat Commun.* 9, 5290.

Yanai, O., Shani, E., Dolezal, K., Tarkowski, P., Sablowski, R., Sandberg, G., Samach, A., Ori, N. (2005). Arabidopsis KNOXI proteins activate cytokinin biosynthesis. *Curr. Biol.* 15, 1566–1571.

Yang, S., Johnston, N., Talideh, E., Mitchell, S., Jeffree, C., Goodrich, J., Ingram, G. (2008). The endosperm-specific ZHOUPI gene of Arabidopsis thaliana regulates endosperm breakdown and embryonic epidermal development. *Development* 135, 3501–3509.

Yang, Y., Sun, M., Yuan, C., Han, Y., Zheng, T., Cheng, T., Wang, J., Zhang, Q. (2019). Interactions between WUSCHEL- and CYC2-like transcription factors in regulating the development of reproductive organs in *Chrysanthemum morifolium*. *Int. J. Mol. Sci.* 20, 1276.

Yi, J., Moon, S., Lee, Y.S., Zhu, L., Liang, W., Zhang, D., Jung, K.H., An, G. (2016). Defective tapetum cell death 1 (DTC1) regulates ROS levels by binding to metallothionein during tapetum degeneration. *Plant Physiol.* 170, 1611–1623.

Yu, L.P., Miller, A.K., Clark, S.E. (2003). POLTERGEIST encodes a protein phosphatase 2C that regulates CLAVATA pathways controlling stem cell identity at Arabidopsis shoot and flower meristems. *Curr. Biol.* 13, 179–188.

Zeng, J., Dong, Z., Wu, H., Tian, Z., Zhao, Z. (2017). Redox regulation of plant stem cell fate. *EMBO J.* 36, 2844–2855.

Zhang, D., Liu, D., Lv, X., Wang, Y., Xun, Z., Liu, Z., Li, F., Lu, H. (2014). The cysteine protease CEP1, a key executor involved in tapetal programmed cell death, regulates pollen development in *Arabidopsis*. *Plant Cell* 26, 2939–2961.

Zhang, W., Sun, Y., Timofejeva, L., Chen, C., Grossniklaus, U., Ma, H. (2006). Regulation of Arabidopsis tapetum development and function by DYSFUNCTIONAL TAPETUM1 (DYT1) encoding a putative bHLH transcription factor. *Development* 133, 3085–3095.

Zhang, X., Henriques, R., Lin, S.S., Niu, Q.W., Chua, N.H. (2006). Agrobacterium-mediated transformation of Arabidopsis thaliana using the floral dip method. *Nat Protoc.* 1, 641–646.

Zhao, Z., Andersen, S.U., Ljung, K., Dolezal, K., Miotk, A., Schultheiss, S.J., Lohmann, J.U. (2010). Hormonal control of the shoot stem-cell niche. *Nature* 465, 1089.

Zhou, Y., Liu, X., Engstrom, E.M., Nimchuk, Z.L., Pruneda-Paz, J.L., Tarr, P.T., Yan, A., Kay, S.A., Meyerowitz, E.M. (2015). Control of plant stem cell function by conserved interacting transcriptional regulators. *Nature* 517, 377–380.

Zhou, Y., Yan, A., Han, H., Li, T., Geng, Y., Liu, X., Meyerowitz, E.M. (2018). HAIRY MERISTEM with WUSCHEL confines CLAVATA3 expression to the outer apical meristem layers. *Science* 361, 502–506.

Zhu, H., Hu, F., Wang, R., Zhou, X., Sze, S.H., Liou, L.W., Barefoot, A., Dickman, M., Zhang, X. (2011). Arabidopsis Argonaute10 specifically sequesters miR166/165 to regulate shoot apical meristem development. *Cell* 145, 242–256.

Zhu, J., Chen, H., Li, H., Gao, J.F., Jiang, H., Wang, C., Guan, Y.F., Yang, Z.N. (2008). Defective in Tapetal development and function 1 is essential for anther development and tapetal function for microspore maturation in Arabidopsis. *Plant J.* 55, 266–277.

Zimmermann, P., Heinlein, C., Orendi, G., Zentgraf, U. (2006). Senescence specific regulation of catalases in *Arabidopsis thaliana* (L.) Heynh. *Plant Cell Environ*. 29, 1049–1060.